Spring 1-30-1956

The Variations of Stress Induced in an Eccentrically Located Bolt Securing a Flanged Joint

Verne E. Blake Jr.

VARIATIONS OF STRESS — Blake

THE VARIATIONS OF STRESS INDUCED IN AN ECCENTRICALLY LOCATED BOLT SECURING A FLANGED JOINT

By

Verne E. Blake, Jr.

A Thesis

Submitted in Partial Fulfillment of the

Requirements for the Degree of

Master of Science in Mechanical Engineering

The University of New Mexico

1956

This thesis, directed and approved by the candidate's committee, has been accepted by the Graduate Committee of the University of New Mexico in partial fulfillment of the requirements for the degree of

MASTER OF SCIENCE

E H Castetter

DEAN

1/30/1956

DATE

THE VARIATIONS OF STRESS INDUCED IN AN ECCENTRICALLY LOCATED BOLT SECURING A FLANGED JOINT

By

Verne E. Blake, Jr.

Thesis committee

R. C. Dorf

CHAIRMAN

C. T. Grace

Eugene Zwoyer

TABLE OF CONTENTS

TABLE OF CONTENTS

LIST OF TABLES

LIST OF FIGURES

Figure

Figure Page

CHAPTER I

INTRODUCTION TO THE PROBLEM

It is common practice in design work to use bolts as a means of attaching load carrying members. In many instances it is not possible to locate the bolt so the line of action of the external load will pass through the bolt axis. As a result, there are secondary loads, resulting from the eccentricity of the load paths, which the bolt must resist in addition to the primary loads. Figure 1 is an example of a typical flanged attachment. Figure 2 is an illustration of the same flanged attachment represented as a free-body diagram with the forces and moments shown. Force F_1 is the externally applied load. Force F_2 is the load applied to the flange by the bolt. This force may exist because of initial tightening of the bolt, because of the external force F_1, or because of a combination of the two. Force F_3 is the resultant force acting on the bottom of the flange and is necessary to place the flange in equilibrium. Force F_3 is equal in magnitude to the product of the average pressure and the area under contact on the lower face of the flange. Its location is at the centroid of the pressure. Moments M_b and M_f are the restoring moments at the bolt and at the external load carrying member respectively that occur when the flange tends to rotate as a result of F_1.

Until recently, very little information was available on the stresses that would be induced in a bolt used in an application similar to that shown in Figure 1. However, formulas are now available which enable the designer to predict stress variations in the bolt of a flanged attachment as long as the joint between the flange and base does not open.[1] Apparently, the problem of bolt stress variations after the joint has started to open has not been investigated.

---

1. T. J. Doland and J. H. McClow, "The Influence of Bolt Tension and Eccentric Tensile Loads on Behavior of a Bolted Joint," *Society of Experimental Stress Analysis*, Vol. 8, No. 1, p. 31.

CHAPTER 1

INTRODUCTION TO THE PROBLEM

It is common practice in design work to use bolts as a means of attaching load carrying members. In many instances it is not possible to locate the bolt so the line of action of the external load will pass through the bolt axis. As a result, there are secondary loads, resulting from the eccentricity of the load paths, which the bolt must resist in addition to the primary loads. Figure 1 is an example of a typical flanged attachment. Figure 2 is an illustration of the same flanged attachment represented as a free-body diagram with the forces and moments shown. Force F_1 is the externally applied load. Force F_2 is the load applied to the flange by the bolt. This force may exist because of initial tightening of the bolt, because of the external force F_1, or because of a combination of the two. Force F_3 is the resultant force acting on the bottom of the flange and is necessary to place the flange in equilibrium. Force F_3 is equal in magnitude to the product of the average pressure and the area under contact on the lower face of the flange. Its location is at the centroid of the pressure. Moments M_1 and M_2 are the restoring moments at the bolt and at the external load carrying member respectively that occur when the flange tends to rotate as a result of F_1.

Until recently, very little information was available on the stresses that would be induced in a bolt used in an application similar to that shown in Figure 1. However, formulas are now available which enable the designer to predict stress variations in the bolt of a flanged attachment as long as the joint between the flange and base does not open.[1] Apparently, the problem of bolt stress variations after the joint has started to open has not been investigated.

---

1. T. J. Doland and J. H. McClow, "The Influence of Bolt Tension and Eccentric Tensile Loads on Behavior of a Bolted Joint," Society of Experimental Stress Analysis, Vol. 8, No. 1, p. 31.

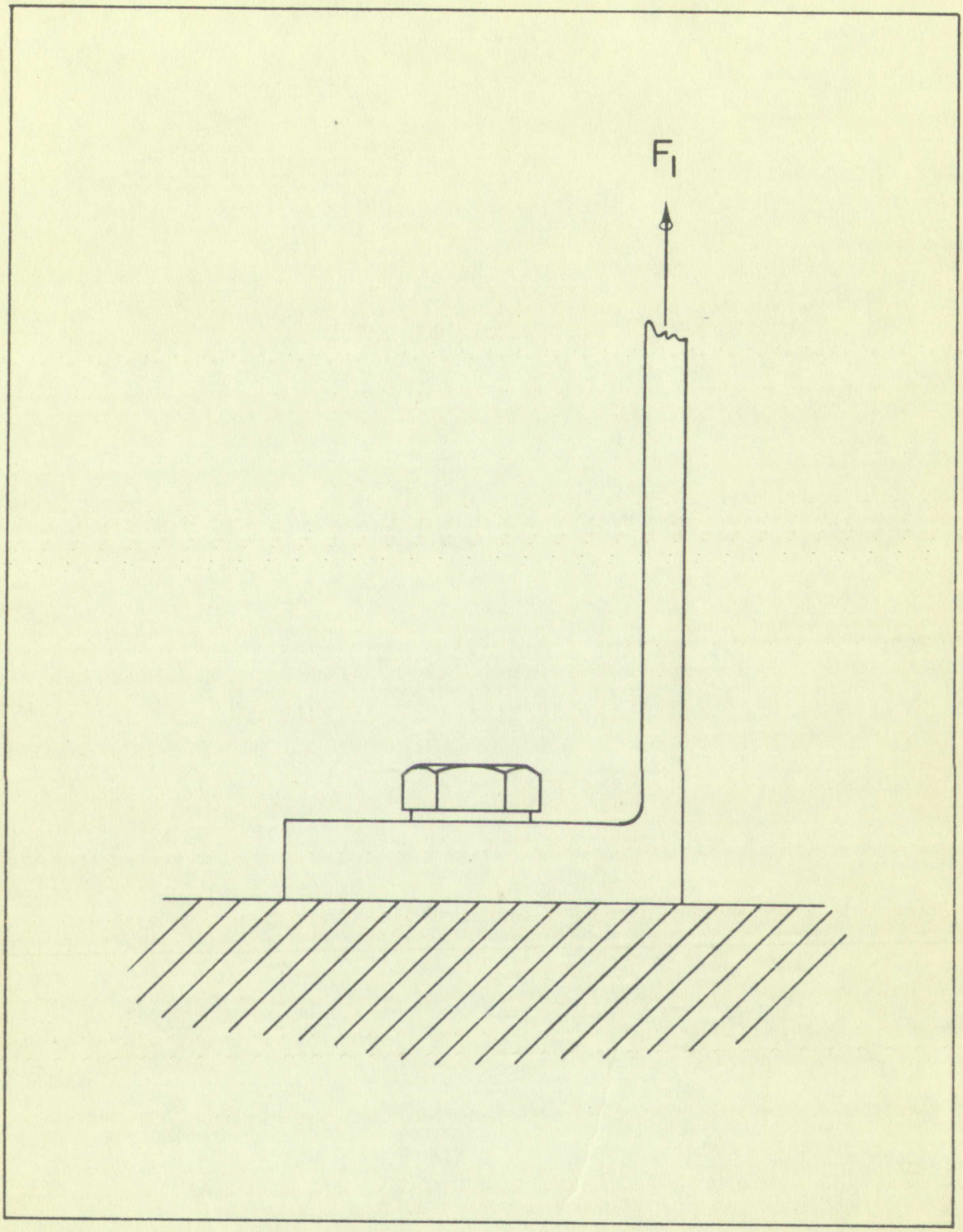

FIGURE 1

TYPICAL FLANGE ATTACHMENT

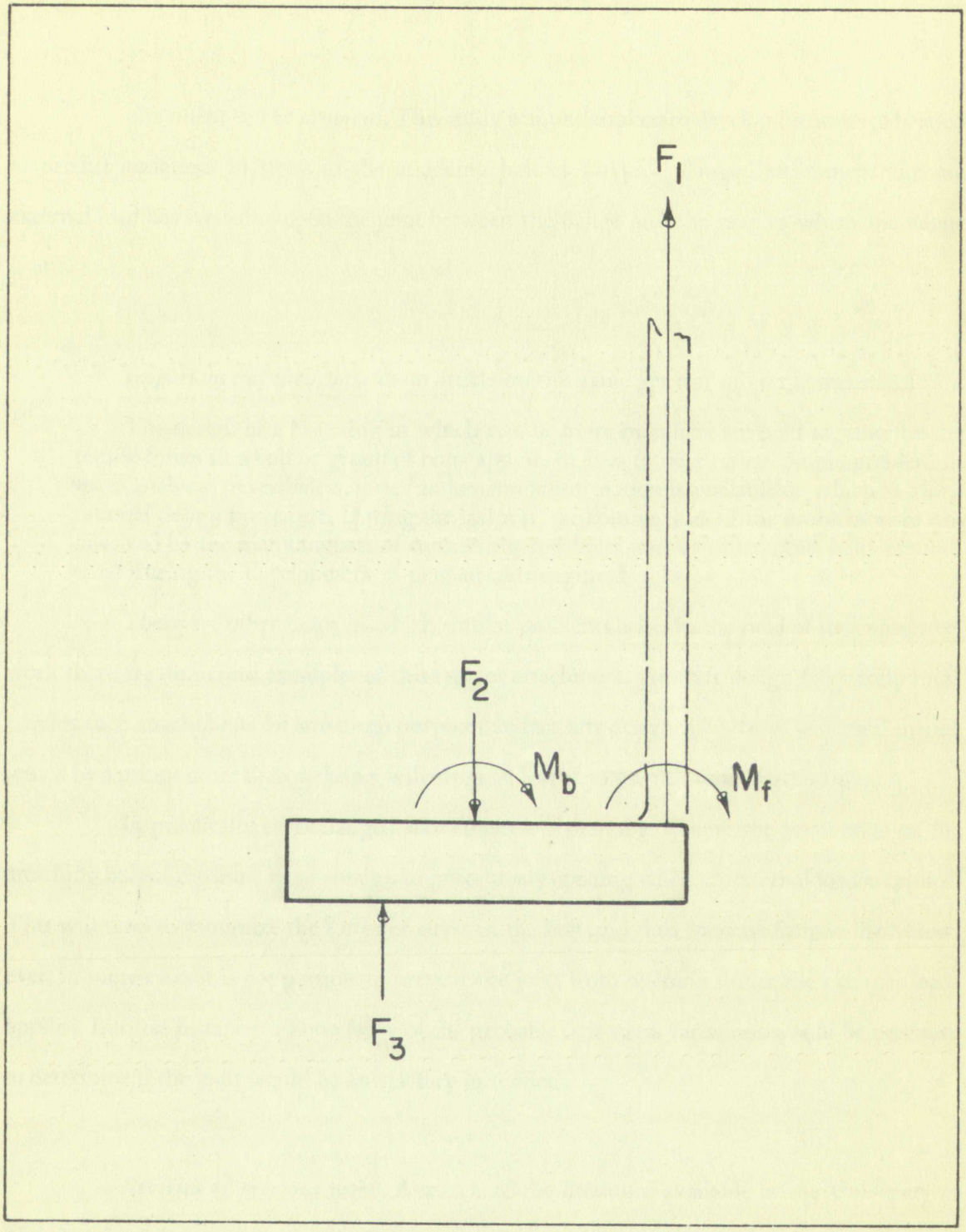

FIGURE 2

FREEBODY DIAGRAM OF FLANGE ATTACHMENT

Statement of the problem. This study was undertaken to develop formulas to be used to predict variations in stress in the attaching bolt of a typical flanged attachment after an external load has started to open the joint between the flange and the base to which the flange is attached.

Importance of the study. In an article on this same general subject it was stated:

> The design of a fastening in which two or more members are held together by the tensile forces in a bolt or group of bolts appears at first to be a rather simple problem in stress analysis; nevertheless, little fundamental information is available on which to base a rational design procedure. During the last war, the complexities of the problem were emphasized by the many failures of connecting rod bolts and cylinder head bolts encountered during the development of new aircraft engines.[2]

There are other fields in which similar problems arise. In the field of structural steel work there are numerous examples of this type of attachment. Aircraft design frequently must employ such attachments for structural purposes. In fact, any designer who uses structural shapes, joined by a means other than welding, will often be forced to use this type of attachment.

In practically every flanged attachment it is desirable to have the pre-tension on the attaching bolt of the joint large enough to prevent any opening when an external load is applied. This will tend to minimize the range of stress in the bolt and thus increase fatigue life.[3] However, in some cases it is not possible to prevent the joint from opening under the external loads applied. In these instances a knowledge of the probable bolt stress variations would be necessary to determine if the joint would be satisfactory in service.

Reviews of previous work. A search of the literature available at the University of New Mexico Library, at the Sandia Corporation Technical Library, and of other sources, failed

2. *Ibid.*, p. 29.

3. *Ibid.*, p. 41.

to uncover any work directly applicable to this subject. However, two articles were found which are indirectly applicable.[4, 5] These articles cover the behavior of bolted attachments before there is any separation of the flange from the base as a result of an external load.

Definition of terms used. The following terms are used frequently throughout the text. It is felt that a definition of these terms will be of advantage in understanding the work to follow.

Load Bolt. A strain gaged capscrew used for measuring the magnitude of the load applied to the flange being tested.

Test Bolt. A strain gaged capscrew used to bolt the Test Flange into the Test Jig. The capscrew was strain gaged to detect both axial and bending loads.

Test Jig. The apparatus used for applying an external load to the Test Flange.

Test Section. The portion of the Test Jig in which the Test Flange was mounted.

Test Flange. Any one of a number of different configurations of flanges used in the test portion of this study.

Eccentrically loaded. A term used to denote that the line of action of an external load in a flanged attachment does not coincide with the center line of the bolt securing the flanged attachment.

---

4. *Ibid.*, pp. 29-43.

5. M. F. Spotts, "Effect of Initial Stress on Eccentrically Loaded Bolt," *Machine Design and Manufacturing Bulletin*, Vol. 20, No. 7, pp. 1-5.

CHAPTER II

DESIGN AND CONSTRUCTION OF THE TEST APPARATUS

This chapter is devoted to the design of the test apparatus, a description of the various parts of the apparatus, and a description of the various pieces of commercial equipment used in conjunction with the testing. The various parts are identified by means of photographs as well as written descriptions.

Basic design. The Test Jig consisted of two primary groups of parts. Photographs showing the general test setup and identifying the various parts of the apparatus may be found in Figures 3 and 4. The first group, the main body of the jig, was made up of two main beams, one upper and one lower, with a compression column between the beams at one end and a hydraulic jack at the other end. The second group, the Test Section, was made up of a Test Flange, a strain gaged capscrew for attaching the Test Flange to the base (the Test Bolt), a thick washer, a mounting base, and several parts, including a second strain gaged capscrew, which were used to attach the Test Flange to the upper beam. The latter strain gaged capscrew (the Load Bolt) was used for measuring the input load to the Test Flange.

Details of various parts. The following paragraphs contain more detailed descriptions of the various parts of the Test Jig.

Each main beam of the jig was fabricated from two pieces of 3 inch structural steel channel bolted together, back to back, with three 0.25 inch thick spacers between them. The beams were used as levers to apply the load to the Test Section.

The compression collumn, located at one end of the jig was made of wood and served

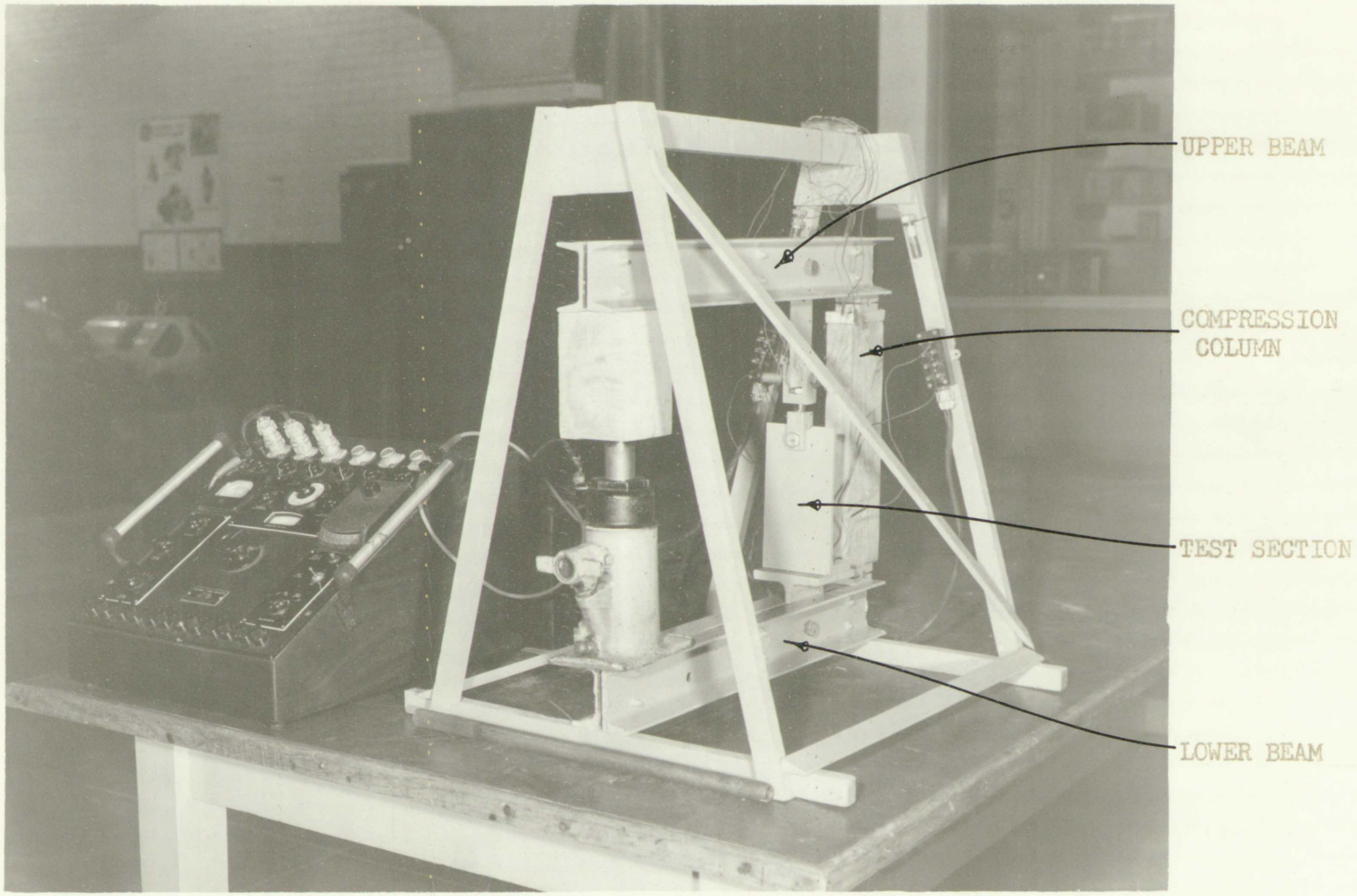

FIGURE 3

TEST SETUP

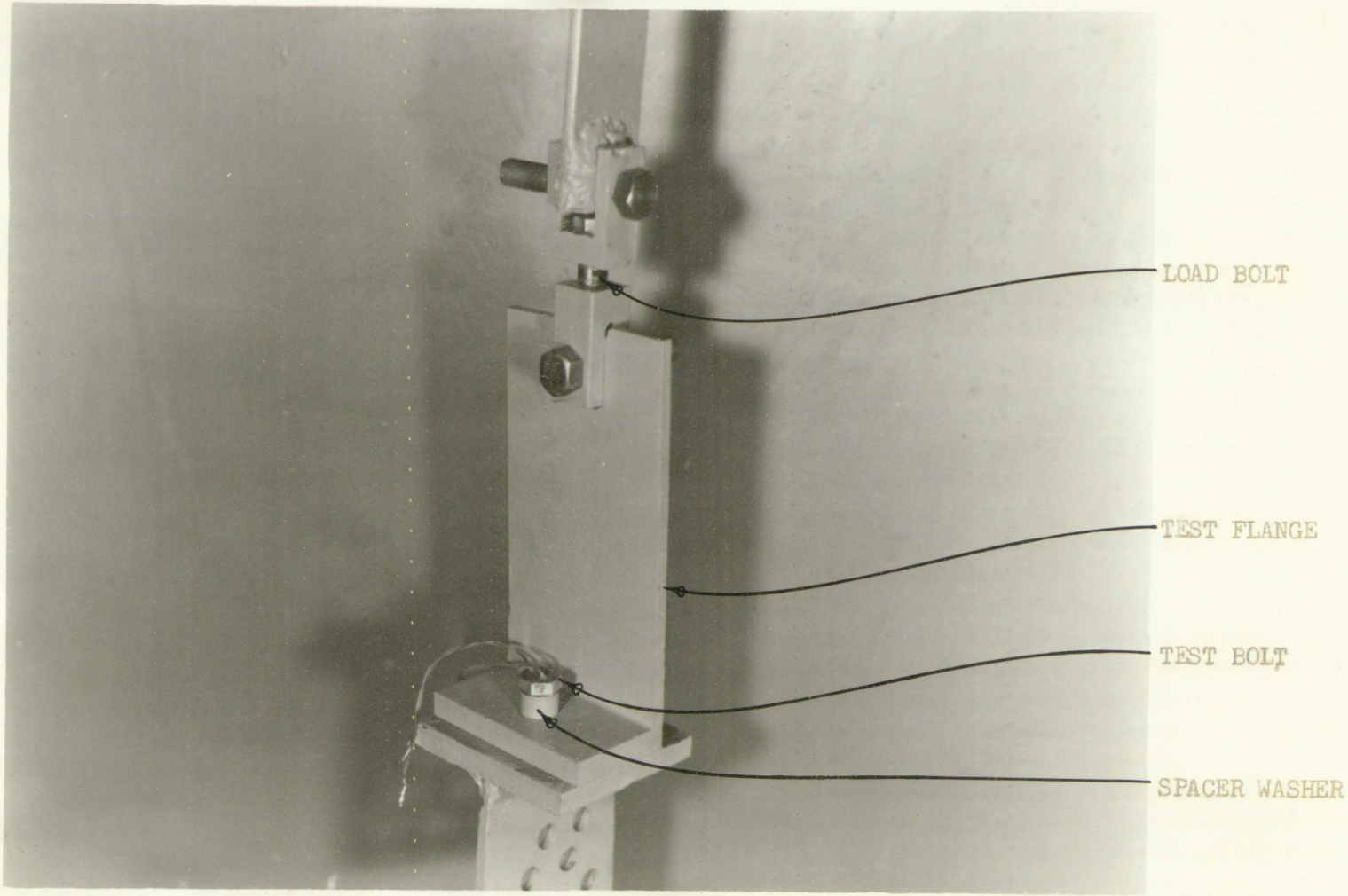

FIGURE 4

TEST SECTION

as a fixed reaction point for the beams.

A hydraulic jack was located at the other end of the beam. A wooden spacer block was placed between the jack and the upper beam to avoid over-extending the hydraulic cylinder of the jack during the tests. The hydraulic jack was used to force the beams apart at one end and thus load the Test Section.

Each Test Flange had the appearance of a 4 inch length of angle with one leg about 2 inches long and the other leg about 7 inches long. The shorter leg was the flange attachment portion, while the longer leg served as the external load carrying member. The longer legs of all Test Flanges were 0.25 inches thick. The shorter legs of the Test Flanges were of varying thicknesses. In all, nine Test Flanges were fabricated. Of these, three had the shorter leg 0.25 inches thick, three had the leg 0.50 inches thick,and three had the leg 0.88 inches thick. In each group of three flanges of the same thickness, one flange was drilled so the mounting bolt and load path were eccentric by 1.44 inches, one flange eccentric by 1.12 inches, and one flange eccentric by 0.81 inches. Figure 5 is a photograph of all of the flanges tested. The detailed drawing of the flanges may be found in Appendix B.

The strain gaged capscrews were fabricated from 0.50 inch diameter steel bolts having an ultimate tensile strength of 125,000 pounds per square inch. Two electric strain gages were bonded to the opposite sides of each bolt with the center of the gages 0.62 inches from the underside of the bolt head. Two curved shims of steel, 0.03 inches thick, were soldered to the bolt between the gages to protect them from abrasion during use. The electrical leads were brought out through two holes drilled in the head of each bolt. A close-up photograph of the two strain gaged bolts may be found in Figure 6. The detailed dawing of the bolts is contained in Appendix B.

In order to use the same test capscrew for all three flange thicknesses, it was necessary to provide spacers between the bolt head and flange for each application. The spacers consisted

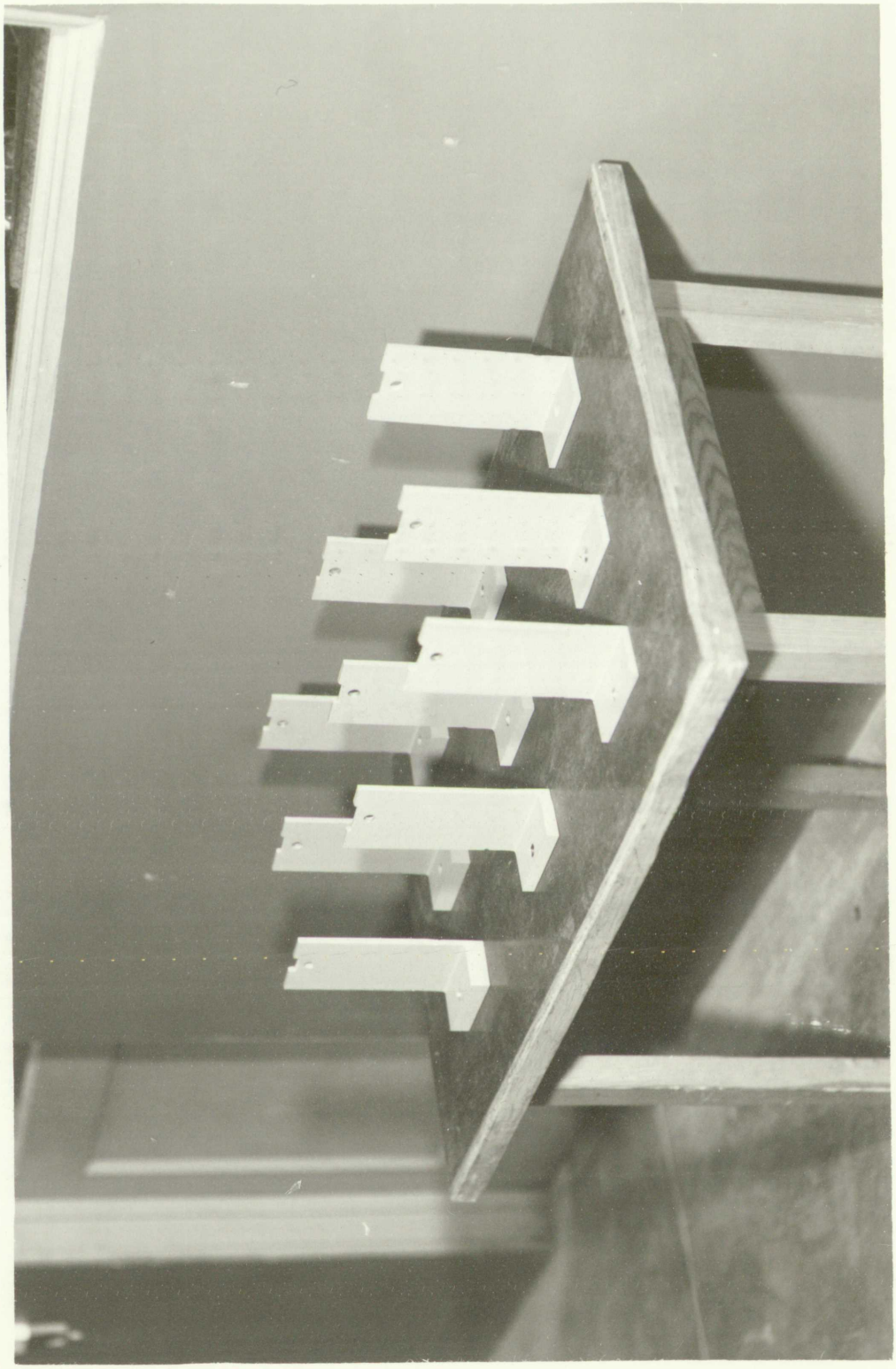

FIGURE 5

TEST FLANGES

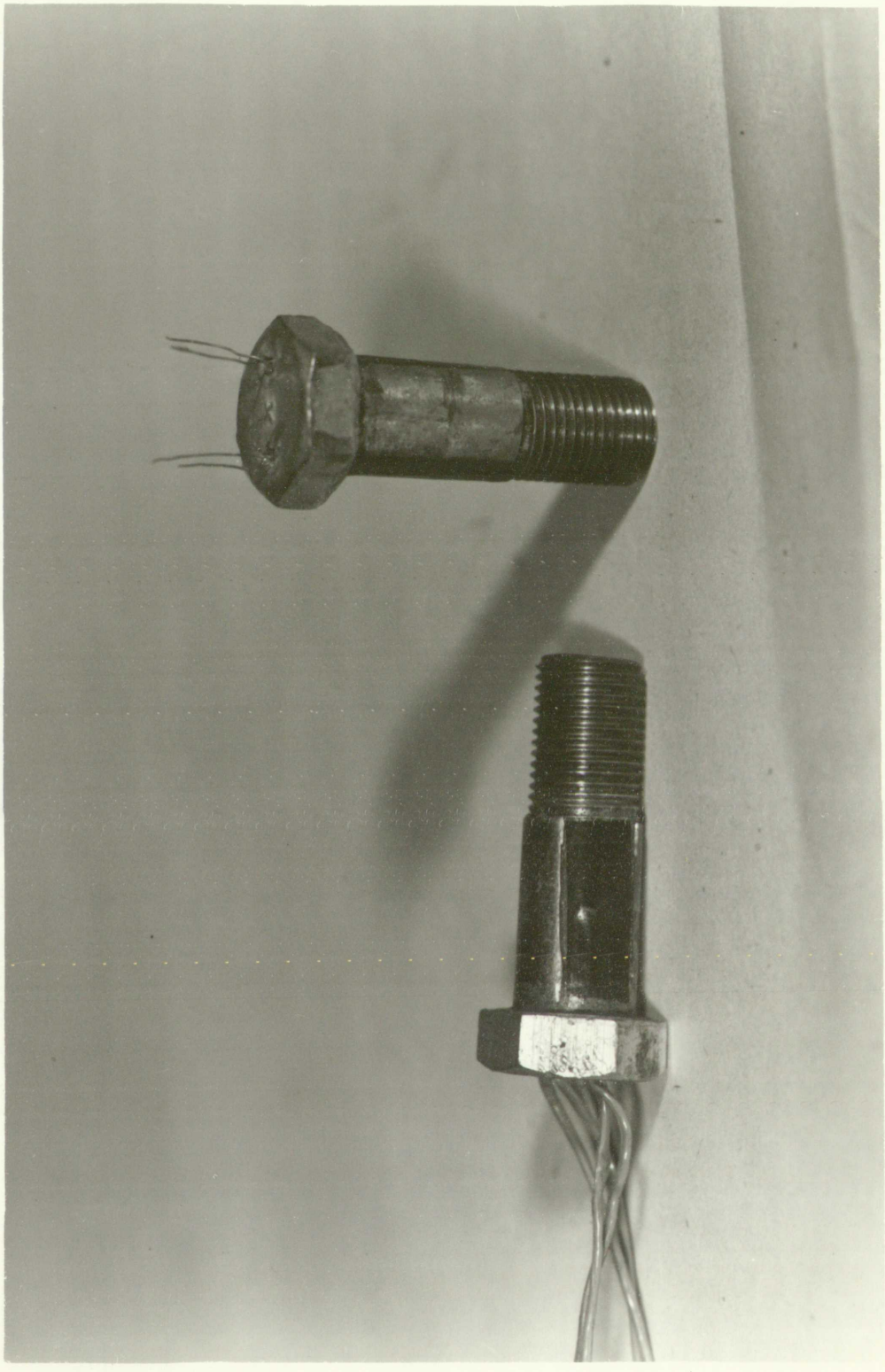

FIGURE 6

STRAIN GAGED BOLTS

of thick washers 0.56 inches inside diameter by 0.75 inches outside diameter. The thickness of each washer was controlled so the sum of the flange thickness and the washer thickness totaled 0.938 inches for each flange. The washers were made of steel having an ultimate tensile strength of 125,000 pounds per square inch. Figure 7 is a photograph of the three washers, shown on a stepped block that corresponds to the three different thicknesses of flanges. Appendix B contains the detailed drawing of the washers.

The mounting base consisted of a 4 inch square piece of 0.50 inch thick steel plate with a second 4 inch square piece of 0.25 inch steel plate welded to the bottom side to form a "T" shaped member. Two tapped holes were located near the center of the 0.50 inch plate directly above the 0.25 inch plate. One of these holes was used for boltingthe Test Flange in place. Two holes were provided so a number of different load path eccentricties could be examined if necessary. In use, the 0.25 inch leg of the "T" was slipped between the channels of the lower beam and pinned in place with a 0.50 inch bolt. Six holes were provided in the vertical leg of the "T" so that, in combination with the two tapped holes, a total of twelve different eccentricities could be accommodated. However, only three eccentricities were tested

The severall parts used to attach the Test Flange to the upper beam were fabricated from steel plate and bar. Figure 8 is a photograph of the various parts assembled together. The lowest portion consisteed of a clevis type part that was pinned with a 0.50 inch bolt to the Test Flange. This piece had a tapped hole in the top into which the Load Bolt was screwed. A second clevis shaped piece, with a clearance hole in the end for the LoadBolt, was the next part in the assembly. A strap was pinned between this second clevis and theupper beam with a 0.50 inch bolt. The Load Bolt was passed through the upper clevis and screwed into the lower clevis to complete the assembly.. The parts were fabricated with two of the pinned joints at right angles so the assembly would not tend to introduce any moments into the system.

The Test Jigg was mounted in a wooden "A" frame forconvenience in testing.

of thick washers 0.56 inches inside diameter by 0.75 inches outside diameter. The thickness of each washer was controlled so the sum of the flange thickness and the washer thickness totaled 0.938 inches for each flange. The washers were made of steel having an ultimate tensile strength of 125,000 pounds per square inch. Figure 7 is a photograph of the three washers, shown on a stepped block that corresponds to the three different thicknesses of flanges. Appendix B contains the detailed drawing of the washers.

The mounting base consisted of a 4 inch square piece of 0.50 inch thick steel plate with a second 4 inch square piece of 0.25 inch steel plate welded to the bottom side to form a "T" shaped member. Two tapped holes were located near the center of the 0.50 inch plate directly above the 0.25 inch plate. One of these holes was used for bolting the Test Flange in place. Two holes were provided so a number of different load path eccentricities could be examined if necessary. In use, the 0.25 inch leg of the "T" was slipped between the channels of the lower beam and pinned in place with a 0.50 inch bolt. Six holes were provided in the vertical leg of the "T" so that, in combination with the two tapped holes, a total of twelve different eccentricities could be accommodated. However, only three eccentricities were tested.

The several parts used to attach the Test Flange to the upper beam were fabricated from steel plate and bar. Figure 8 is a photograph of the various parts assembled together. The lowest portion consisted of a clevis type part that was pinned with a 0.50 inch bolt to the Test Flange. This piece had a tapped hole in the top into which the Load Bolt was screwed. A second clevis shaped piece, with a clearance hole in the end for the Load Bolt, was the next part in the assembly. A strap was pinned between this second clevis and the upper beam with a 0.50 inch bolt. The Load Bolt was passed through the upper clevis and screwed into the lower clevis to complete the assembly. The parts were fabricated with two of the pinned joints at right angles so the assembly would not tend to introduce any moments into the system.

The Test Jig was mounted in a wooden "A" frame for convenience in testing.

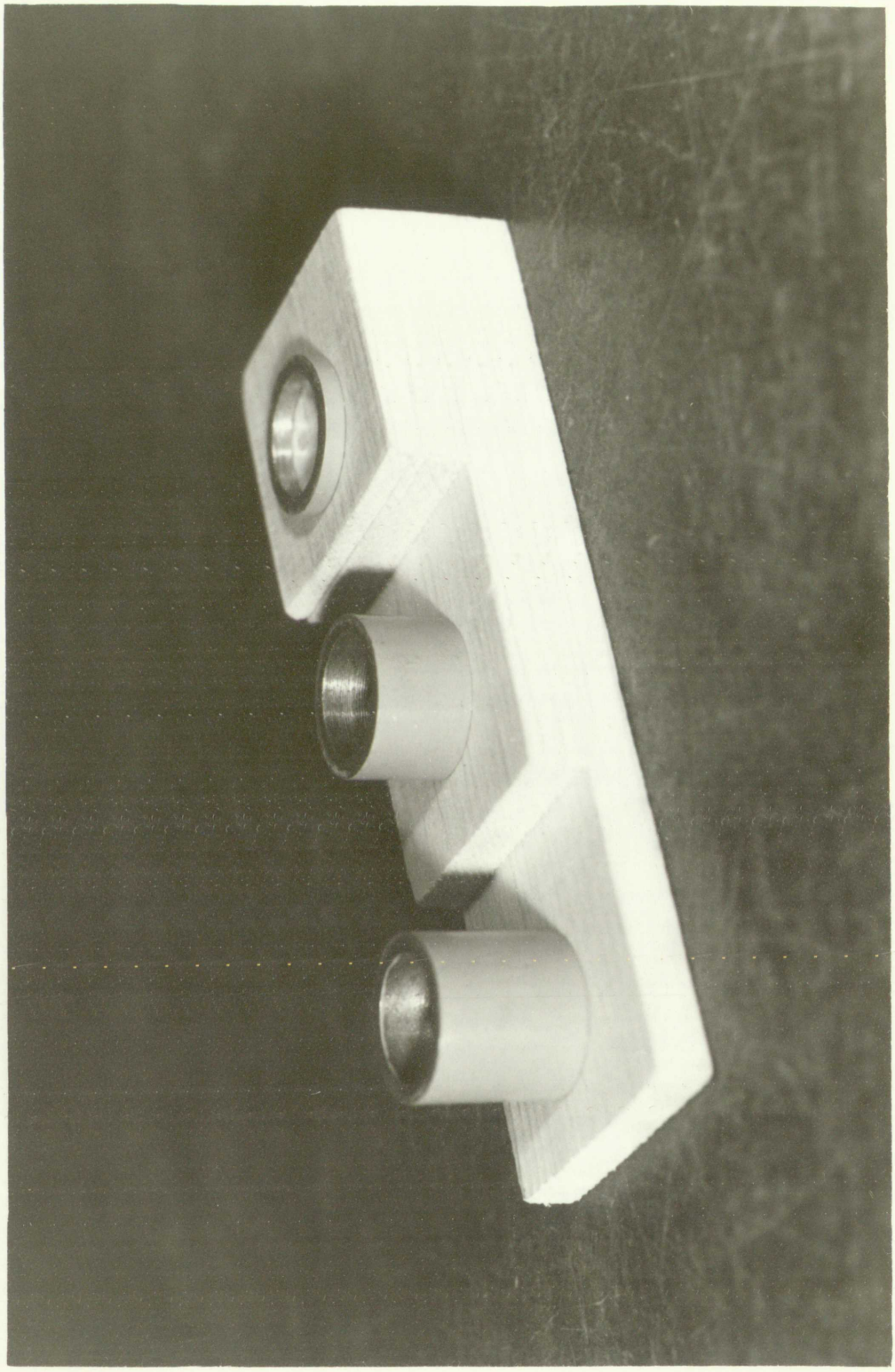

FIGURE 7

SPACER WASHERS

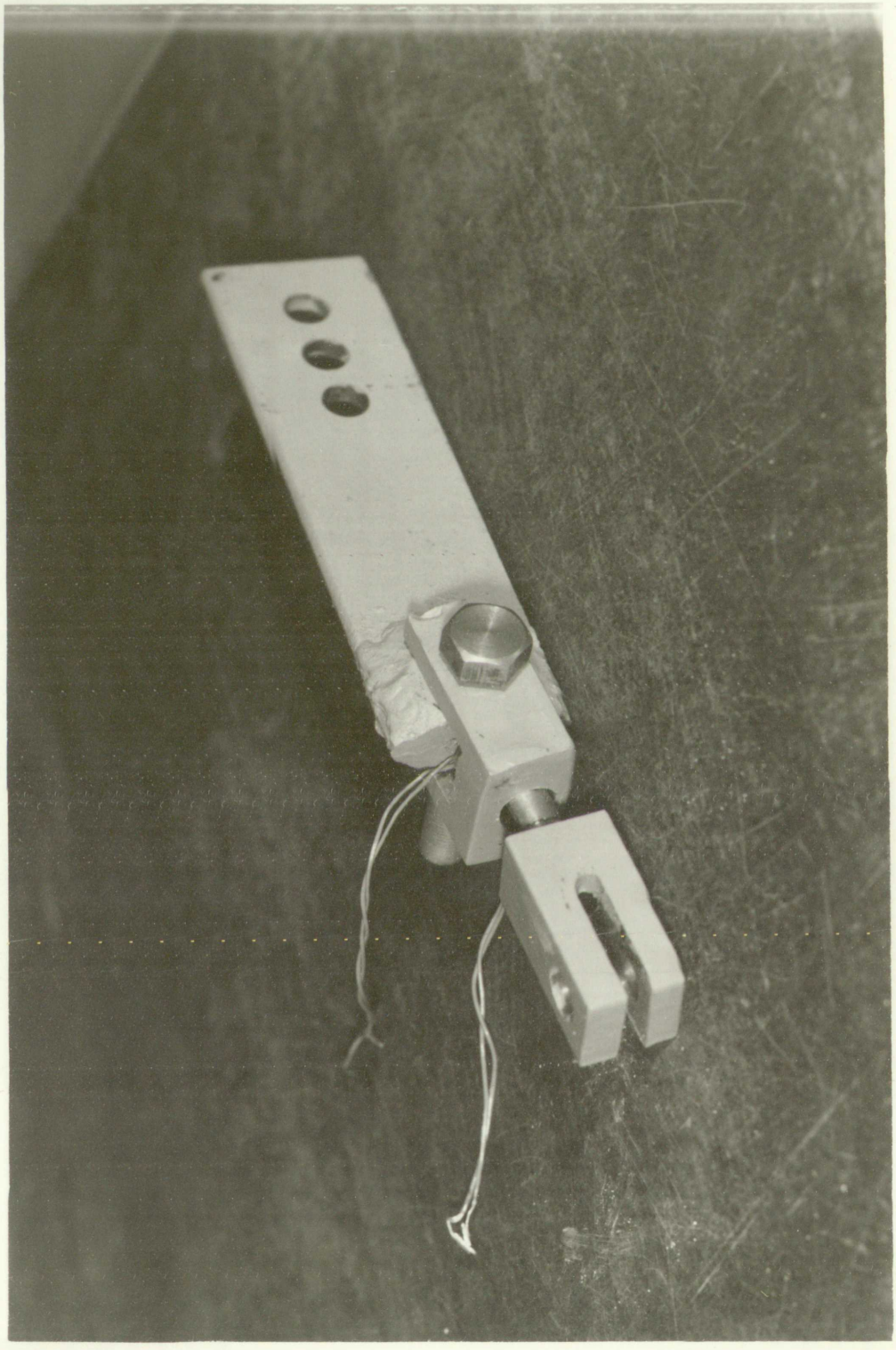

FIGURE 8

UPPER TEST SECTION

Commercial equipment. The instrument used for measuring the induced strains in the system was a Portable Strain Indicator, type RS-10, serial number 4229-1, manufactured by the Hathaway Instrument Company of Denver, Colo.

The commercial external bridge circuits used with the strain gages were type WA, serial numbers 4229-2 and 4229-3, also manufactured by the Hathaway Instrument Company. Figure 9 is a photograph of the Portable Strain Indicator and two of the external bridge circuits used in the experiments.

The batteries used were standard 12 volt Delco automobile batteries. Both batteries were connected to a trickle charger when not in use, to keep the voltages high and nearly equal.

The strain gages used were of the electrical resistance type (SR-4) manufactured by the Baldwin-Lima-Hamilton Company of Philadelphia, Pa. Type A-7 gages with a nominal resistance of 120 ohms were used. These gages have an overall length of 0.75 inches and a width of 0.25 inches. The gage length is 0.25 inches.

The hydraulic jack used with the Test Jig was a Buda model 5-8.5 having a capacity of 10,000 pounds. The jack was manufactured by the Buda Company of Harvey, Ill.

FIGURE 9

PORTABLE STRAIN INDICATOR AND EXTERNAL BRIDGES

CHAPTER III

TEST PROCEDURE

This chapter deals primarily with the procedures followed in measuring the strains induced in the Test Bolt. The results of pre-test trial runs to check out the equipment, and a description of the types of readings taken and their significance, are also included.

Significance of readings taken. As noted in Chapter II, both the Test Bolt and Load Bolt were strain gaged with two gages on each. These gages were located on opposite sides of the bolts.

On the Load Bolt, the strain gages were electrically connected in opposite arms of the strain gage bridge so that all bending strains would automatically cancel.[6] The strain readings taken were the sum of the strains detected by the two gages. Normally, it would be necessary to divide this reading by two in order to obtain the average axial strain. However, the Portable Strain Indicator used on these tests was calibrated so this was accomplished automatically.[7]

The Load Bolt was mounted in a section in which pinned joints were used to transmit the load so that, for all practical purposes, no bending loads were transmitted. For this reason it was unnecessary to instrument the Load Bolt to detect any loads other than axial.

On the Test Bolt the strain readings of each gage were recorded separately. In this case, it was necessary to double each reading obtained since the Portable Strain Indicator is calibrated for 2 gages additively.

With the strain readings on the Test Bolt recorded separately, it was possible to

---

6. C. C. Perry, and H. R. Lissner, *The Strain Gage Primer* (New York: McGraw-Hill Book Company, Inc., 1955), p. 61.

7. *Hathaway Type RS-10 Portable Strain Indicator Instruction Book H-172* (Denver, Colorado: Hathaway Instrument Company), p. 11.

CHAPTER III

TEST PROCEDURE

This chapter deals primarily with the procedures followed in measuring the strains induced in the Test Bolt. The results of pre-test trial runs to check out the equipment, and a description of the types of readings taken and their significance, are also included.

Significance of readings taken. As noted in Chapter II, both the Test Bolt and Load Bolt were strain gaged with two gages on each. These gages were located on opposite sides of the bolts.

On the Load Bolt, the strain gages were electrically connected in opposite arms of the strain gage bridge so that all bending strains would automatically cancel.[1] The strain readings taken were the sum of the strains detected by the two gages. Normally, it would be necessary to divide this reading by two in order to obtain the average axial strain. However, the Portable Strain Indicator used on these tests was calibrated so this was accomplished automatically.[2]

The Load Bolt was mounted in a section in which pinned joints were used to transmit the load so that, for all practical purposes, no bending loads were transmitted. For this reason it was unnecessary to instrument the Load Bolt to detect any loads other than axial.

On the Test Bolt the strain readings of each gage were recorded separately. In this case, it was necessary to double each reading obtained since the Portable Strain Indicator is calibrated for 2 gages additively.

With the strain readings on the Test Bolt recorded separately, it was possible to

---

6. C. C. Perry and H. R. Lissner, *The Strain Gage Primer* (New York: McGraw-Hill Book Company, Inc., 1955), p. 61.

7. Baldwin-Lima-Hamilton Corporation, *Operating Instructions and Parts List for Portable Strain Indicator Type P-3500* (Baldwin-Lima-Hamilton Corporation, Electronic Instrument Company), p. 11.

mathematically reduce the data to an axial load and a bending load. However, the problem was somewhat complicated by the fact that the gages were not always orientedso the strain gage axis was coincident with the axis where the maximum bending strains occured. (It was assumed that the theoretical axis of maximum bending was in a plane perpendicular to the intersection of the two legs of the Test Flange.) Figure 10 shows the relation between the various axes. This problem arose since the gages, which were bonded to the bolt, would rotate as the bolt was screwed into the tapped hole in the mounting base. The final angle between the gage axis and the axis of maximum bending would then be a function of the flange thickness, the spacer washer thickness, and the bolt pre-tension. The sum of the flange thickness and washer thickness was controlled by carefully grinding the washer until its thickness was such that the gage axis, with the Test Bolt snug but not tightened, was between 20 and 50 degrees of the axis of maximum bending. The washer thickness was chosen so that additional tightening would first decrease the angle to zero, and then would increase it to a larger angle on the other side of the axis of maximum bending. In this way, it was possible to run all of the tests with the angle between the gage axis and the axis of maximum bending less than 50 degrees. The angle between the gage axis and the theoretical axis of maximum bending was kept as small as possible since the correction factor involved division by the cosine of the angle, and one over the cosine of the angle does not vary greatly for angles less than 50 degrees. The equations for reducing the data are given in Appendix C.

Pre-test trial runs. A series of tests were run before the data of this study were actually collected. These runs were made primarily to gain familiarity with the equipment and to establish a consistent method of taking data.

A test was run in this early series to determine if the direction the flange faced, toward or away from the hydraulic jack, would have any significant effect on the readings.

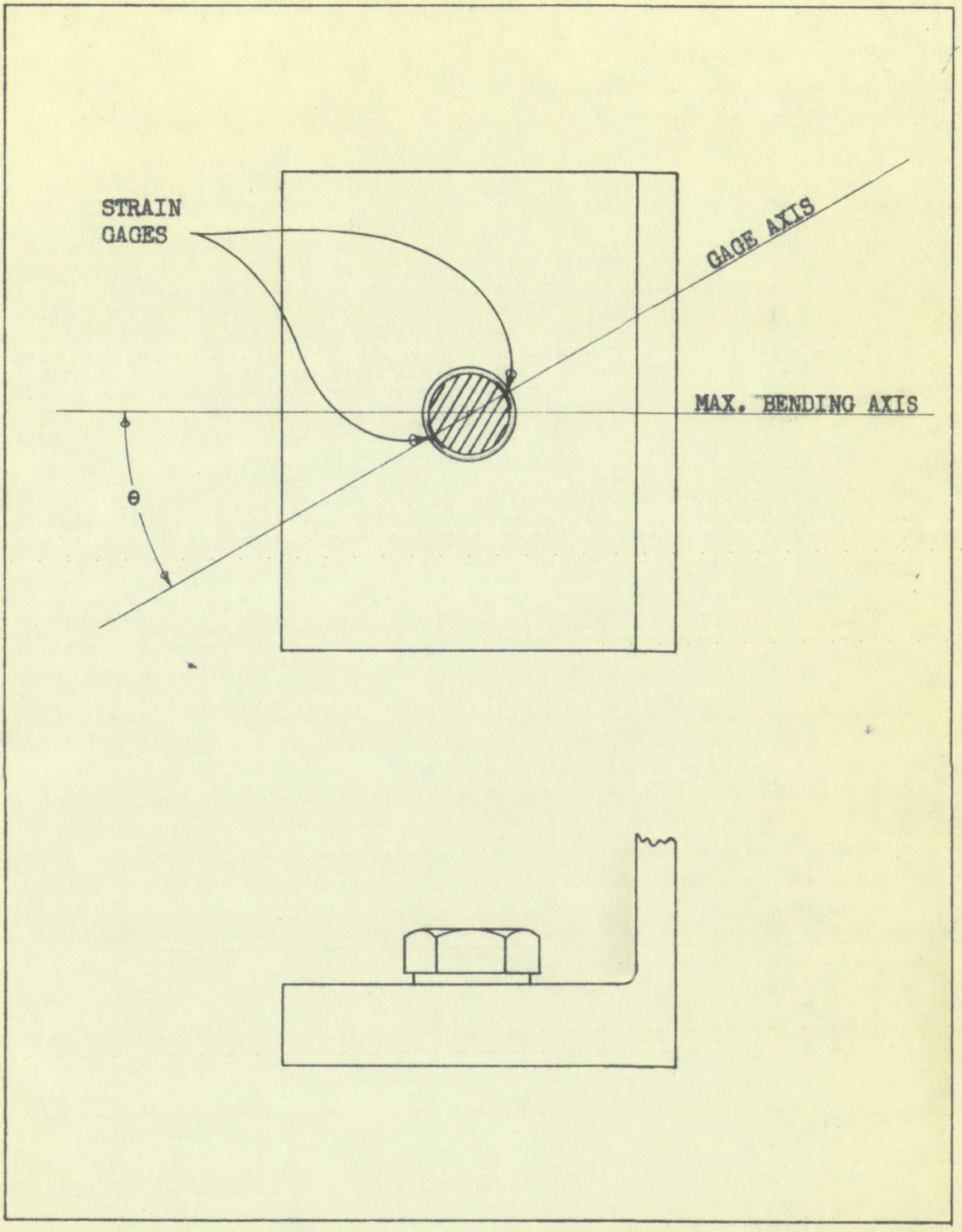

FIGURE 10

RELATION BETWEEN MAXIMUM BENDING AXIS AND MEASURED BENDING AXIS

The results of this test showed no discernible difference in the readings. However, to be consistent, the flange was faced away from the jack in subsequent studies.

It was found in these early runs that the apparent Test Bolt pre-tension due to tightening would drop appreciably after the first test at a given external load. In a second test at the same load there would be a small decrease. A third test at the same load usually would result in no significant change in pre-tension. The strains recorded on each test at the maximum load would be essentially the same for all three tests. If a fourth test were made at a still higher external load, the pre-tension would again decrease. A fifth run at this higher external load would usually show no significant change. There was no evidence of the bolt turning and thus contributing to this effect. Figure 11 is a graph of the results of the tests performed as indicated above. From this behavior of the Test Bolt pre-tension it was concluded that an additional problem existed. The new problem was that of determining how much the pre-tension of a bolt would decrease in use. The original problem was that of determining the variations of Test Bolt loads as a function of external load, after the pre-tension had reached a state of equilibrium. The solution to both problems is obviously needed to completely evaluate a given design. Since the latter problem was considered more likely to lend itself to a theoretical solution, it was decided to investigate this problem only, for this study. The problem of the decrease in bolt pre-tension is left for a separate study.

To prevent this pre-tension loss from affecting the tests, a set procedure was followed on each test run. The bolt was first torqued until the strain gages indicated 20 to 40 percent greater pre-tension than desired. The external load was taken to the maximum for the test and then released. This was repeated until there was no further shift in the zero readings. When the zero readings were consistent a test run was made. If, after the run, the zero readings had again shifted, the test was repeated. In this way any effects on the results of a decrease in pre-tension during the test were eliminated.

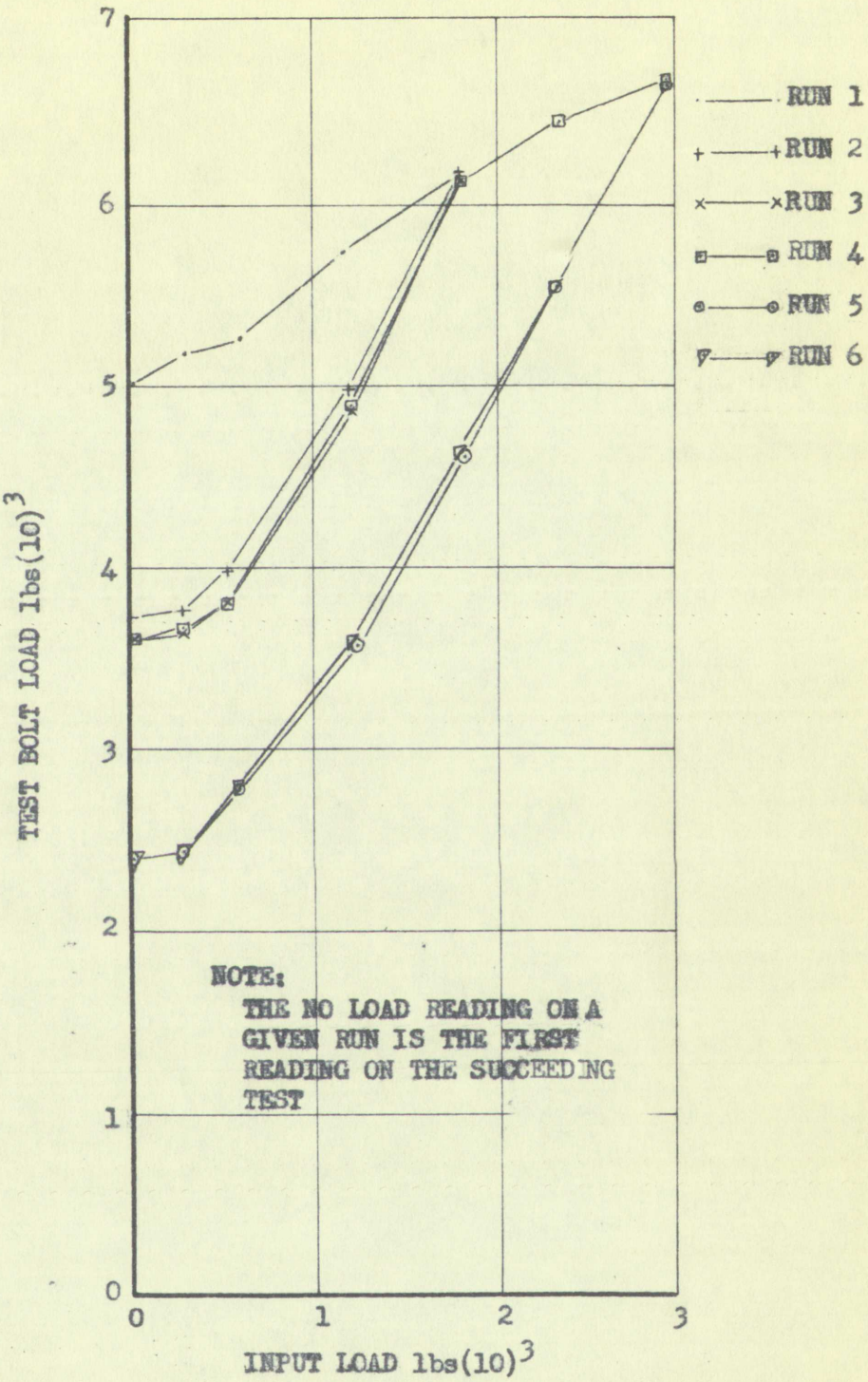

FIGURE 11

DECREASE IN INITIAL BOLT PRE-TENSION DUE TO INCREASED INPUT LOAD

Recommended test procedures. The following procedures wereused throughout all tests reported in this study. The same sequence and procedure were followed so that variations which might affect the results would not be introduced.

1. As soon as a series of runs was started, all of the strain gageswere connected into the circuit. Because of the circuit in the type of strain indicator used, all of the gages were continuously carrying current throughout the test. The current was large, about 50 milliamperes, so there evidently was some heating. It usually took about 10 to 15 minutes for the readings to become consistent.

2. While the system was warming up, the battery voltages werecarefully compared and adjusted. With this type of strain indicator the two power sources musthave the same voltage since the reading is based on comparing the voltage drop in an internal bridge with the voltage drop in an external bridge. A wiring schematic may be found in Figure 12.

3. The galvanometer was carefully zeroed and the internal bridge balanced.

4. The external bridge circuits were balanced. Each external circuit is provided with a potentiometer which can be adjusted so that each gage reads zero. When all of the gage readings had ceased changing, the external bridge circuits were rebalanced to zero, where necessary, and the test was started.

5. The Test Bolt was torqued until the value of pre-tension was 20 to 40 percent above the desired value. The angle between the strain gage axis on the bolt and the axis of maximum bending was measured and recorded.

6. The external load was increased to the maximum value and released. This process was repeated until the pre-tension at zero load no longer shifted.

7. A test was run with approximately equally spaced increment of input load until the maximum load was reached. The load was then released and the no load value of pre-tension

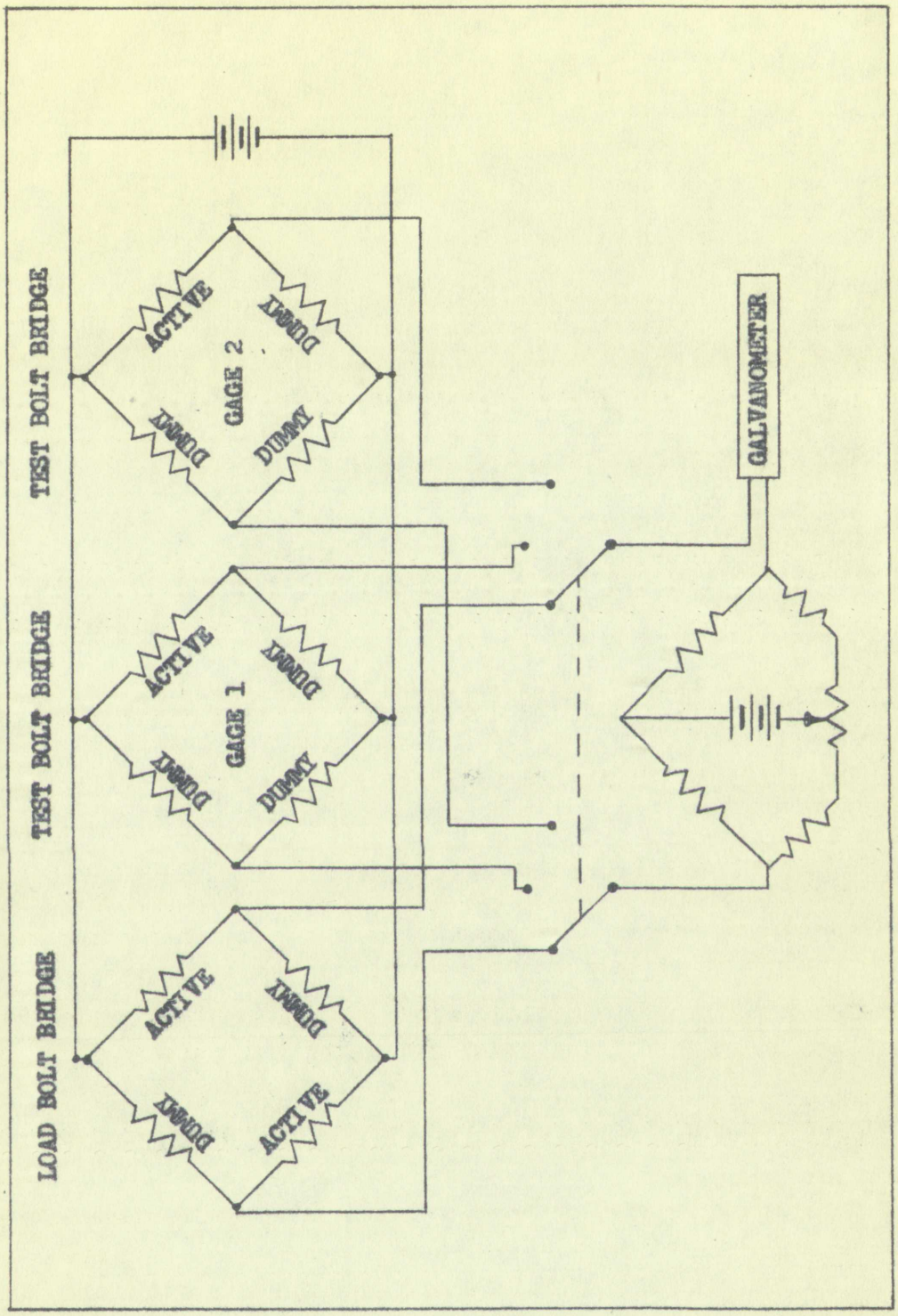

FIGURE 12

WIRING DIAGRAM OF TEST ARRANGEMENT

rechecked. If any appreciable shift had occurred, the test was rerun.

8. The Test Bolt was loosened and all of the gage readings rechecked to make sure no appreciable zero shifts had occurred during the test. If an appreciable shift had occurred, the test was repeated. It was found that very few tests had to be repeated because of a shift in zero readings.

9. The Test Bolt was torqued to a new value of pre-tension and steps 5 through 8 were repeated. The battery voltages were checked frequently throughout the tests to make sure they remained equal.

rechecked. If any appreciable shift had occurred, the test was void.

8. The Test Bolt was loosened and all of the gage readings rechecked to make sure no appreciable zero shifts had occurred during the test. If an appreciable shift had occurred, the test was repeated. It was found that very few tests had to be repeated because of a shift in zero readings.

9. The Test Bolt was torqued to a new value of pre-tension and steps 5 through 8 were repeated. The battery voltages were checked frequently throughout the tests to make sure they remained equal.

CHAPTER IV

TEST RESULTS

The results obtained from the tests are presented in this chapter. Tables of the raw data, as well as the method of reducing the data, are covered in Appendix C.

The results are shown graphically in this chapter. The system used for numbering the different tests is also presented. The final paragraphs contain some observations and conclusions concerning the test results.

Test numbering system. It was evident early in the program that it would be advantageous to have a system of numbering each test run that would tend to identify the run with a given flange. Therefore, every test run was identified by three numbers, each separated by a dash. The first number was used to identify the thickness of the flange being tested. The number selected was the number of eighths of an inch in the thickness of the flange. That is, a 7 for the first number would identify a 0.88 inches flange thickness. The second number was used to identify the amount of eccentricity between the load path and the Test Bolt centerline. Since only three different eccentricity ratios were tested, these were identified at 1, 2, and 3. Number 1 represented the greatest eccentricity and number 3 the least. The third number of the three digit identifying number represented the test run on the particular flange identified by the previous two numbers. These were numbered consecutively from 1 to 4, there being four runs at different bolt pre-tensions on each flange. The higher the number, the greater the pre-tension. Thus, a complete identifying number of 4-3-4 would identify a 0.50 inch thick flange, with the least eccentricity, and the test run would be the one with the highest pre-tension.

CHAPTER IV

TEST RESULTS

The results obtained from the tests are presented in this chapter. Tables of the raw data, as well as the method of reducing the data, are covered in Appendix C.

The results are shown graphically in this chapter. The system used for numbering the different tests is also presented. The final paragraphs contain some observations and conclusions concerning the test results.

Test numbering system. It was evident early in the program that it would be advantageous to have a system of numbering each test run that would tend to identify the run with a given flange. Therefore, every test run was identified by three numbers, each separated by a dash. The first number was used to identify the thickness of the flange being tested. The number selected was the number of eighths off an inch in the thickness of the flange. That is, a 7 for the first number would identify a 0.88 inches flange thickness. The second number was used to identify the amount of eccentricity between the load path and the Test Bolt centerline. Since only three different eccentricity ratios were tested, these were identified as 1, 2, and 3. Number 1 represented the greatest eccentricity and number 3 the least. The third number of the three digit identifying number represented the test run on the particular flange identified by the previous two numbers. These were numbered consecutively from 1 to 4, there being four runs at different bolt pre-tensions on each flange. The higher the number, the greater the pre-tension. Thus, a complete identifying number of 4-3-4 would identify a 0.50 inch thick flange, with the least eccentricity, and the test run would be the one with the highest pre-tension.

Reduction of test data. The graphs shown in Figures 13 through 21 represent the results of tests on the nine Test Flanges. The left-hand portion of each graph is a plot of the resulting axial bolt load versus the input load. These curves pass through the origin of the graph only for zero pre-tension on the Test Bolt. Thus the points on the graph for zero input load represent the axial load resulting from the torque applied to the Test Bolt. The right-hand portion of each graph is a plot of the maximum bending moment induced at the head of the bolt versus the input load. A small cross-section drawing to scale of the flange tested is also shown on each graph. (Detailed drawings of the Test Flanges may be found in Appendix B.)

The graphs shown in Figures 22 through 24 are plots of maximum stress versus input load for the different flanges. The data for these graphs were obtained by adding the maximum bending stress to the axial tensile stress.

Preliminary tests were conducted on all of the 0.25 inch thick flanges to determine the yield load of each flange since the flange stress in some cases was near the yield strength. The actual tests were carried to a load below the yield strength of the flange so that no permanent set would occur in any of the flanges. This resulted in the lowered input loads on flanges 2-1 and 2-2.

Discussion of test results. A study of the results obtained on the nine Test Flanges revealed the following:

1. The plot of the induced axial Test Bolt load versus the input load for each test run was comprised of three portions: a first portion with a relatively small and constant slope; a second portion with a gradually increasing slope; and a third portion with a relatively large and approximately constant slope.

2. The plot of the induced bending moment versus the input load on many of the Test Bolts was also comprised of three portions: a first portion with a relatively small and con-

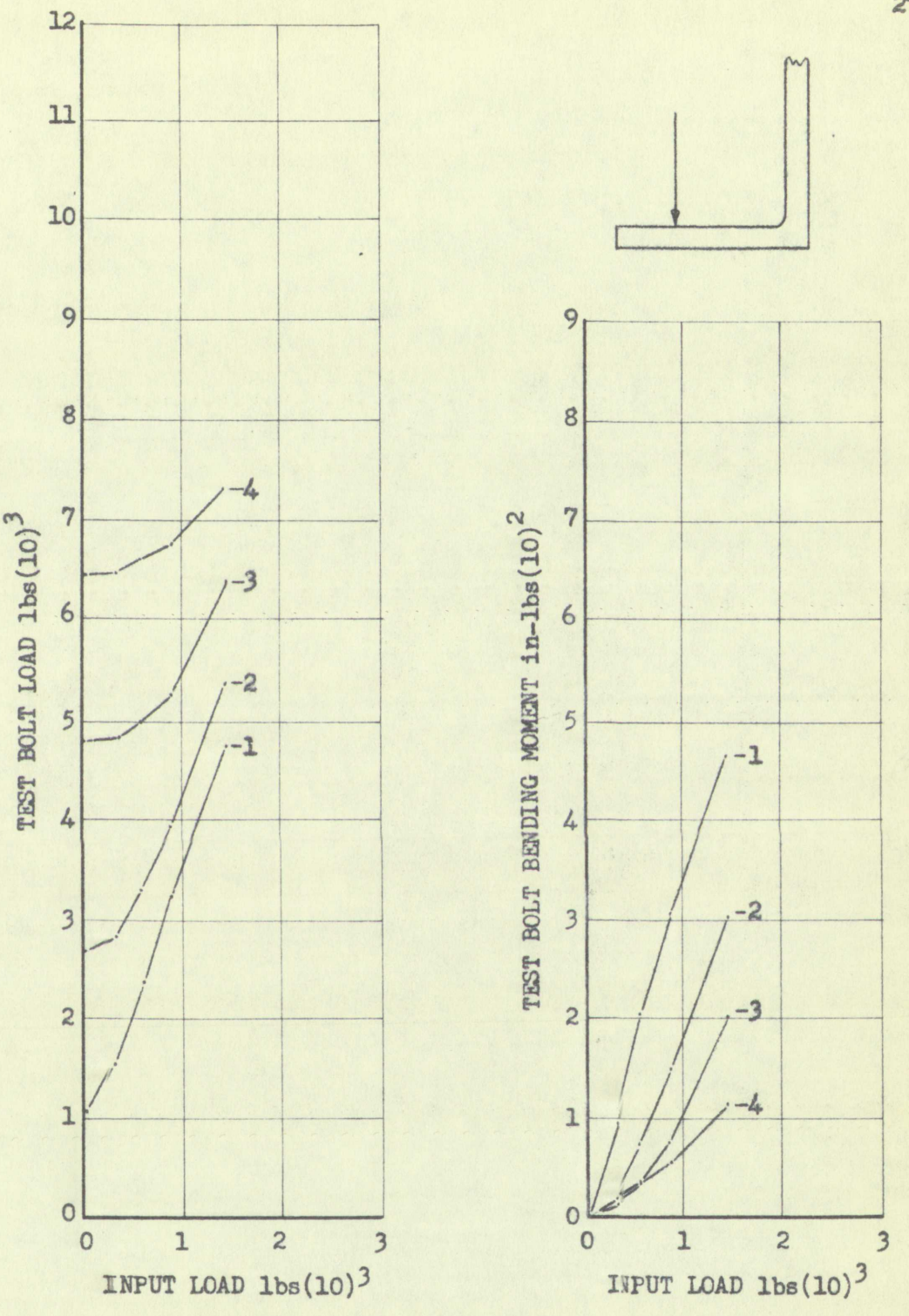

FIGURE 13

TEST FLANGE 2-1, BOLT TENSILE AND BENDING LOADS

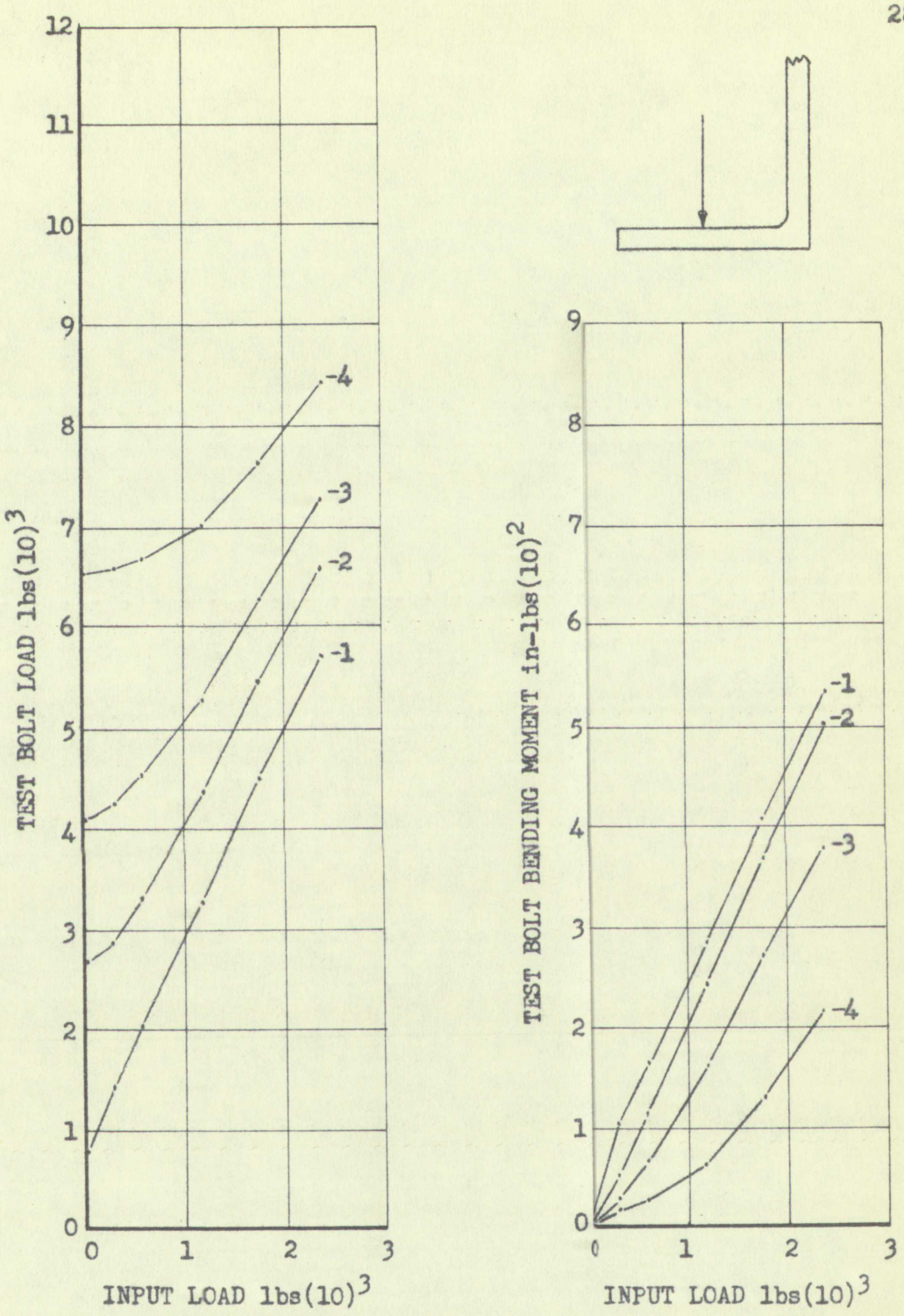

FIGURE 14

TEST FLANGE 2-2, BOLT TENSILE AND BENDING LOADS

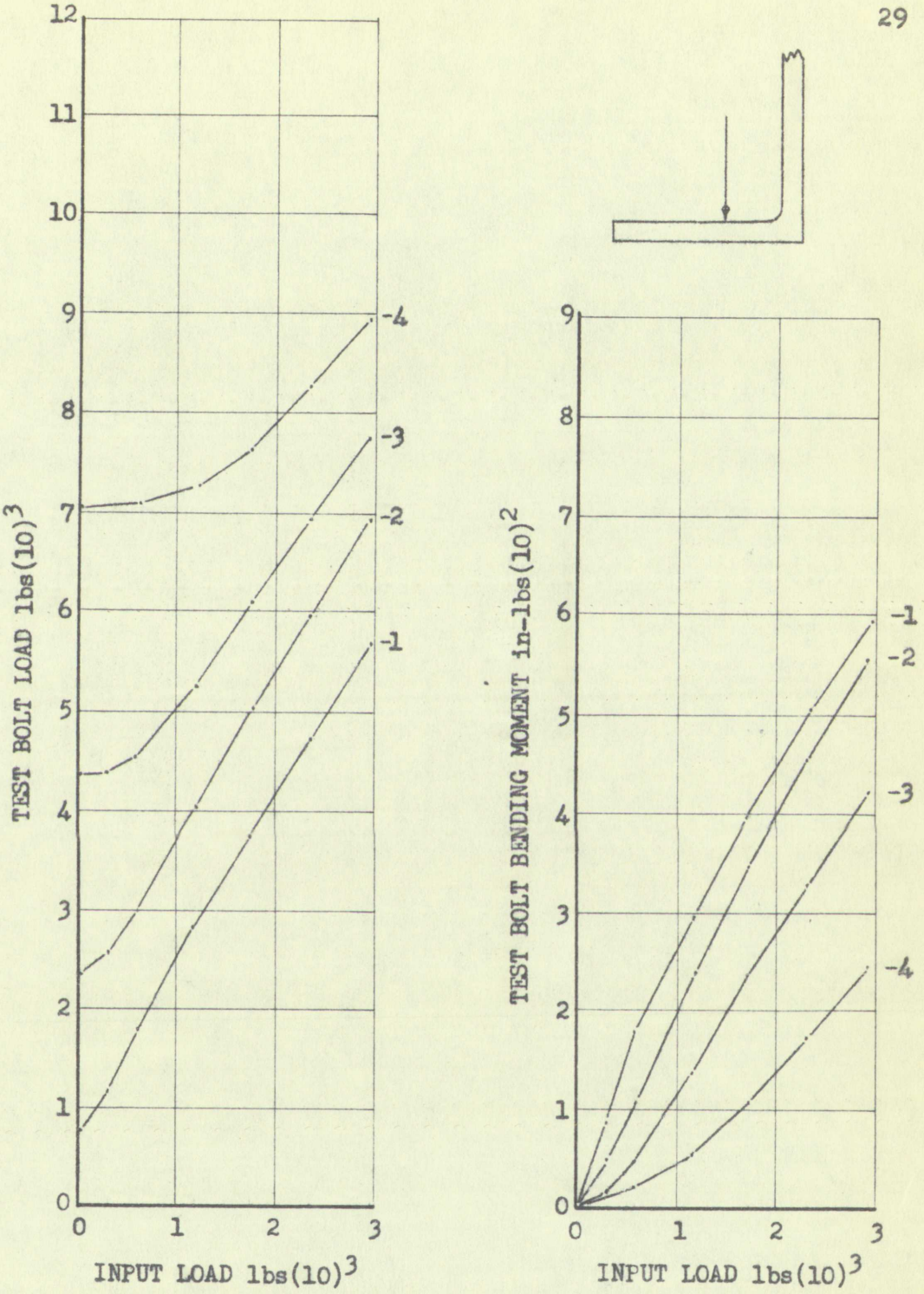

FIGURE 15

TEST FLANGE 2-3, BOLT TENSILE AND BENDING LOADS

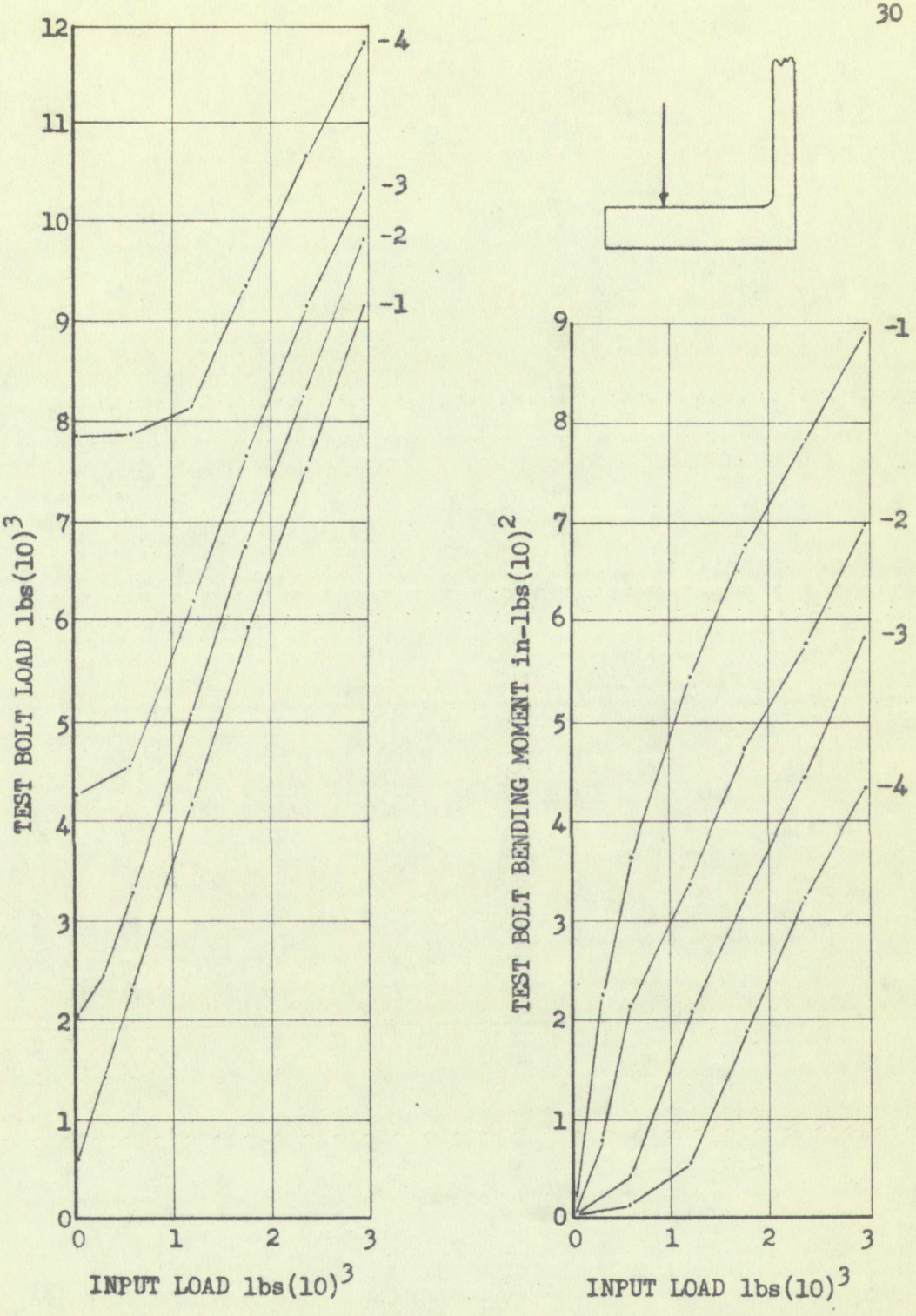

FIGURE 16

TEST FLANGE 4-1, BOLT TENSILE AND BENDING LOADS

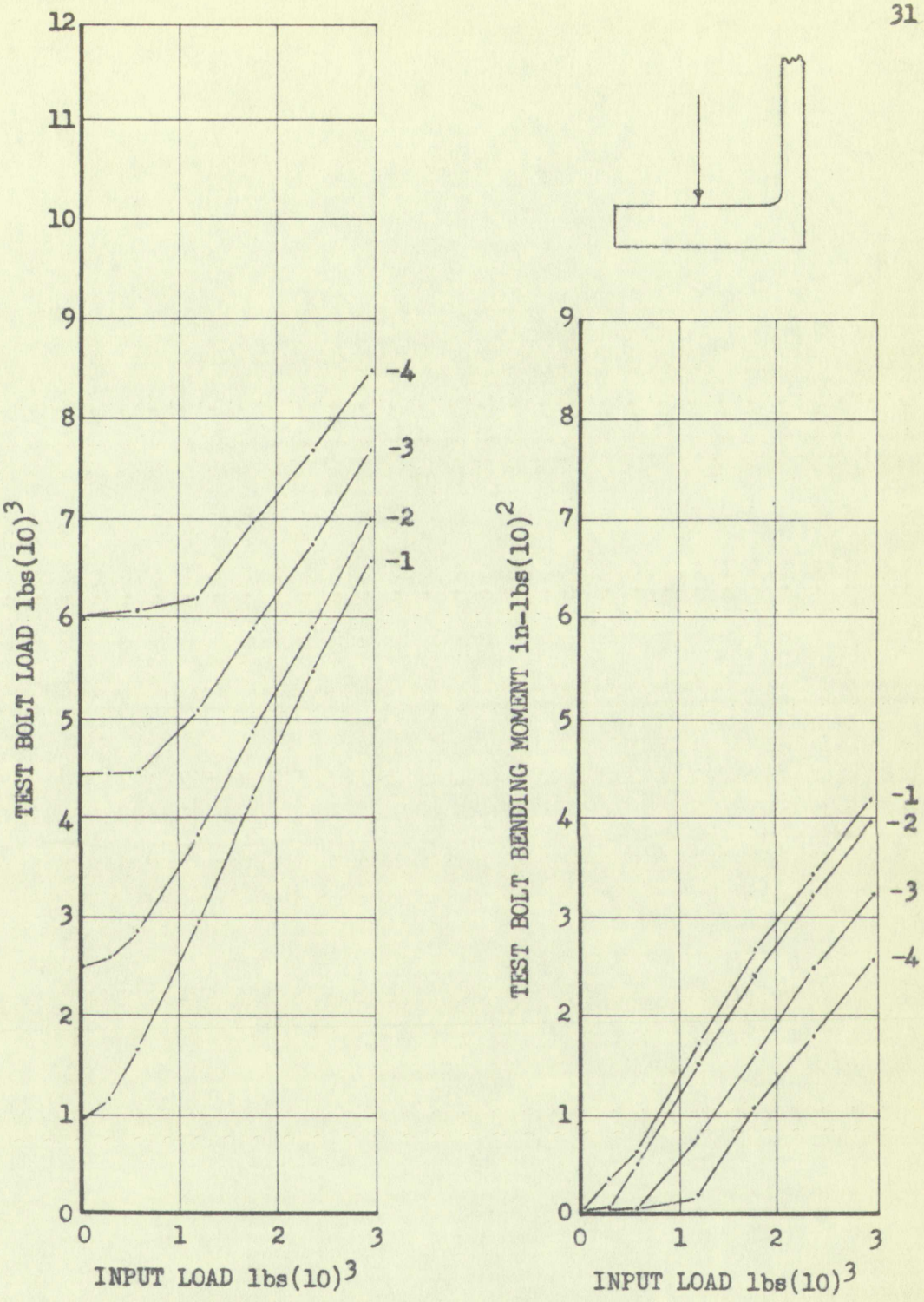

FIGURE 17

TEST FLANGE 4-2, BOLT TENSILE AND BENDING LOADS

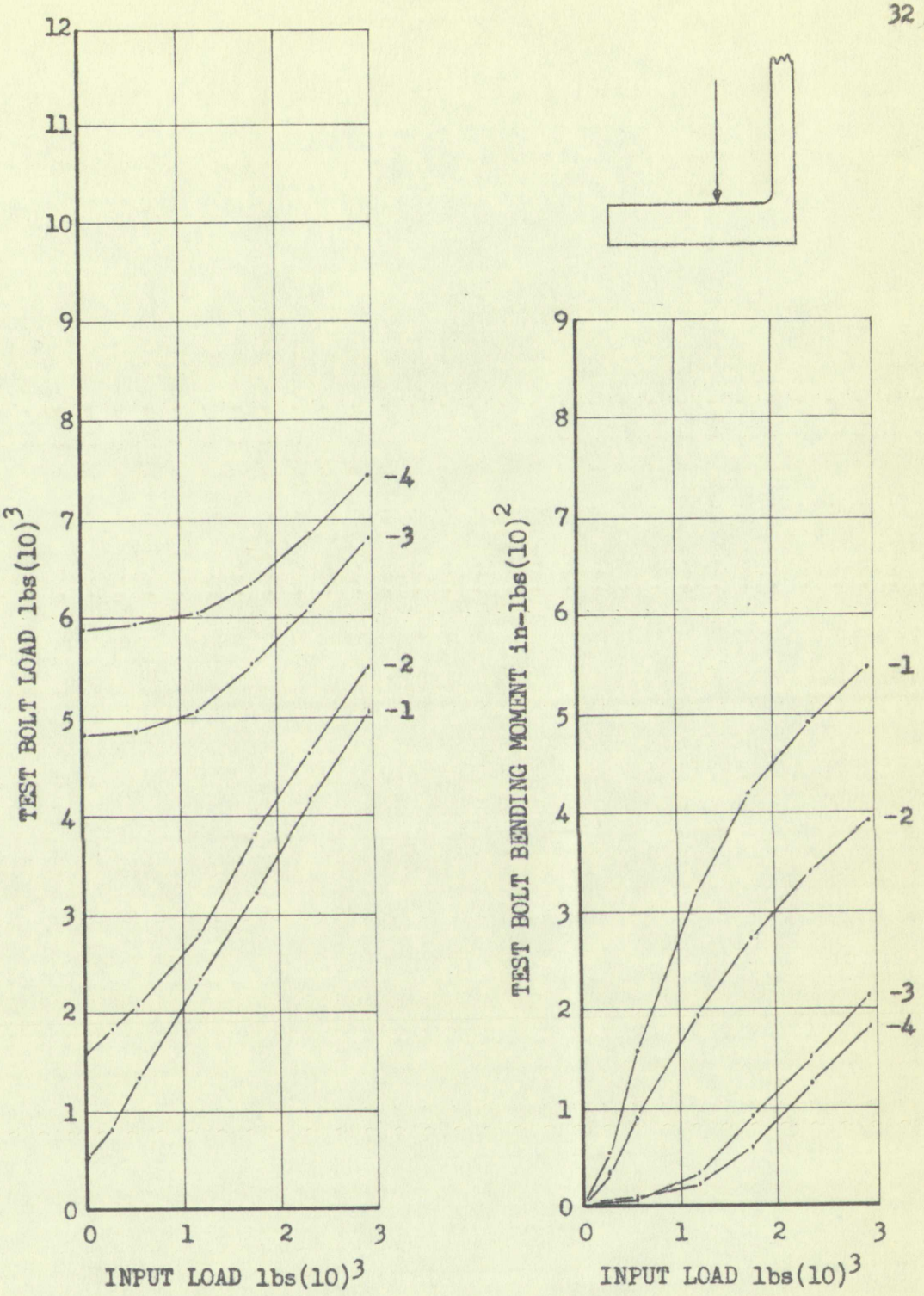

FIGURE 18

TEST FLANGE 4-3, BOLT TENSILE AND BENDING LOADS

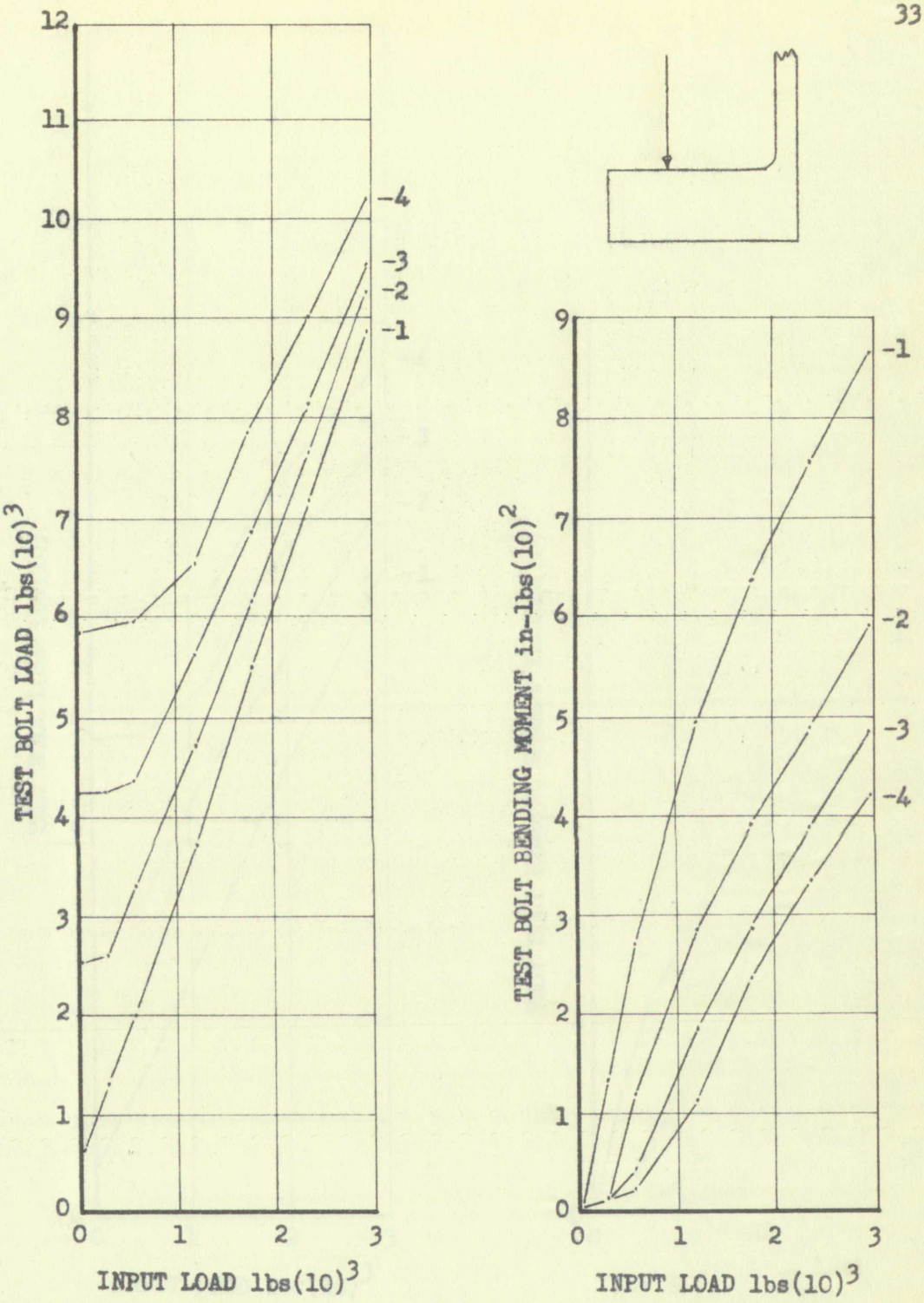

FIGURE 19

TEST FLANGE 7-1, BOLT TENSILE AND BENDING LOADS

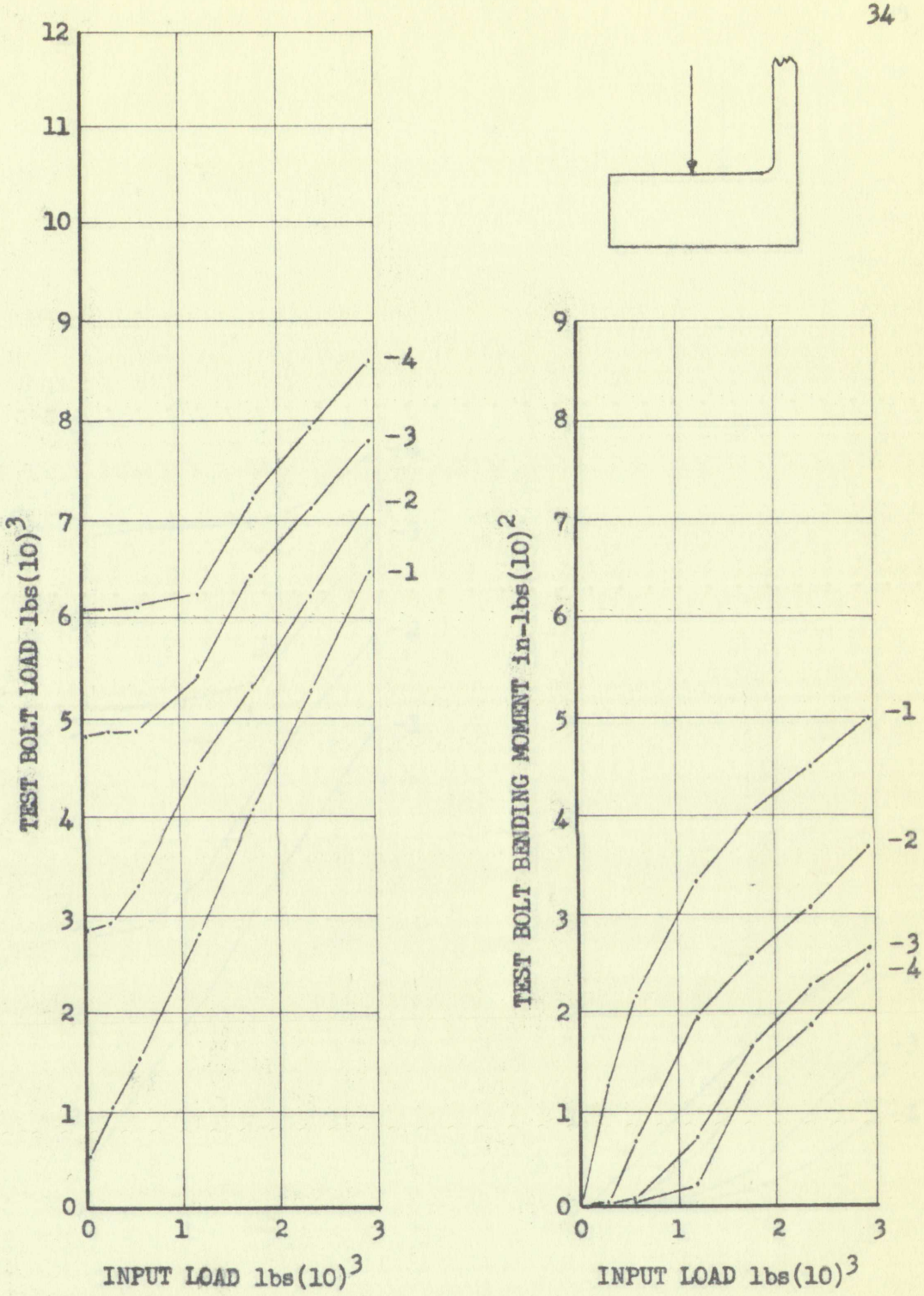

FIGURE 20

TEST FLANGE 7-2, BOLT TENSILE AND BENDING LOADS

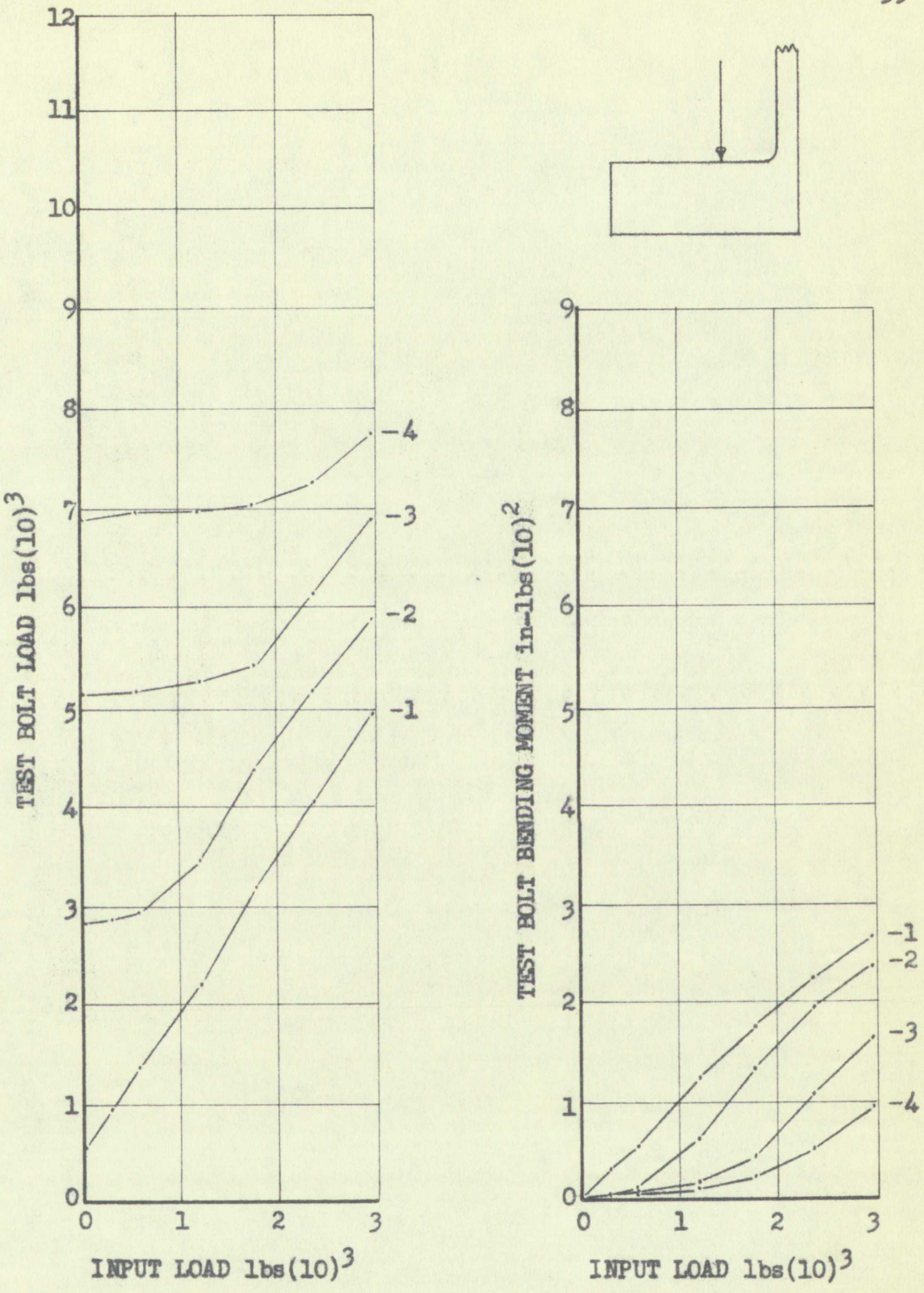

FIGURE 21

TEST FLANGE 7-3, BOLT TENSILE AND BENDING LOADS

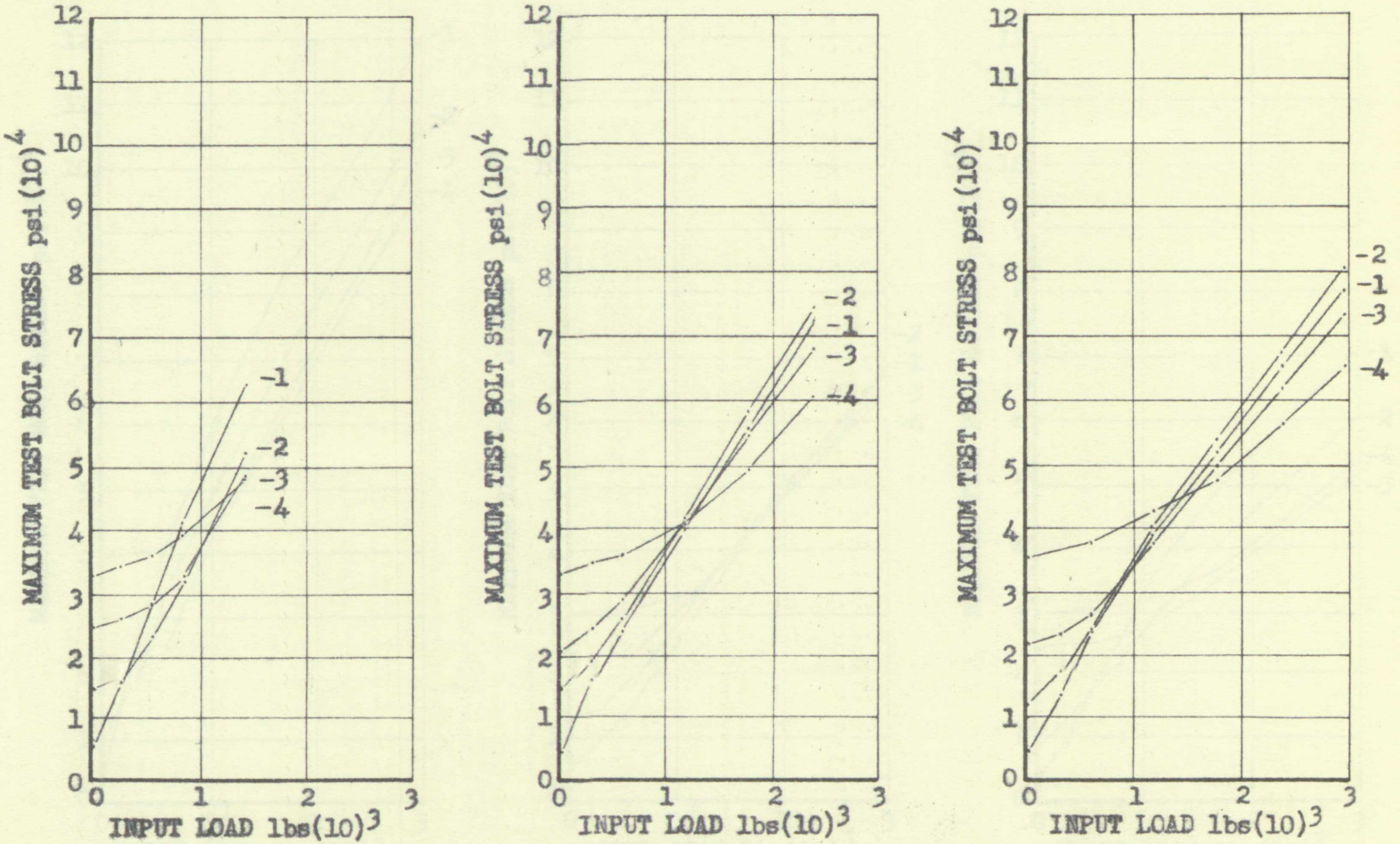

FIGURE 22

MAXIMUM TEST BOLT STRESS VERSUS INPUT LOAD

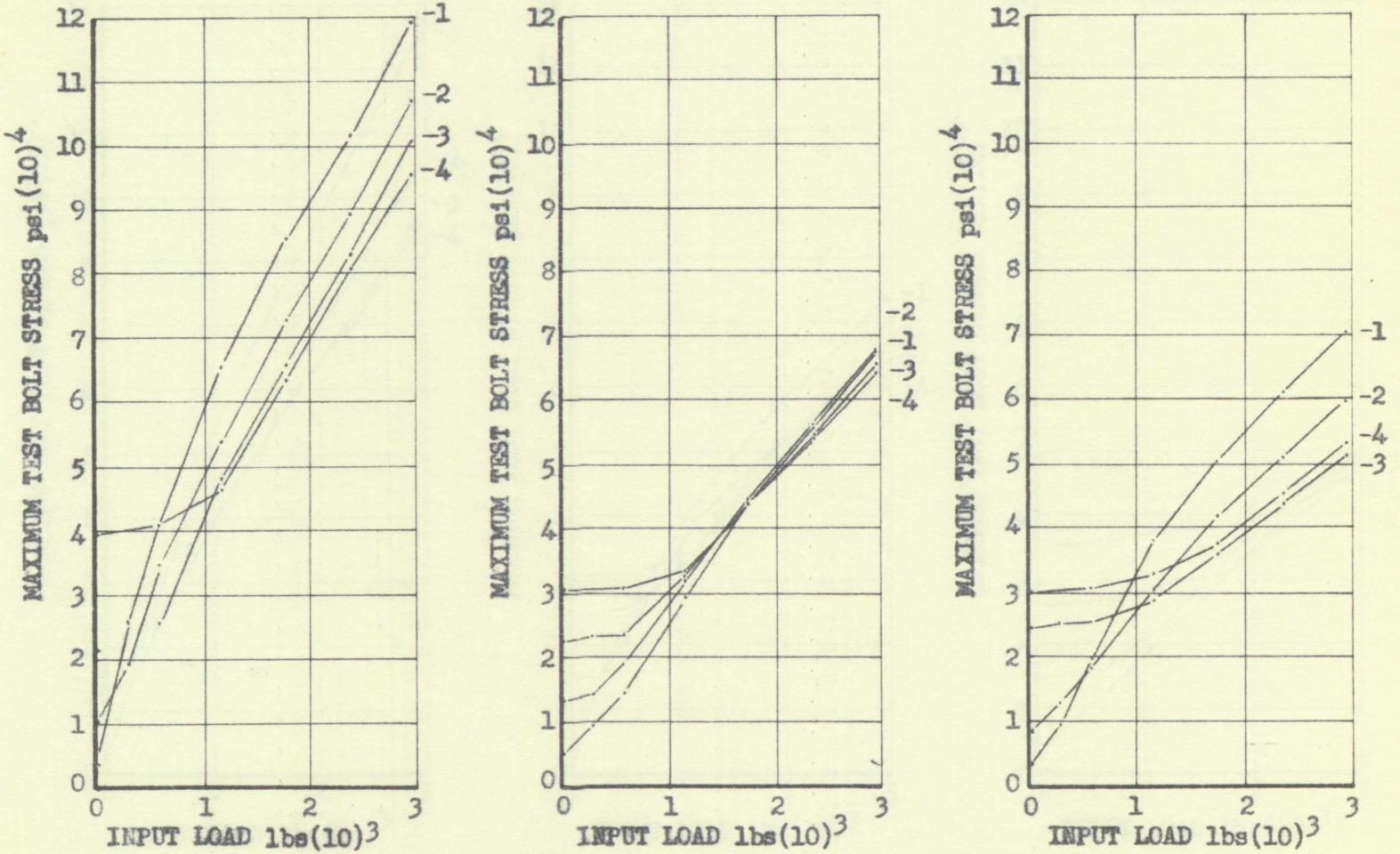

FIGURE 23

MAXIMUM TEST BOLT STRESS VERSUS INPUT LOAD

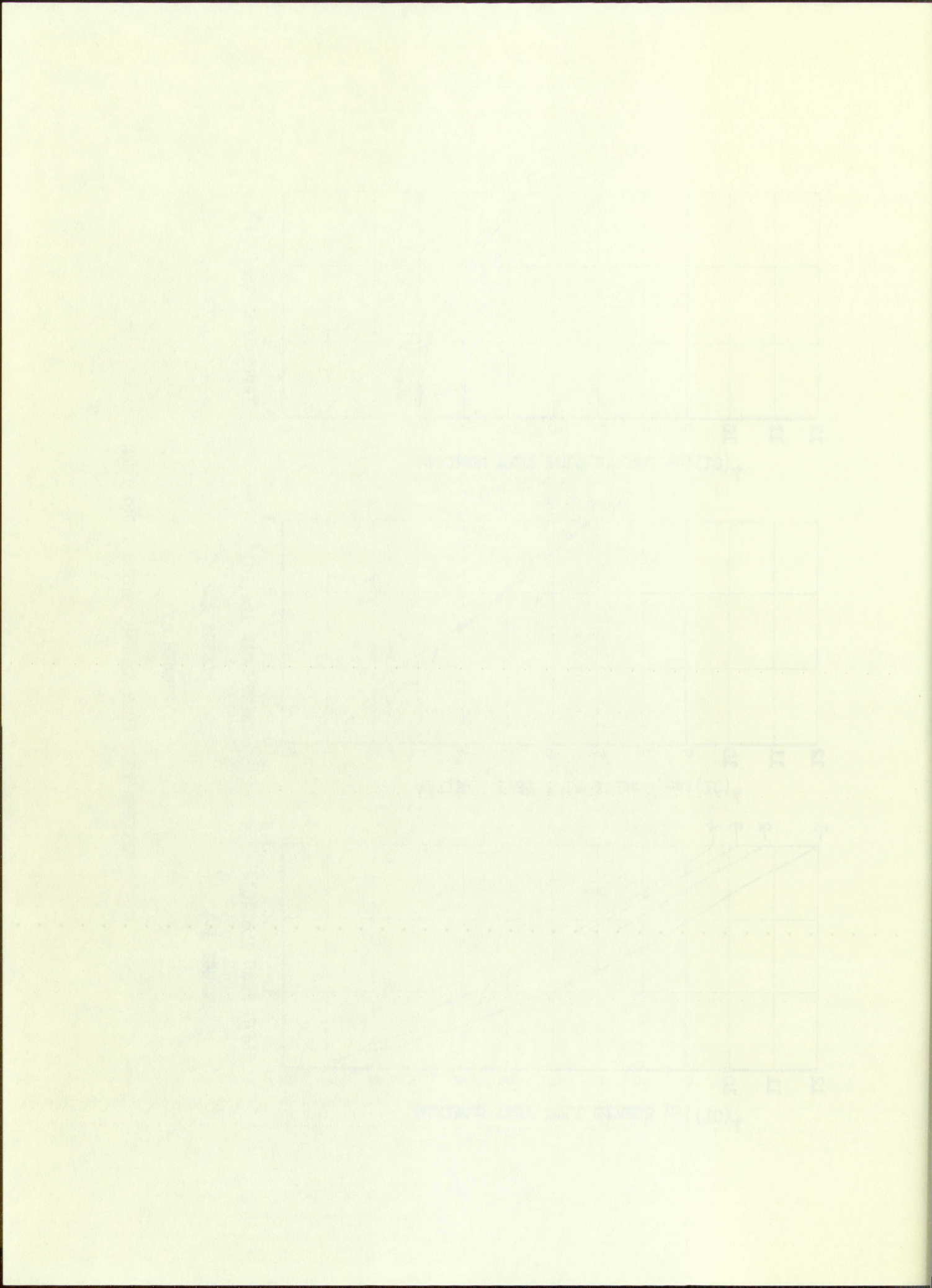

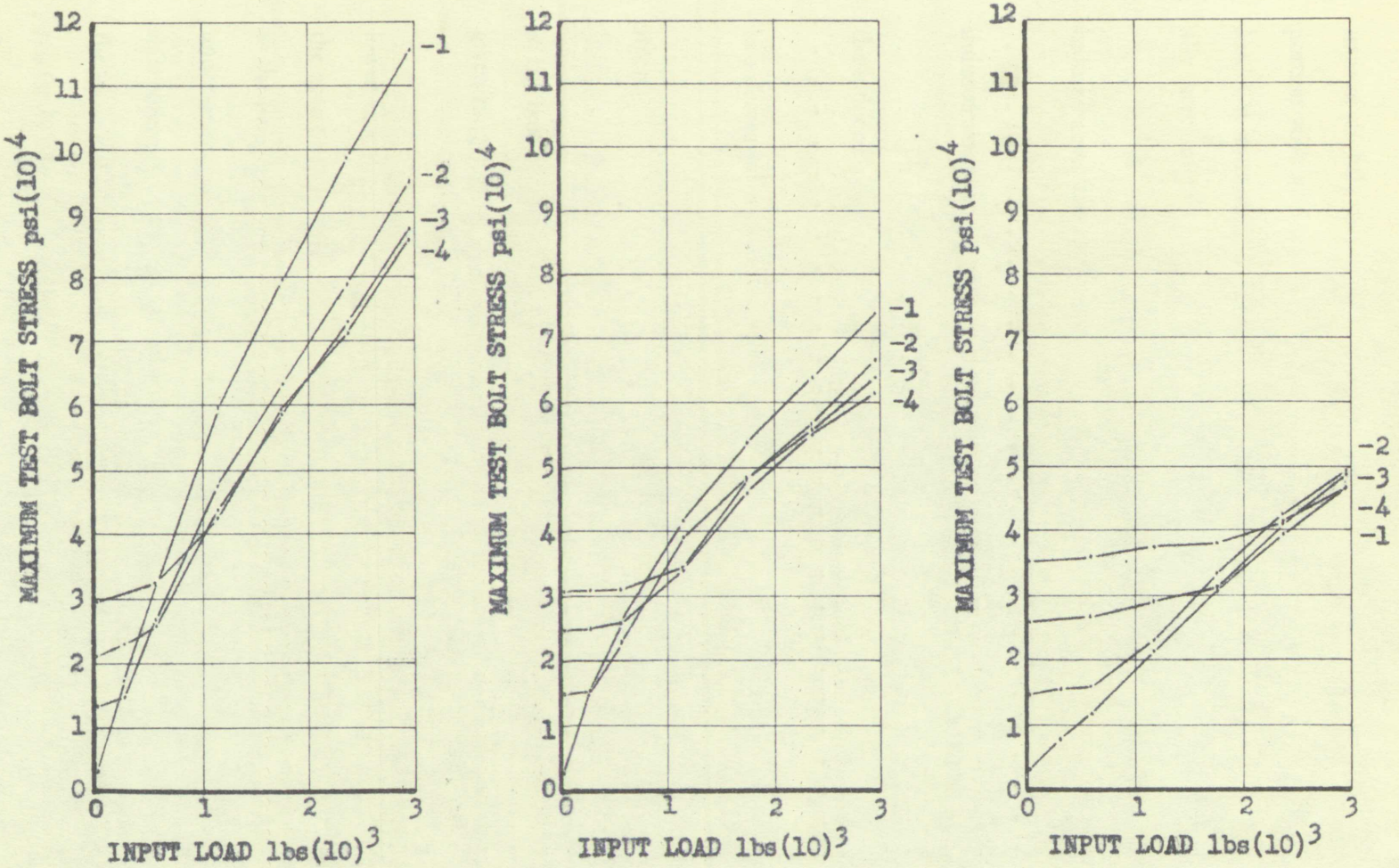

FLANGE 7-1 FLANGE 7-2 FLANGE 7-3

FIGURE 24

MAXIMUM TEST BOLT STRESS VERSUS INPUT LOAD

stant or slightly increasing slope; a second portion with a gradually increasing slope; and a third portion with an initially relatively steep slope that gradually decreased with increasing input load. On some of the test runs the first two portions seemed to blend into one portion of gradually increasing slope.

3. With increasing initial bolt pre-tension, the first portion of the curves for both induced axial load and induced bending became proportionately larger.

4. With increasing initial bolt pre-tension, the third portion of the curves for both induced axial load and induced bending became proportionately smaller.

5. With increasing initial bolt pre-tension, the slope of the third portion of both the induced axial load and induced bending curves was decreased.

6. Decreasing the eccentricity between the external load and the Test Bolt resulted in a decreased maximum bolt stress.

7. Increasing the thickness of the flange resulted in a decreased maximum bolt stress.

8. Increasing the pre-tension on the Test Bolt resulted in a decreased stress range in the bolt, (the difference between maximum and minimum stress due to external load) for a given range of external load, although not necessarily a reduction in the maximum stress.

9. The three portions of each curve indicate the following about the pressure on the lower face of the flange: 1) the first portion of the curve represents that phase of the test when the area under pressure is constant, but the center of pressure is moving toward the outer edge of the flange, 2) the second portion of the curve represents that phase of the test when the area under pressure is decreasing (as a result of flange separation from the base) and both the area and the center of pressure are moving toward the outer edge of the flange, and 3) the third portion of the curve represents that phase of the test when the area under pressure has become small but relatively constant, and both the area and the center of pressure are near the outer edge of the flange.

Summary. A study of the test results showed that generally consistnt trends were obtained for the three main parameters investigated, namely 1) the effect of nitial bolt pre-tension; 2) the effect of flange thickness; and 3) the effect of eccentricity betwen the external load and the Test Bolt.

The tests also bear out the contention of many designers that increasng flange thickness and decreasing load path eccentricity in a flanged joint will decrease bolt stresses.

The tests showed that increasing the bolt pre-tension will decrease he stress range for a given range of external load. However, the increased pre-tension will not necessarily decrease the maximum stress.

CHAPTER V

DERIVATION OF FORMULAS

This chapter discusses the derivation of four sets of formulas which describe the behavior of a typical flanged joint. Each set is based on a different theory. The first derivation is for a Rigid Flange Theory, the second for a Flexible Flange Theory, and the third for a Modified Rigid Flange Theory. The fourth derivation is based on handling the data by the methods of Dimensional Analysis. The detailed derivations of the formulas for the different theories are contained in Appendices D, E, and F.

The development of each system of formulas opens with the assumption made for the derivation, presents the final derived formulas, and closes with a discussion of the results of using the formulas and the shortcomings of the theory. The chapter closes with a summary of the results obtained from the developed formulas.

I. RIGID FLANGE THEORY

Assumptions. This theory was based on the assumption that the flange would not bend. However, it was assumed that it would deform elastically on the lower face, due to compressive loads. It was further assumed that the base to which the flange was bolted would not bend or deform. In addition, the area of the flange was assumed to be relatively large compared to the area of the bolt. (No corrections were made for the hole in the flange in any of the derivations.)

Derived Formulas. The complete derivations of the formulas may be found in Appendix D, along with drawings of the flanges showing the dimensions involved. Appendix A

CHAPTER V

DERIVATION OF FORMULAS

This chapter discusses the derivation of four sets of formulas which describe the behavior of a typical flanged joint. Each set is based on a different theory. The first derivation is for a Rigid Flange Theory, the second for a Flexible Flange Theory, and the third for a Modified Rigid Flange Theory. The fourth derivation is based on handling the data by the methods of Dimensional Analysis. The detailed derivations of the formulas for the different theories are contained in Appendices D, E, and F.

The development of each system of formulas opens with the assumption made for the derivation, presents the final derived formulas, and closes with a discussion of the results of using the formulas and the shortcomings of the theory. The chapter closes with a summary of the results obtained from the developed formulas.

1. RIGID FLANGE THEORY

Assumptions. This theory was based on the assumption that the flange would not bend. However, it was assumed that it would deform elastically on the lower face, due to compressive loads. It was further assumed that the base to which the flange was bolted would not bend or deform. In addition, the area of the flange was assumed to be relatively large compared to the area of the bolt. (No corrections were made for the hole in the flange in any of the derivations.)

Derived Formulas. The complete derivations of the formulas may be found in Appendix D, along with drawings of the flanges showing the dimensions involved. Appendix A

contains the definitions of all symbols used.

The first problem was to determine formulas for the behavior of the flange due to the load produced by the pre-tension on the bolt. It was found that two cases existed, one when the bolt was located within the middle 1/3 of the flange, and the other when the bolt was not located within the middle 1/3 of the flange. The important thing to be determined was the compressive deformation of the flange at the bolt. The deformation, e_2, was needed for the other derivations. It was found, when the bolt was located between 1/3 d and 2/3 d, the deformation is equal to

$$e_2 = \frac{F_t}{Sd}\left(\frac{3\,(2b-d)^2}{d^2}+1\right). \tag{1}$$

When the bolt was located between 0 and 1/3 d, the deformation is equal to

$$e_2 = \frac{4\,F_t}{9\,bS}. \tag{2}$$

When the bolt was located between 2/3 d and d, the deformation is equal to

$$e_2 = \frac{4\,F_t}{9\,(d-b)\,S}. \tag{3}$$

It was then necessary to derive formulas for the relation between the external load F_1, the resulting bolt load F_2, the initial bolt pre-tension F_t, and the various dimensions of the flange, before the joint had started to open. The important thing determined was that the relation between the external load F_1 and the resulting bolt load F_2 was linear. In other words, only 2 points on the curve need be determined in order to draw the curve. Since one of the points may be taken as $F_2 = F_t$ when $F_1 = 0$, only one additional point must be determined. (It was found to be easier to determine this second point by using the derivation of the following paragraph and letting f, the distance from the outer edge of the flange to the point of opening, be equal to b, the distance from the outer edge of the flange to the bolt.)

Finally, it was necessary to derive formulas for the relation between F_2 and F_1 after

contains the definitions of all symbols used.

The first problem was to determine formulas for the behavior of the flange due to the load produced by the pre-tension on the bolt. It was found that two cases existed, one when the bolt was located within the middle 1/3 of the flange, and the other when the bolt was not located within the middle 1/3 of the flange. The important thing to be determined was the compressive deformation of the flange at the bolt. The deformation, e_b, was needed for the other derivations. It was found, when the bolt was located between 1/3t and 2/3t, the deformation is equal to

$$e_b = \frac{P}{24}\left(\frac{3\,(2b-d)^2}{d^2}+1\right)$$

When the bolt was located between 0 and 1/3 t, the deformation is equal to

$$e_b = \frac{4P_1}{9.85}$$

When the bolt was located between 2/3 t and t, the deformation is equal to

$$e_b = \frac{4P_1}{9\,(t-2)}$$

It was then necessary to derive formulas for the relation between the external load P_1, the resulting bolt load P_2, the initial bolt pre-tension P_i, and the various deformations of the flange, before the joint had started to open. The important thing determined was that the relation between the external load P_1 and the resulting bolt load P_2 was linear. In other words, only 2 points on the curve need be determined in order to draw the curve. Since one of the points may be taken as $P_2 = P_1$ when $P_1 = 0$, only one additional point must be determined. It was found to be easier to determine this second point by using the derivation of the following paragraph and letting λ, the distance from the outer edge of the flange to the point of opening, be equal to b, the distance from the outer edge of the flange to the bolt.

Finally, it was necessary to derive formulas for the relation between P_2 and P_1 after

the flange had started to open from the base. In this case it was necessary to solve for another force F_3, the resulting force acting on the base of the flange. In the derivations of Appendix D, it was determined that

$$F_1 = \frac{Sf^2(e_1+e_2)\left[gf-\left(b+\frac{RK}{b}\right)-\frac{2R}{fbs}\right]-\frac{R}{b}(e_1+e_2)[2(b-f)-SKf^2]}{SKf^2\left[gf-\left(b+\frac{RK}{b}\right)-\frac{2R}{fbs}\right]-\left(b-a+\frac{RK}{b}\right)[2(b-f)-SKf^2]}, \tag{4}$$

$$F_3 = \frac{Sf^2(KF_1-e_1-e_2)}{2(b-f)-SKf^2}, \tag{5}$$

$$F_2 = F_1+F_3, \tag{6}$$

and

$$M_b = \left(KF_2+\frac{2F_3}{Sf}-e_1-e_2\right)\frac{R_b}{b}. \tag{7}$$

In these equations, g has the value of 1/3.

The two results that were desired were the expressions for F_2 and M_b. To solve a typical problem, a given value of f is substituted into equation (4) along with e_2 from equation (1), (2), or (3). The values of F_1 and f are substituted into equation (5) to obtain F_3. The force F_2 is then obtained from F_1 and F_3 by equation (6). The bending moment is determined by substituting the values of F_2, F_3 and f into equation (7).

Results. The results of applying these formulas to a given set of conditions may be found in Figure 25. The calculations were based on the conditions of test 7-2-3. As can be seen, neither the tensile load F_2 nor the bending moment M_b agree with test results in the third portion of each curve (the part with the relatively steep slope). The first portions are in reasonable agreement. Of course, the calculated bending moment, which is a function of F_2 and F_1, could not be expected to agree well when F_2 and F_1 are incorrect.

Also plotted on the tensile load portion of the graph is a line with the slope of a/b. This line represents the calculated relation between F_1 and F_2 when it is assumed that there is no

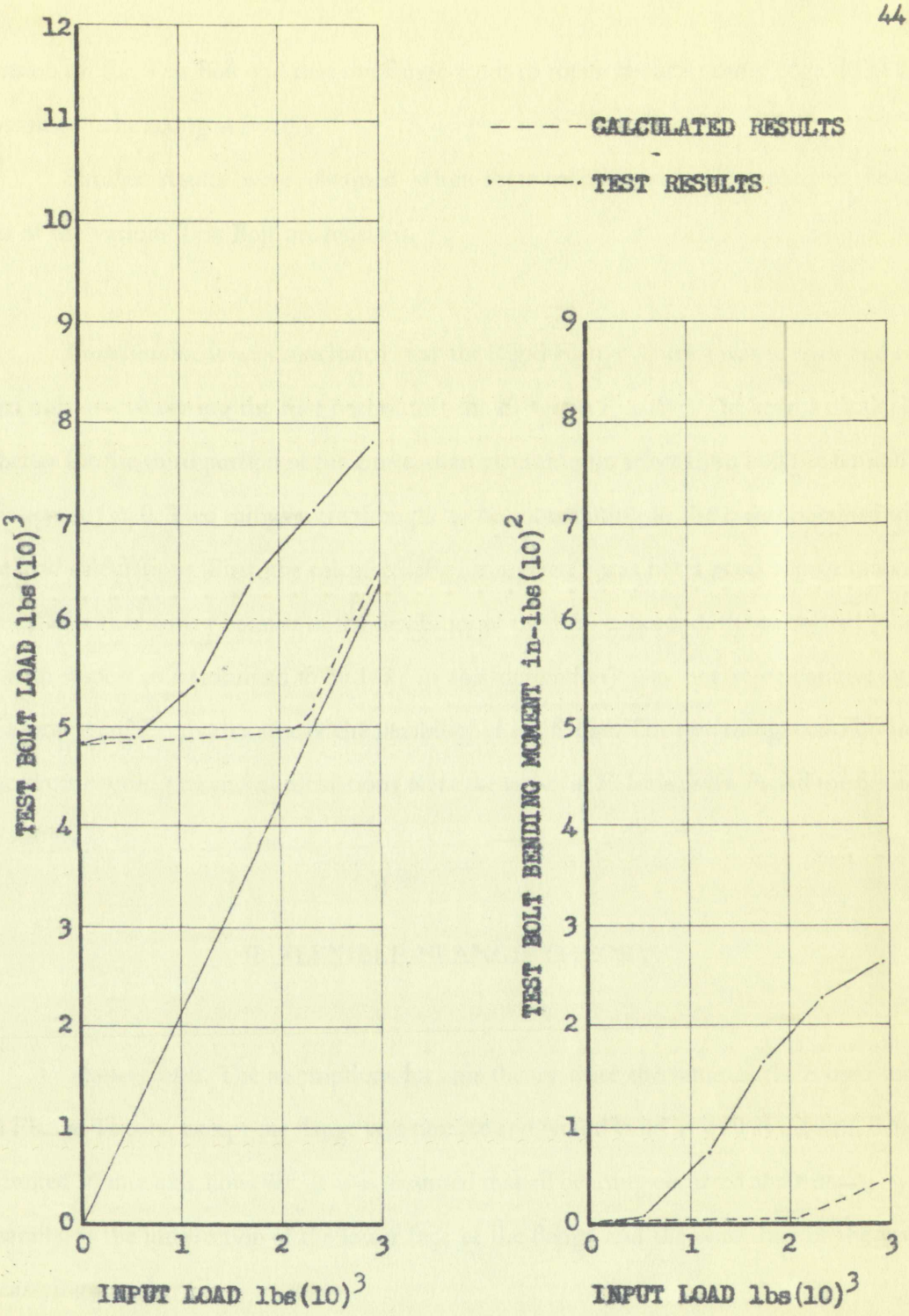

FIGURE 25

CALCULATED RESULTS OF RIGID FLANGE THEORY - FLANGE 7-2

pre-tension on the Test Bolt and that the flange tends to rotate about its outer edge. (The force F_3 is assumed to be acting at $f = 0$.)

Similar results were obtained when these calculations were applied to the other flanges at the various Test Bolt pre-tensions.

Conclusions. It was concluded that the Rigid Flange Theory was in error and could be used only in calculating the first portion of the F_2 versus F_1 curve. The results obtained are little better for the third portion of the curve, than assuming no effect from bolt pre-tension and that F_3 acts at $f = 0$. Two things were thought to be contributing to the errors obtained in the tensile load calculations. First, the calculated F_3 for a given f was not a good approximation of the true F_3 for that same f because of the flexibility of the flange. Second, the calculated location of F_3 with respect to f (assumed to be $1/3\ f$ in this derivation) was not representative of the correct location of F_3, also because of the flexibility of the flange. The two things contributing to the incorrect bending moment calculations were the errors in F_2 for a given F_1 and the flexibility of the flange.

II. FLEXIBLE FLANGE THEORY

Assumptions. The assumptions for this theory were the same as those used for the Rigid Flange Theory, except the flange was flexible and would bend as well as deform. Bending was limited to one axis however. It was assumed that all bending occurred about an axis which was parallel to the intersection of the lower face of the flange and the outer face of the vertical load carrying member.

Derived formulas. The complete derivation of the formulas may be found in Appen-

dix E along with a drawing showing the dimensions involved.

Since the equations derived were complicated, all were reduced to simple forms by combining terms into constants. In this case the desired formulas were

$$F_1 = \frac{A_{11} A_{13} - A_7 A_{14}}{A_{10} A_{14} - A_8 A_{11} A_{12}} , \tag{8}$$

$$F_4 = \frac{F_1 A_8 A_{12} + A_{13}}{A_{14}} , \tag{9}$$

$$F_2 = (F_1 + F_4) A_8 , \tag{10}$$

and

$$M_b = R_b (F_2 A_{15} + F_4 A_{16} + A_{17}) . \tag{11}$$

These equations may be solved for any given f to obtain the desired relations between F_1 and F_2, and F_1 and M_b. The definitions of the various constants may be found in Appendix A.

Results. The results of applying these calculations to test 7-2-3 were little better than those obtained with the Rigid Flange Theory. A plot of the results may be found in Figure 26. The center portion of the tensile load curve, the transition from the low slope portion to the steep slope portion, was better than that obtained by the Rigid Flange Theory, but the remainder was approximately the same. In addition the slope of the bending moment curve is nearer the correct angle although the influence of the incorrect F_2 and F_1 still tend to produce poor results. To check this, the correct F_2 and F_1 from test results, along with the calculated f, were substituted into equation (11) to obtain the third curve shown on the plot of Bending Moment versus Input Load. This gives a better approximation of the actual bending moment curve. When calculations were applied to the thinner flanges, it was found that erratic results were obtained. This was caused by the fact that the flexure curve of the beam from 0 to b had a great enough change of slope that the base line would be forced to pass below the point zero as shown in Figure 41, page 109. This presented serious complications since most of the equations of Appendix E would then have to be re-derived because the lower limit of integration was no longer zero.

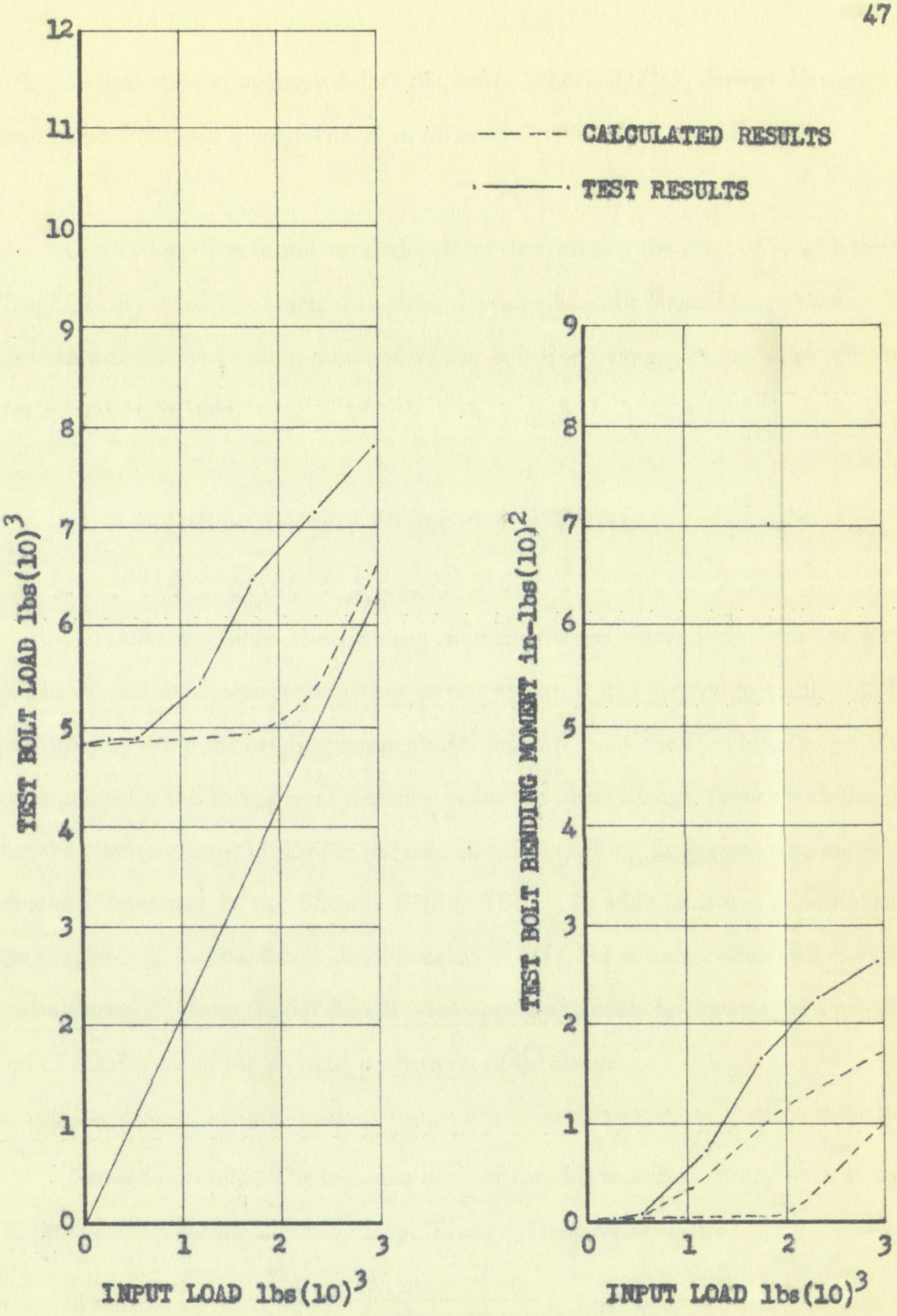

FIGURE 26

CALCULATED RESULTS OF FLEXIBLE FLANGE THEORY - FLANGE 7-2

No further derivations were attempted since the test run checked, 7-2-3, showed the theory to be little better than the Rigid Flange Theory in those areas where both could be applied.

Conclusions. The formulas developed for determining the value of F_2 with the Flexible Flange Theory were little better than those developed for the Rigid Flange Theory. However, the formula for the bending moment on the bolt does show promise when the correct values of F_2 and F_1 are used.

III. MODIFIED RIGID FLANGE THEORY

Assumptions. Since the bending moment M_b as determined from the Flexible Flange Theory, did show promise of giving correct results, it was decided to modify the Rigid Flange Theory by using the bending moments M_b and M_f from the Flexible Flange Theory. The assumptions for this theory were the same as for the Rigid Flange Theory with the exception that the relative change in slope at the bolt and the attaching flange was determined from the equations developed in the Flexible Flange Theory. In addition it was assumed that the force on the lower face of the flange, F_4 did not act at $1/3\,f$, but at some point equal to gf where g was to be determined from the test data. It was hoped that g could be shown to be a predictable function of f and some of the physical parameters of the flange.

Derived Formulas. The formulas derived for this modified theory were of similar form to those derived for the Flexible Flange Theory. These formulas are

$$F_1 = \frac{A_{13}\,A_{19} - A_7\,A_{20}}{A_{18}\,A_{20} - A_{12}\,A_{19}}\,, \tag{12}$$

$$F_4 = \frac{F_1\,A_{12} + A_{13}}{A_{20}}\,, \tag{13}$$

$$F_2 = F_1 + F_4\,, \tag{14}$$

and

$$M_b = R_b (F_2 A_{15} + F_4 A_{16} + A_{17}) . \tag{15}$$

Results. For each value of f, it was necessary to calculate a g value that would result in a calculated F_2 on the experimentally determined curve of F_2 versus F_1. The flange selected for comparison was flange 7-2. For this theory, results are shown in Figure 27 for test runs 7-2-1 through 7-2-4. In this case the calculated points for F_2 versus F_1 correspond to the test results since they were forced to by the proper choice of g. The resulting bending moment versus input load curves were a reasonably good approximation of the test data. Figure 28 shows the relation between g and f for each of the four tests shown in Figure 27. The same methods were used to calculate results for other flanges. The plots of bending moment versus input load were always a reasonable approximation of the results obtained from the tests, and the plots of g versus f were of the same general form. However, no predictable pattern governing the shape of the g versus f curves could be determined.

Conclusions. If it were possible to determine the relation between g and f, this theory would give satisfactory results. The solution for the bending moment on the Test Bolt is reasonably good, provided the proper solution of the relation between F_2 and F_1 has already been determined. However, since this relation is not known, it may be concluded that this theory is also unsatisfactory.

IV. DIMENSIONAL ANALYSIS

Since the previous derivations did not give satisfactory results for the relation between F_2 and F_1 after the flange had started separating from the base, it was decided to try to express

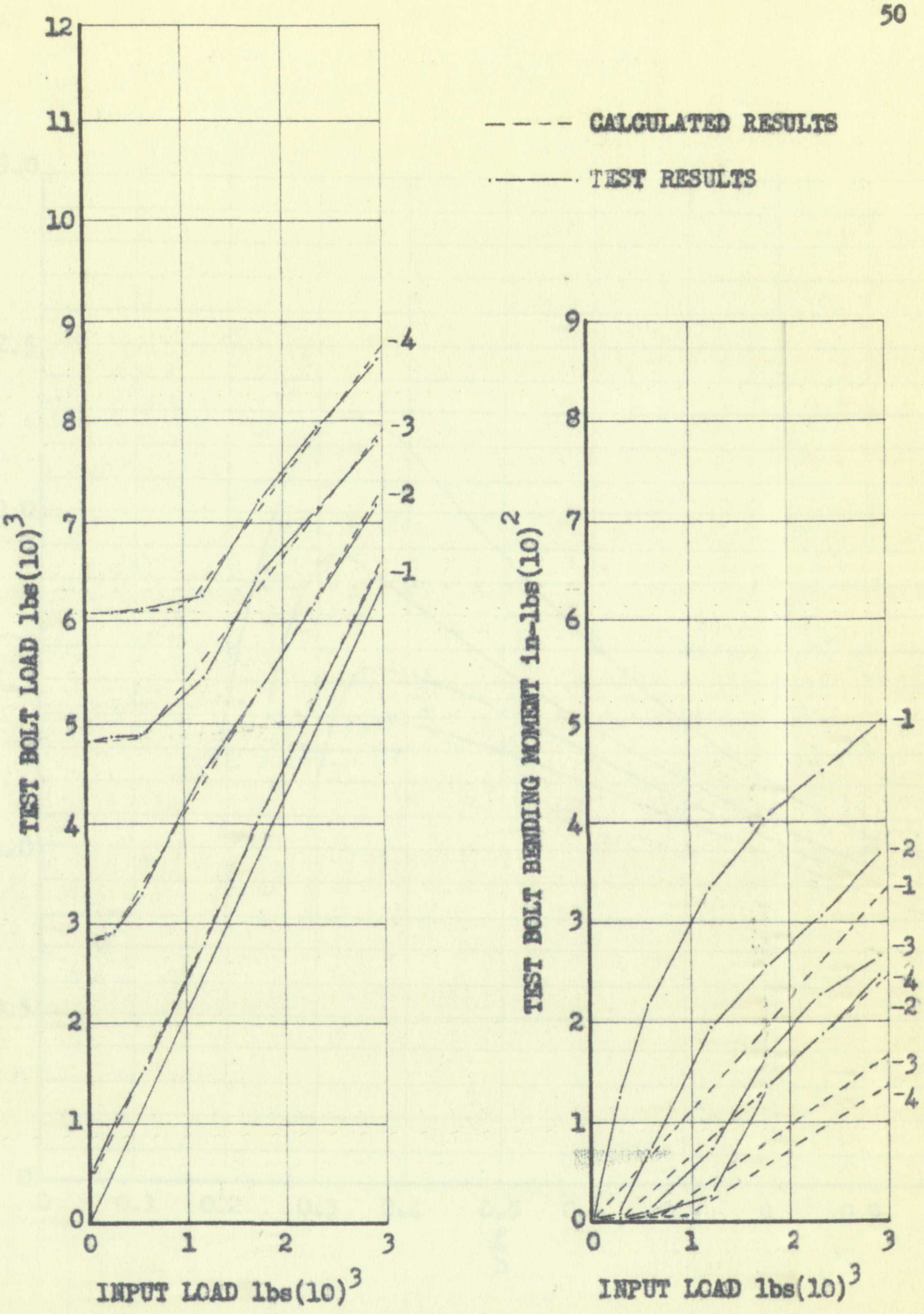

FIGURE 27

CALCULATED RESULTS OF MODIFIED RIGID FLANGE THEORY - FLANGE 7-2

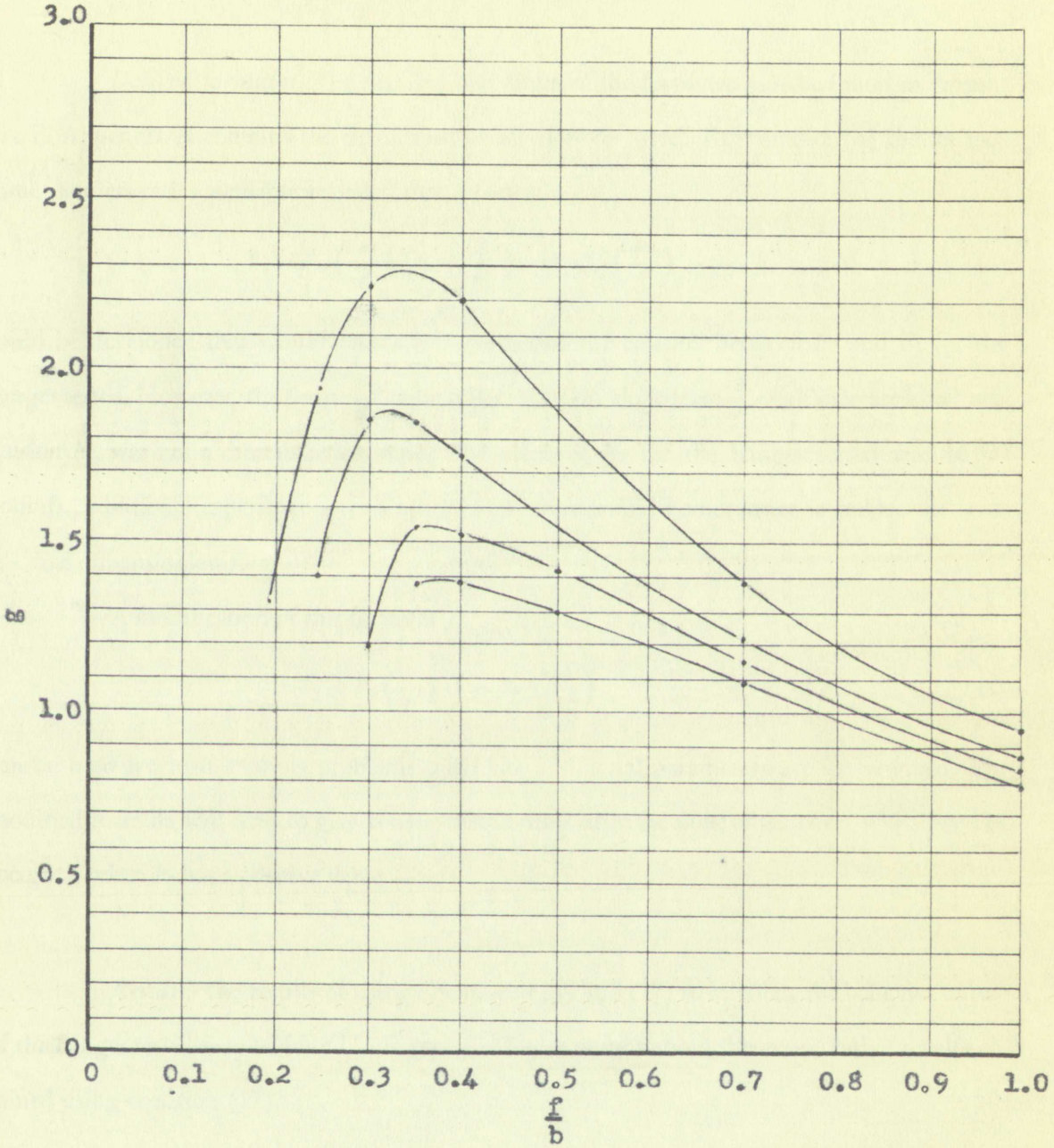

FIGURE 28

PLOT OF g VERSUS $\frac{f}{b}$ FOR FLANGE 7-2

the relation as some function of dimensionless ratios.

Derived formulas. The detailed derivation of the formulas may be found in Appendix F. Appendix A contains the definitions of all symbols used. Examination of the various dimensionless ratios available revealed that a formula

$$F_2 = F_1 \left(\frac{a}{b}\right)\left(1 - \frac{F_t}{B_1}\right) + F_t B_2 \left(\frac{bh}{a^2}\right) \tag{16}$$

could be developed that would satisfactorily describe the relation between F_2 and F_1 for the flanges tested. However, the term $\frac{F_t}{B_1}$, which decreases the slope term $\frac{a}{b}$ with increased bolt pretension F_t, was not a dimensionless ratio. The value of B_1 for the flanges tested was 16,000 pounds. Additional experiments with other parameters would be necessary to reduce the term $\frac{F_t}{B_1}$ to a dimensionless ratio.

A modification of this formula

$$F_2 = F_1 \left(\frac{a}{b}\right) + F_t B_2 \left(\frac{bh}{a^2}\right) \tag{17}$$

can be used for load analysis problems until the additional parameters are investigated. The modified formula will tend to give conservative results since the slope of the curve will always be too great when F_t has a positive value.

Results. The results of using equations (16) and (17) to calculate the behavior of two of the flanges tested may be found in Figure 29. These graphs show the conservative results obtained using equation (17).

Conclusions. The use of Dimensional Analysis has provided a means of calculating the relation between F_2 and F_1 after the flange has started to separate from the base. Additional experiments using the parameters not investigated for this problem should be made so the proper

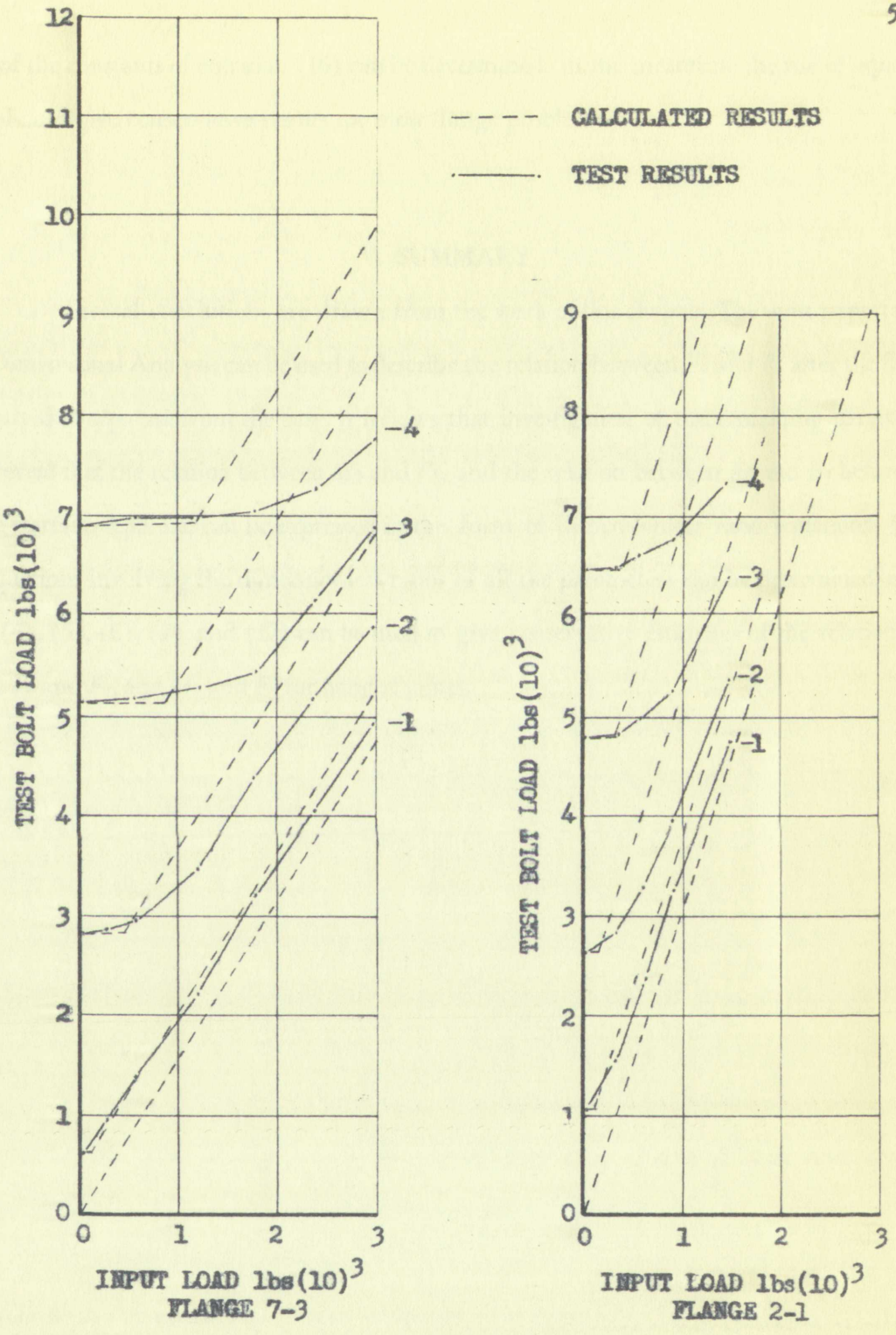

FIGURE 29

PLOT OF FLANGES 7-3 AND 2-1 USING DIMENSIONAL ANAYLSIS THEORY

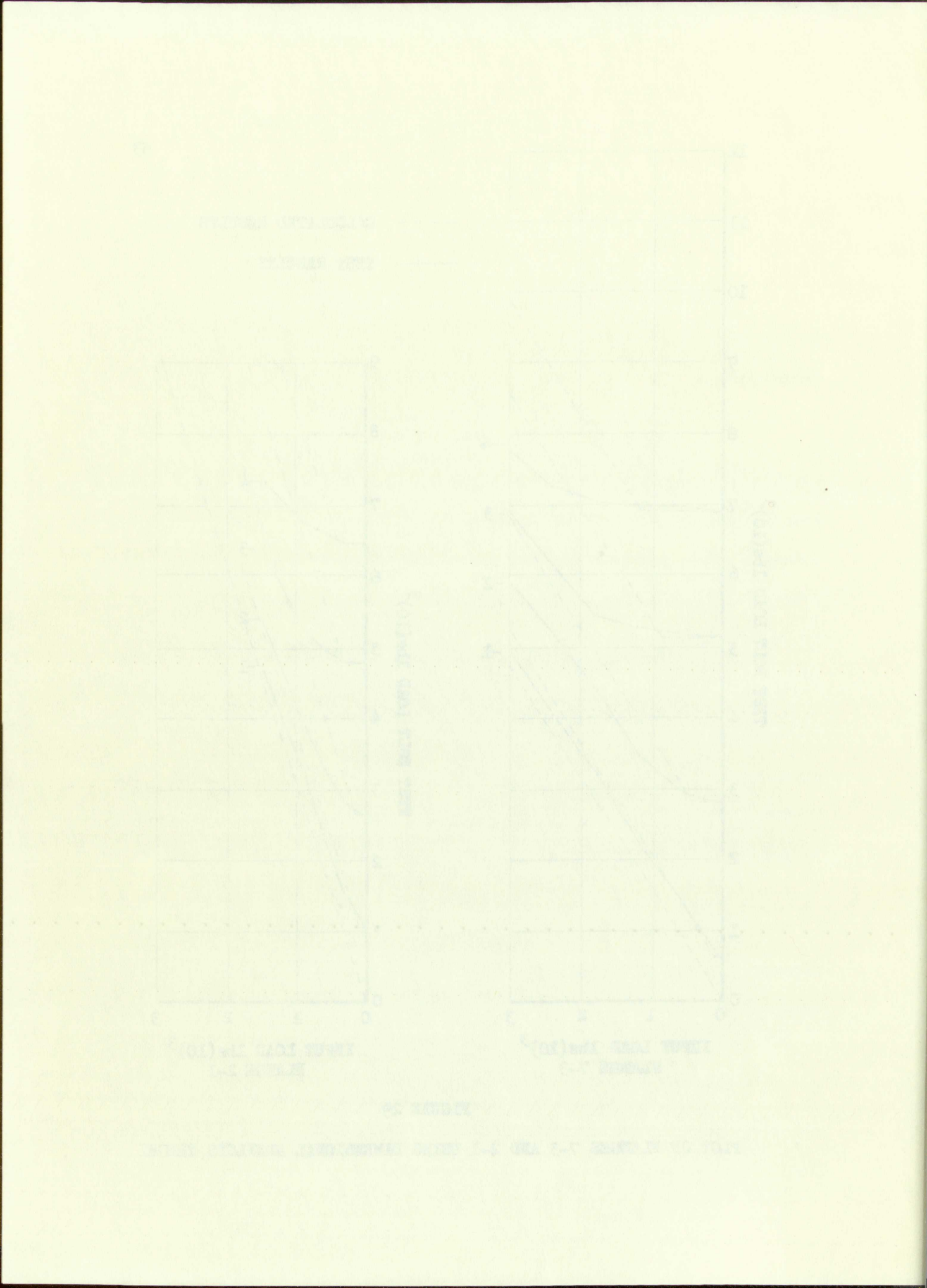

form of the constants of equation (16) can be determined. In the meantime the use of equation (17) should give conservative results for most flange problems.

V. SUMMARY

Several conclusions are drawn from the work of this chapter. The most important is that Dimensional Analysis can be used to describe the relation between F_2 and F_1 after the flange has started to separate from the base. It follows that investigation of the remaining parameters may reveal that the relation between M_b and F_1, and the relation between F_2 and F_1 before the flange starts to separate, can be expressed in the form of dimensionless ratio equations. Until the equations involving the dimensionless ratios of all the parameters can be determined, equations (4), (5), (6), (7), and (17) can be used to give conservative estimates of the relations between F_2 and F_1, and M_b and F_1 for flanged joints.

CHAPTER VI

RECOMMENDED PROCEDURE FOR SOLUTION OF FLANGED JOINT PROBLEMS

This chapter presents the procedures recommended for use in solving for the forces and moments encountered in flanged joint design. Also presented is a sample problem which is solved using the recommended procedures. The chapter concludes with comments concerning the use of the recommended procedures and the results to be expected.

Recommended Procedure. The stress variations in the attaching bolt of a flanged joint subjected to external loading are reasonably complicated. Therefore, it is recommended that any problem be solved by constructing graphs of F_2 versus F_1 and M_b versus F_1 similar to those shown in Figures 13 through 21 of Chapter IV. The recommended methods for constructing the graphs involve use of parts of the Rigid Flange Theory, the Flexible Flange Theory, and the Dimensional Analysis Theory. The solutions obtained in the Rigid Flange Theory are used to plot the first part of the F_2 versus F_1 curve, the part with the small slope. The third part, where the F_2 versus F_1 curve is relatively steep, is plotted using the Dimensional Analysis Theory. The second part of the F_2 versus F_1 curve, where the slope is increasing from the small slope of the first portion to the steep slope of the third portion, was not determined for the solutions herein developed. (The test data showed that no significant error would be introduced by doing this.) The graph of M_b versus F_1 is plotted by use of both the Flexible Flange Theory and the Rigid Flange Theory.

The first step, in a typical solution, is to plot the F_2 versus F_1 relation for the flange. The plot of the steeper sloped portion of the curve is constructed by use of equation (17) of Chapter V. The definitions of all the variables used in the solution of the equations are contained in Appendix A. The plot of the curve for the lower sloped portion is made using equa-

CHAPTER VI

RECOMMENDED PROCEDURE FOR SOLUTION OF FLANGED JOINT PROBLEMS

This chapter presents the procedures recommended for use in solving for the loads and moments encountered in flanged joint design. Also presented is a sample problem which is solved using the recommended procedures. The chapter concludes with comments concerning the use of the recommended procedures and the results to be expected.

Recommended Procedure. The stress variations in the matching pair of flanged joint subjected to external loading are reasonably complicated. Therefore, it is recommended that any problem be solved by constructing graphs of F_2 versus F_1 and M_3 versus F_1 similar to those shown in Figures 13 through 21 of Chapter IV. The recommended methods for constructing the graphs involve use of parts of the Rigid Flange Theory, the Flexible Flange Theory, and the Dimensional Analysis Theory. The solutions obtained in the Rigid Flange Theory are used to plot the first part of the F_2 versus F_1 curve, the part with the small slope. The third part, where the F_2 versus F_1 curve is relatively steep, is plotted using the Dimensional Analysis Theory. The second part of the F_2 versus F_1 curve, where the slope is increasing from the small slope of the first portion to the steep slope of the third portion, was not determined for the solutions that were developed. (The test data showed that no significant error would be introduced by doing this.) The graph of M_3 versus F_1 is plotted by use of both the Flexible Flange Theory and the Rigid Flange Theory.

The first step, in a typical solution, is to plot the F_2 versus F_1 relation for the flange. The plot of the steeper sloped portion of the curve is constructed by use of equation 4.67 of Chapter V. The definitions of all the variables used in the solution of the equations are contained in Appendix A. The plot of the curve for the lower sloped portion is made using data

tions (4) through (6) of Chapter V. This curve can be plotted from only two points since it was shown in Appendix D to be a straight line. One point is known; $F_2 = F_t$ when $F_1 = 0$. The additional point is located by solving equation (4) of Chapter V when f is equal to b. The required F_2 versus F_1 curve is the line starting at $F_2 = F_t$ when $F_1 = 0$ and extending to the steeper portion of the curve and then up the steeper curve. Additional curves of F_2 versus F_1 for different F_t values may now be drawn, if required, since the shallower sloped portions are parallel as are the steeper sloped portions. The intersections of the steeper and shallower sloped portions of all curves are on a straight line extending through the origin of the graph and the intersection of the two curves originally plotted. The plot of the family of curves of the F_2 versus F_1 values may prove valuable at this stage of the solution since they may enable the designer to select an F_t which will be large enough to prevent the flange from separating from the base. This should always be the aim of the engineer who designs to a fluctuating external load since the range of stress variation in the attaching bolt will be reduced if the flange joint is prevented from opening.

After the desired F_t is chosen from the plots of F_2 versus F_1, it is necessary to construct the M_b versus F_1 curve. This is done by the use of a modification of equation (15) of Chapter V. The modification consists of omitting the $F_4 A_{16}$ and A_{17} terms from the equation so that

$$M_b = R_b (F_2 A_{15}) . \tag{1}$$

Elimination of these terms is justified since they are relatively small compared to the $F_2 A_{15}$ term. Elimination of these terms did not materially affect the results obtained in solving for the curves of the flanges tested for this paper.

An examination of the results obtained from the flanges tested shows that little bending of the bolt is encountered until the flange has started to separate from the base. In order to modify equation (1) so that it will give results consistent with observed results, it is necessary to subtract the constant from the right side which is equal to the value of M_b at $F_2 = F_t$. The modified equation then becomes

$$M_b = R_b A_{15} (F_2 - F_t) , \tag{2}$$

tions (4) through (6) of Chapter V. This curve can be plotted from only two points since it was shown in Appendix D to be a straight line. One point is known; $F_3 = F_1$ when $F_1 = 0$. The additional point is located by solving equation (4) of Chapter V when λ is equal to λ_1. The required F_3 versus F_1 curve is the line starting at $F_3 = F_1$ when $F_1 = 0$ and extending to the steeper portion of the curve and then up the steeper curve. Additional curves of F_3 versus F_1 for different F_1 values may now be drawn, if required, since the shallower sloped portions are parallel as are the steeper sloped portions. The intersections of the steeper and shallower sloped portions of all curves are on a straight line extending through the origin of the graph and the intersection of the two curves originally plotted. The plot of the family of curves of the F_3 versus F_1 values may prove valuable at this stage of the solution since they may enable the designer to select an F_1 which will be large enough to prevent the flange from separating from the base. This should always be the aim of the engineer who designs to a fluctuating external load since the range of stress variation in the attaching bolt will be reduced if the flange joint is prevented from opening.

After the desired F_1 is chosen from the plots of F_3 versus F_1, it is necessary to construct the M_3 versus F_1 curve. This is done by the use of a modification of equation (15) of Chapter V. The modification consists of omitting the $F_1 A_{1s}$ and $J_1 \alpha$ terms from the equation so that

$$M_3 = R_3 (F_3 A_{3s}) . \tag{1}$$

Elimination of these terms is justified since they are relatively small compared to the $F_3 A_{3s}$ term. Elimination of these terms did not materially affect the results obtained in solving for the curves of the flanges tested for this paper.

An examination of the results obtained from the flanges tested shows that little bending of the bolt is encountered until the flange has started to separate from the base. In order to modify equation (1) so that it will give results consistent with observed results, it is necessary to subtract the constant from the right side which is equal to the value of M_3 at $F_3 = F_1$. The modified equation then becomes

$$M_3 = R_3 A_{3s} (F_3 - F_1) , \tag{2}$$

the equation recommended for use in calculating the value of the moment M_b in any flanged joint problem.

Solution of example problem. In order to compare calculated results with the results obtained by test, a particular test which had been run is used as the example for theoretical solution. The test chosen is 4-1-3, the test of the 1/2 inch thick flange with the greatest eccentricity and an initial bolt pre-tension (F_t) of 4260 pounds. The problem is to determine the variation in maximum expected stress from an external load varying between 0 and 3000 pounds.

The first thing determined is the relation between F_2 and F_1 for the steeper portion of the curve. From an observation of the flange drawings in Appendix B, it can be seen that $a = 2.125$ inches, $b = 0.688$ inches and $c = 1.437$ inches. By substituting these values into equation (17) of Chapter V along with an F_t of 4260 pounds, an equation of F_2 versus F_1 is obtained. This equation may be solved at $F_1 = 0$ and $F_1 = 3000$ pounds to obtain two points on the straight line relation between F_2 and F_1 after the flange has started separating from the base. This line is plotted on the graph of Figure 30 as the line ab. The plot of the straight line relation between F_2 and F_1 at the lower slope is made by using equations (4) through (6) of Chapter V. In order to solve these equations several constants must first be determined. These constants are K, S, R_b, R_f, e_2, and e_1. The definitions of these constants may be found in Appendix A.

The constant K is the number of inches the attaching bolt will elongate when subjected by the flange to a load of one pound. In this example the attaching bolt is not the only member which contributes to this elongation. The thick washer which is used under the bolt head also compresses thus contributing to the effective elongation. Therefore the elongation is made up of the sum of the elongation of the bolt due to one pound and the compression of the washer due to one pound. The value of K for this problem is equal to 2.735 (10^{-7}) inches per pound.

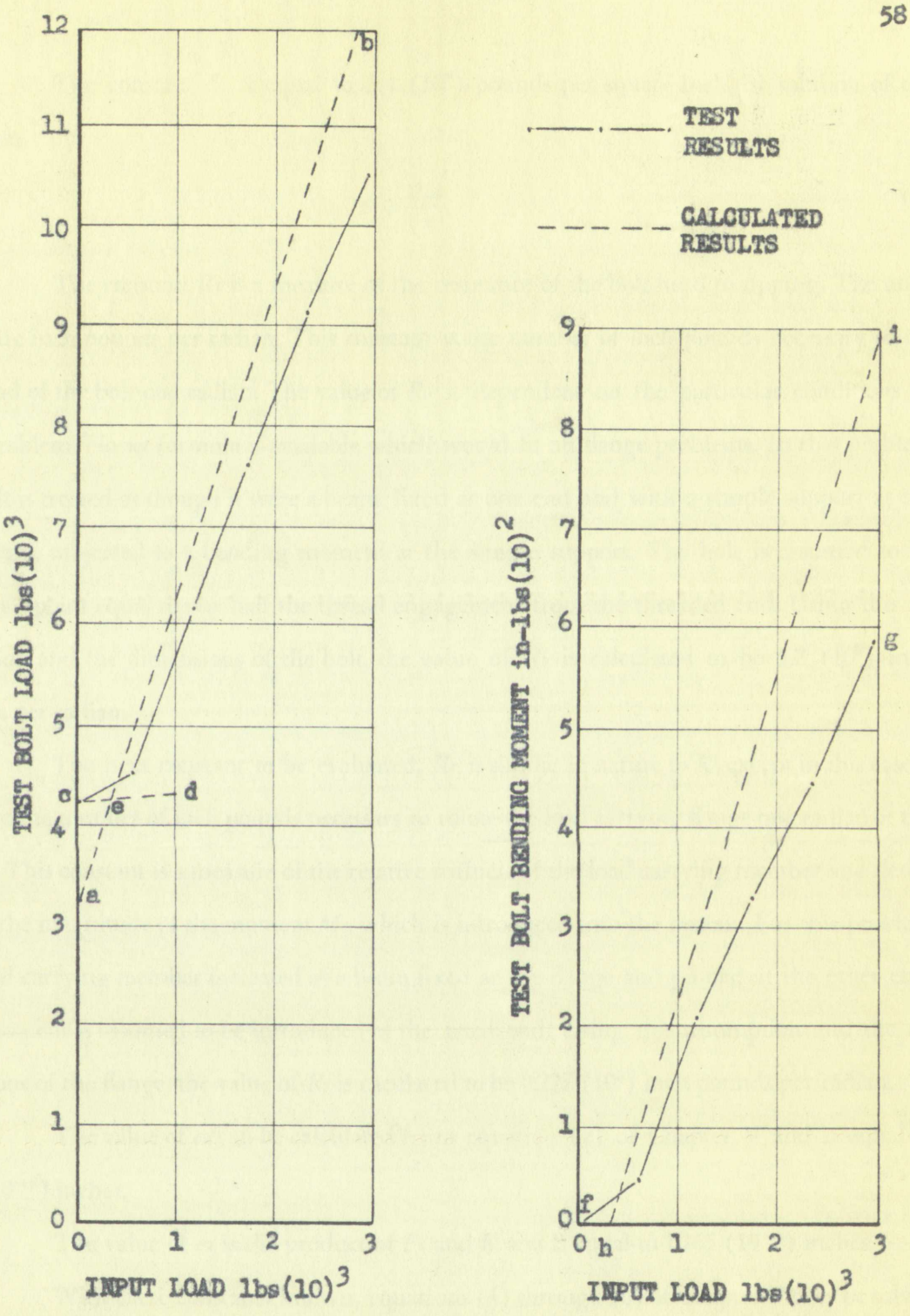

FIGURE 30

CALCULATED RESULTS OF EXAMPLE PROBLEM

The constant S, is equal to 2.4 (10^8) pounds per square inch, by solution of the equation

$$S = \frac{E_f w}{t} . \tag{3}$$

The constant R_b is a measure of the resistance of the bolt head to tipping. The units of R_b are inch pounds per radian. This constant is the number of inch pounds necessary to tilt the head of the bolt one radian. The value of R_b is dependent on the particular conditions of each problem. No set formula is available which would fit all flange problems. In this problem the bolt is treated as though it were a beam, fixed at one end and with a simple support at the other end, subjected to a bending moment at the simple support. The bolt is assumed to be fixed at a point equal to one half the thread engagement from the threaded end. Using this assumption and the dimensions of the bolt, the value of R_b is calculated to be 2.2 (10^5) inch pounds per radian.

The next constant to be evaluated, R_f, is similar in nature to R_b except in this case is equal to the number of inch pounds necessary to rotate the load carrying flange one radian at the flange. This constant is a measure of the relative stiffness of the load carrying member and determines the magnitude of the moment M_f, which is introduced into the system. For this problem the load carrying member is treated as a beam fixed at the flange and pinned at the other end. The moment is assumed to be introduced at the fixed end. Using this assumption and the dimensions of the flange, the value of R_f is caculated to be 0.227 (10^5) inch pounds per radian.

The value of e_2 can be calculated from equation (2) of Chapter V and is equal to 1.15 (10^{-5}) inches.

The value of e_1 is the product of F_t and K and is equal to 1.165 (10^{-3}) inches.

With these constants known, equations (4) through (6) of Chapter V may be solved to determine the relation between F_1 and F_2. By solving these equations at $f = b$ a point is found at $F_2 = 4285$ pounds when $F_1 = 1045$ pounds. This point is plotted on the left-hand graph of

Figure 30 as point d. A second point is known since $F_2 = F_t$ when $F_1 = 0$. This point is plotted as point c. The straight line cd is then drawn which intersects the line ab previously drawn at the point e. The desired relation between F_2 and F_1 over the range of F_1 from 0 pounds to 3000 pounds is the line ceb.

The plot of M_b versus F_1 is then made using the graph just constructed along with equation (2) of this chapter. This curve is the line fhi on the M_b versus F_1 graph Figure 30. The test results are shown as the line fg.

Figure 31 is a graph of maximum stress versus F_1, the input load. This graph was drawn in order to show the results that are obtained from the various solutions of the problem. The line agh represents the result that was obtained in the test of the flange. The line acd is the result that was obtained by using the equations recommended in this chapter. Two additional curves were plotted in order to compare the calculated and test results with the results obtained by two of the more commonly used solutions. One of these solutions assumes that no additional bolt loading will occur until the external load exceeds the pre-tension load and also that the flange will tend to pivot about its outer edge. This solution ignores any induced bending stresses. The results of this calculation are shown by the curve afj. Another similar solution makes the same assumptions, except the flange is assumed to pivot about a point 1/3 the distance from the outer edge to the bolt. This solution is shown by the curve aei.

Conclusion. The recommended formulas for the determination of the loads and moments in a flanged joint are presented in this chapter. An example of the application of these formulas and the comparison of the calculated and test results are included. The example showed that the commonly used solutions for the bolt stresses in flanged joint problems can be far lower than the actual stresses encountered in the joint. The reason for this error lies principally in the lack of any expresion for the probable bending stresses to be encountered. It is also demonstrated that the formulas recommended for use tend to give conservative results.

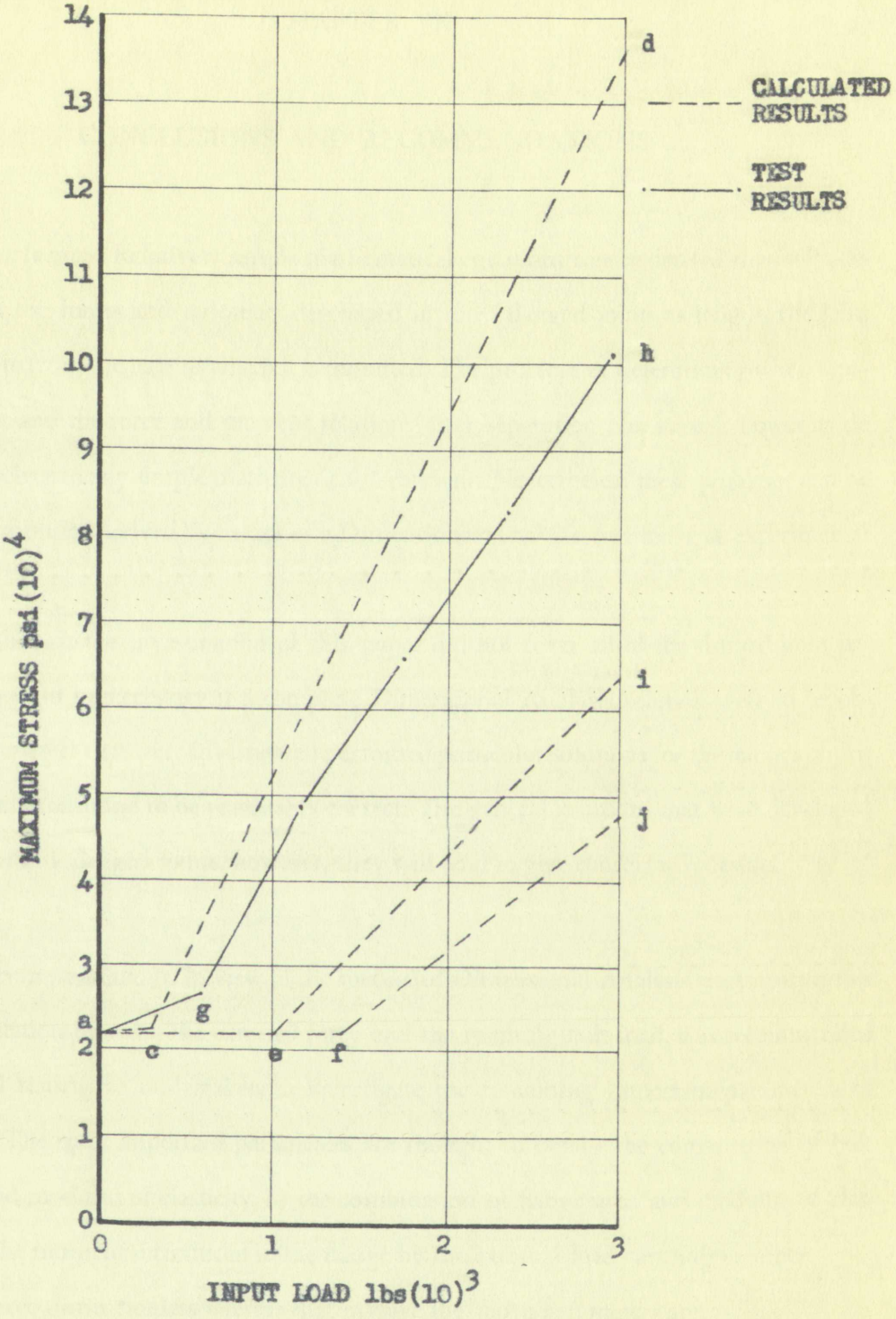

FIGURE 31

MAXIMUM STRESS VERSUS INPUT LOAD FOR EXAMPLE PROBLEM

CHAPTER VII

CONCLUSIONS AND RECOMMENDATIONS

Conclusions. Relatively simple mathematical equations can be derived that will adequately predict the forces and moments developed in most flanged joints as long as the joint does not separate from the base to which it is mounted. The problem of determining when separation will start and the force and moment relations after separation has started, however, do not lend themselves to any simple mathematical treatment. Nevertheless these problems can be handled with formulas derived by means of a Dimensional Analysis treatment of experimental data.

Although the investigation of this paper did not cover all of the flanged joint parameters that would be necessary if a complete Dimensional Analysis solution were to be obtained, the parameters that were investigated permitted particular solutions for the flanges of this problem. These were found to be reasonably correct. The general solutions that were developed may be used for any flanged joints, however, they will tend to give conservative results.

Recommendations. In view of the successful Dimensional Analysis treatment in this paper of the relation between the external force and the resulting bolt load, it is recommended that additional testing be undertaken to investigate the remaining important parameters of flanged joints. The most important parameters are thought to be: 1) the combination of bolt area, length and modulus of elasticity, 2) the combination of flange area and modulus of elasticity, and 3) the moment introduced in the flange by the external load carrying member.

Three dimensionless π terms that involve the above parameters are:

$$\pi_5 = \frac{F_t K}{t}, \tag{1}$$

$$\pi_6 = \frac{E_f a w}{F_t}, \tag{2}$$

and

$$\pi_7 = \frac{R_f}{F_t a}. \tag{3}$$

It may be possible to investigate these π terms by using the flanges of this paper if a new attaching bolt and washers are fabricated. These new items should be of the same dimensions as those used in this problem, but of a material with a different modulus of elasticity. A bolt and washers of a high strength aluminum (24-ST, or 75-ST) would be satisfactory.

A series of tests similar to those conducted for this problem should be run using these new parts. These tests should give an indication of the effect of π_5 on the flange behavior.

The second dimensionless term, π_6, can be investigated by decreasing the width of the Test Flanges and conducting another series of tests using both the aluminum and steel, bolt and washer combinations. For these tests the flange width should be decreased to about 2 inches. Depending on the results obtained, it may be desirable to decrease flange width to 1 inch and run another test series. As a spot check on these tests, several flanges of a different material should be tested to make sure that π_6 is the correct form of the desired dimensionless ratio.

During the above tests for π_5 and π_6, the external load carrying member should be strain gaged at the junction between the flange and the member to detect bending strains. A knowledge of the strains, and thus induced bending moments, over the range of conditions investigated above, should provide a sufficient knowledge of the behavior of π_7, to determine its relation to the problem.

In order to reduce the number of tests, it is recommended that only two bolt pre-tensions be examined for each flange bolt combination. One test at an intermediate pre-tension and one at a higher pre-tension should be sufficient.

It should be noted that the above tests would also serve to investigate several other variables which might also have an influence on flange behavior.

and

Another problem was uncovered during the work for this paper which would bear investigation. This problem, the decrease in apparent bolt pre-tension after initial loading, was pointed out in Chapter III. Since the relation between the forces and moments in a flanged joint is a function of the bolt pre-tension, a knowledge of this phenomena must precede any critical evaluation.

BIBLIOGRAPHY

BIBLIOGRAPHY

Doland, Thomas J., and J. H. McClow, "The Influence of Bolt Tension and Eccentric Tensile Loads on Behavior of a Bolted Joint," *Society of Experimental Stress Analysis,* Vol. 8, No. 1, pp. 29-43.

Hathaway Type RS-10 Portable Strain Indicator Instruction Book H-172. Denver, Colorado: Hathaway Instrument Company. 27 pp.

Perry, Charles C. and Herbert R. Lissner, *The Strain Gage Primer.* New York: McGraw-Hill Book Company, Inc., 1955. 281 pp.

Spotts, Merhyle F., "Effect of Initial Stress on Eccentrically Loaded Bolt," *Machine Design and Manufacturing Bulletin,* Vol. 20, No. 7, Seattle, Washington: University of Washington, March, 1954. pp. 1-5.

APPENDICES

APPENDIX A

DEFINITIONS OF TERMS USED

This appendix contains the definitions of all the symbols used in he text and in the other appendices. A drawing of the Test Flange showing the principal dimeisions is shown in Figure 32.

Symbol	*Definition*	*Units*
A_1	$\frac{a-b}{6E_f I_f a}$	$\frac{1}{\text{in.}^2\text{-lb.}}$
A_2	$\frac{2b^2 (a-b)^2}{6E_f I_f a}$	in.
A_3	$A_1 (2ab - 4b^2)$	$\frac{1}{\text{lb.}}$
A_4	$\frac{b (a^2 - b^2)}{6E_f I_f a}$	$\frac{1}{\text{lb.}}$
A_5	$\frac{R_b}{b}(A_2 + K - A_3 b) + \frac{R_f}{b}(A_2 + K + A_4 b)$	in.
A_6	$\frac{2 (R_b + R_f)}{S b f}$	in.
A_7	$-\frac{e_1 + e_2 (R_b + R_f)}{b}$	in.-lb.
A_8	$\frac{4}{4 - SA_1 f^4}$	dimensionless
A_9	$\frac{15b - 2SA_1 f^5 + 15A_5}{15}$	in.
A_{10}	$A_8 A_9 - a$	in.
A_{11}	$gf - A_6 - A_8 A_9$	in.

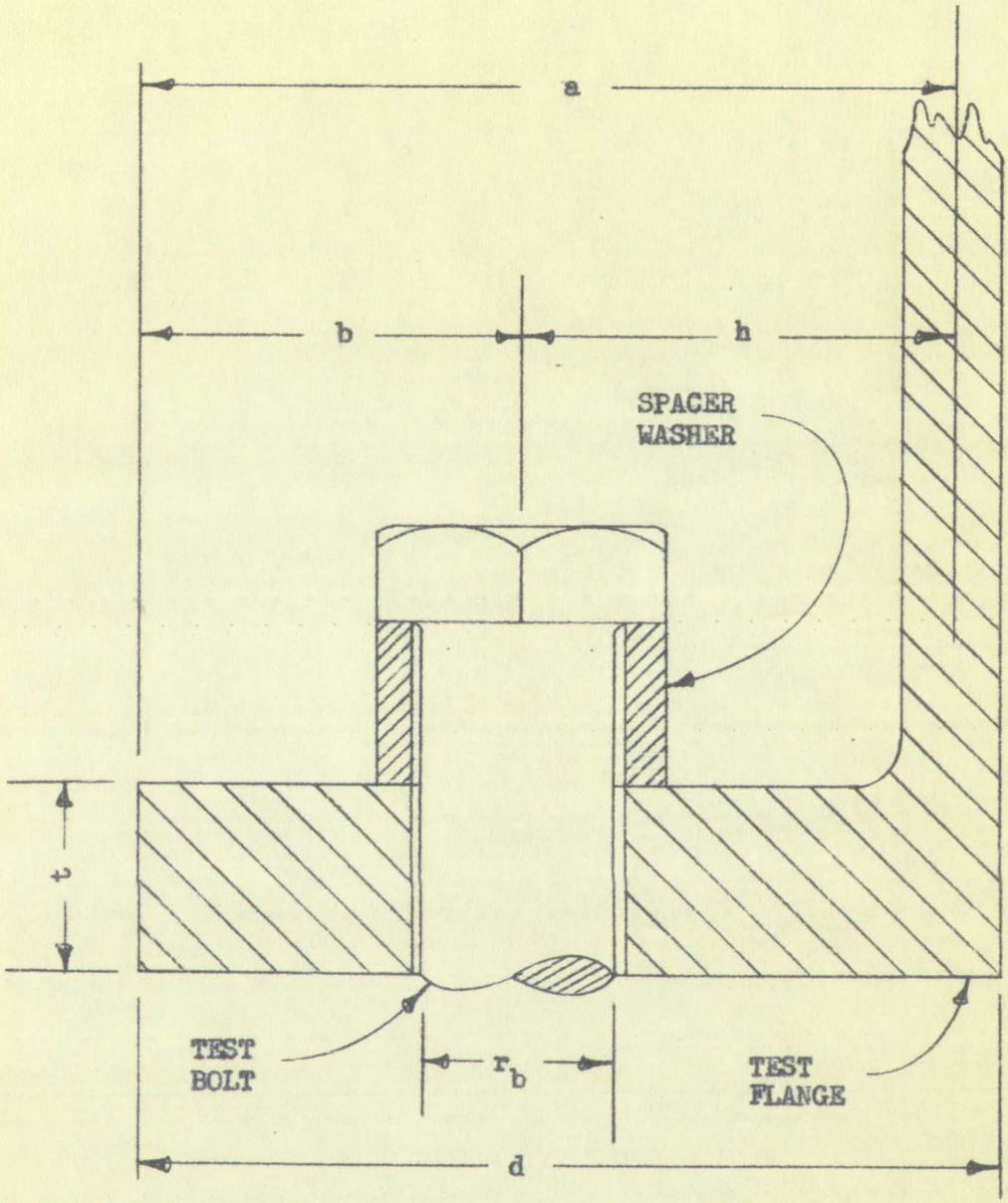

w IS THE WIDTH OF THE FLANGE PERPENDICULAR
TO THE PLANE OF THE PAPER

FIGURE 32

LETTERED DIMENSIONS OF THE FLANGE AND BOLT

Symbol	*Definition*	*Units*
A_{12}	$\frac{-SA_1 bf^2 (2ab - b^2 - f^2) + Sf^2 (A_2 + K)}{2b}$	dimensionless
A_{13}	$\frac{-Sf^2 (e_1 + e_2)}{2b}$	lb.
A_{14}	$1 - A_8 A_{12} - \frac{f}{b}$	dimensionless
A_{15}	$\frac{-A_3 b + A_2 + K}{b}$	$\frac{1}{\text{lb.}}$
A_{16}	$\frac{2}{Sbf}$	$\frac{1}{\text{lb.}}$
A_{17}	$\frac{-(e_1 + e_2)}{b}$	dimensionless
A_{18}	$b - a + A_5$	in.
A_{19}	$gf - b - A_5 - A_6$	in.
A_{20}	$1 - A_{12} - \frac{f}{b}$	dimensionless
a	The distance from the outer edge of the flange to the external load.	in.
B_1	A constant equal to 16,000.	lb.
B_2	A constant equal to 3.48.	dimensionless
b	The distance from the outer edge of the flange to the centerline of the attaching bolt.	in.
c	The distance from the outer edge of the flange to the centroid of pressure on the lower face of the flange.	in.
d	The distance from the outer edge of the flange to the inner edge.	in.
E_b	The modulus of elasticity of the Test Bolt.	$\frac{\text{lb.}}{\text{in.}^2}$

Symbol	*Definition*	*Units*
E_f	The modulus of elasticity of the flange.	$\frac{\text{lb.}}{\text{in.}^2}$
e	The distance from the outer edge of the flange to the force F_4.	in.
F_1	The external load.	lb.
F_2	The total axial load on the Test Bolt.	lb.
F_3	The total load acting on the lower face of the flange.	lb.
F_4	The load acting on the lower face of the flange due to a triangular shaped volume of displaced metal.	lb.
F_5	The load acting on the lower face of the flange due to lens shaped volume of displaced metal.	lb.
F_t	The initial pre-tension on the bolt due to the applied bolt torque.	lb.
f	The distance from the outer edge of the flange to the point where the lower face of the flange separates from the base due to the external load.	in.
g	A dimensionless constant. When multiplied by the distance f, the result will be the distance from the outer edge of the flange to the centroid of pressure on the lower face.	dimensionless
h	The distance from the external load path to the centerline of the attaching bolt.	in.
i	The intercept of the F_2 versus F_1 curve with the y axis in the Dimensional Analysis equation.	lb.
I_b	The moment of inertia of the attaching bolt.	in.^4
I_f	The moment of inertia of the flange. This moment of intertia is equal to $1/12\ w\ t^3$.	in.^4
K	The reciprocal of the spring constant of the attaching members.	$\frac{\text{in.}}{\text{lb.}}$

Symbol	*Definition*	*Units*
M	The total external induced moment acting on the flange.	in.-lb.
M_b	The moment induced on the flange by the attaching member.	in.-lb.
M_f	The moment induced on the flange by the external load carrying member.	in.-lb.
M_3	The bending moment induced in the Test Bolt at the strain gages.	in.-lb.
m_1	The slope of the curve y_1.	dimensionless
m_2	The slope of the curve y_2.	dimensionless
m_3	The slope of the curve y_3.	dimensionless
m_{3a}	The slope of the curve y_3 at the point $x = a$.	dimensionless
m_{3b}	The slope of the curve y_3 at the point $x = b$.	dimensionless
R	The sum of R_b and R_f.	in.-lb.
R_b	The torque necessary to bend the head of the bolt one radian.	in.-lb.
R_f	The torque necessary to bend the external load carrying member one radian at the point of attachment to the flange.	in.-lb.
S	A constant equal to $\frac{E_f w}{t}$.	$\frac{\text{lb.}}{\text{in.}^2}$
t	The thickness of the flange.	in.
w	The width of the flange.	in.
x	The distance from the y axis to the point under consideration.	in.
y	The distance from the x axis to the point under consideration.	in.
y_1	A particular curve of y versus x.	dimensionless
y_2	A particular curve of y versus x.	dimensionless
y_3	A particular curve of y versus x.	dimensionless
y_{2f}	The distance from the x axis to the y_2 curve at the point $x = f$.	in.

Symbol	*Definition*	*Units*
y_{3f}	The distance from the x axis to the y_3 curve at the point $x = f$.	in.
e_1	The elongation of the attaching bolt due to the pre-tension load.	in.
e_2	The compression of the flange at the bolt due to the attaching bolt pre-tension.	in.
e_3	The distance from the mounting base to the bottom of the flange at the bolt.	in.
e_4	The deflection of the flange at the attaching bolt due to bending.	in.
ε_5	The measured strain on the Test Bolt at the gage nearer the external load carrying member.	dimensionless
ε_5'	The strain on the Test Bolt at the gage nearer the external load carrying member after being corrected for initial bending.	dimensionless
ε_6	The measured strain on the Test Bolt at the gage on the side away from the external load carrying member.	dimensionless
ε_6'	The strain on the Test Bolt at the gage on the side away from the external load carrying member after being corrected for initial bending.	dimensionless
ε_7	The net tensile strain on the Test Bolt.	dimensionless
ε_8	The strain on the Test Bolt due to the induced bending moment.	dimensionless
ε_9	The net tensile strain on the Load Bolt.	dimensionless
θ	The angle between the bending axis of the strain gages and the axis of maximum bending on the Test Bolt.	dimensionless
π_1	$\frac{F_1}{F_2}$	dimensionless
π_2	$\frac{F_t}{F_2}$	dimensionless

Symbol	*Definition*	*Units*
π_3	$\frac{a}{b}$	dimensionless
π_4	$\frac{bh}{a^2}$	dimensionless
π_5	$\frac{F_t K}{t}$	dimensionless
π_6	$\frac{E_f a w}{F_t}$	dimensionless
π_7	$\frac{R_f}{F_t a}$	dimensionless

Symbol	Definition	Dim
π_1	$\frac{u}{c}$	dimensionless
π_2	$\frac{hh}{d^2}$	dimensionless
π_3	$\frac{F \cdot K}{t}$	dimensionless
π_4	$\frac{E_{mw}}{P_r}$	dimensionless
π_5	$\frac{K_l}{F_{ra}}$	dimensionless

APPENDIX B

DETAILED DRAWINGS OF THE TEST ITEMS

Drawings of the Test Flanges, strain gaged capscrews, and spacer washers are contained in this Appendix. These drawings are presented so the detailed dimensions of the various parts that can affect the calculations will be available. These drawings are exact copies of the drawings used in the actual fabrication of the test parts.

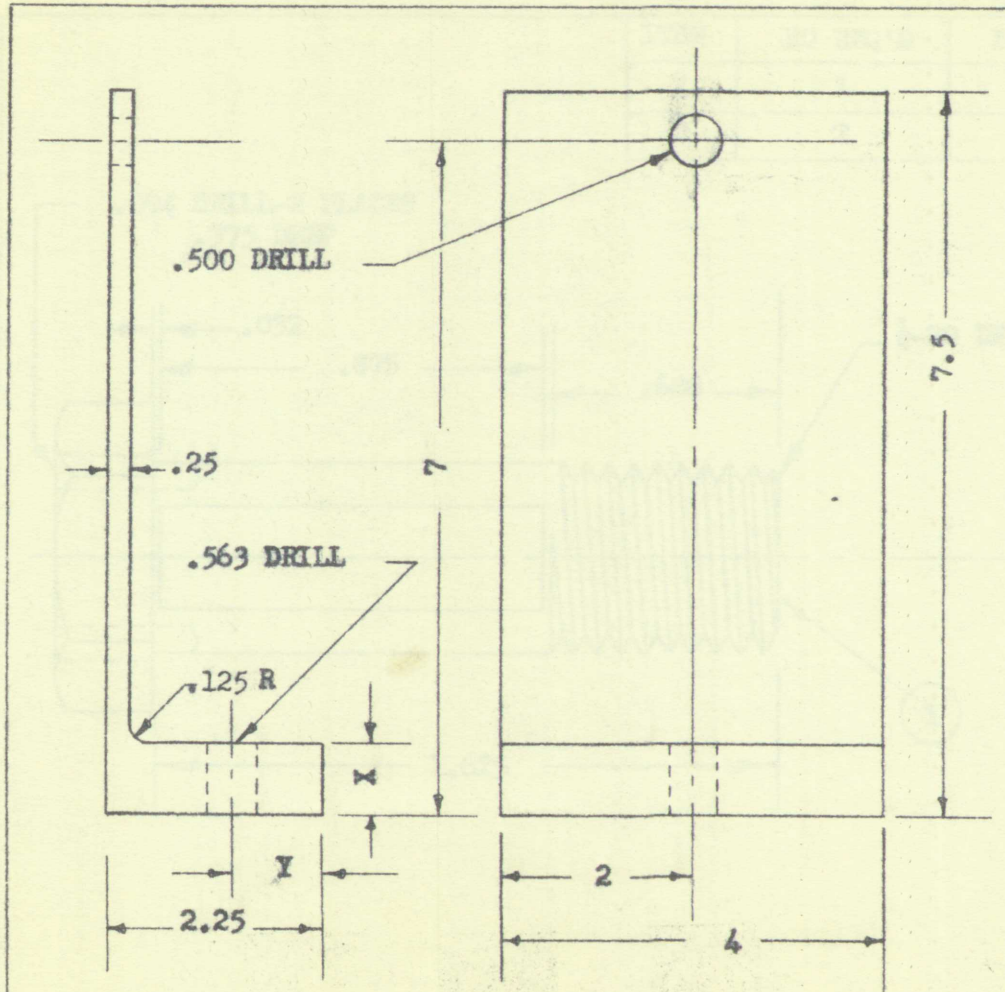

FLANGE	X	Y
2-1	0.25	0.688
2-2	0.25	1.000
2-3	0.25	1.312
4-1	0.50	0.688
4-2	0.50	1.000
4-3	0.50	1.312
7-1	0.88	0.688
7-2	0.88	1.000
7-3	0.88	1.312

NOTE: NINE FLANGES ARE REQUIRED, ONE OF EACH OF THE ABOVE COMBINATIONS

TEST FLANGES	
MATERIAL- STEEL	DATE 1-1-56
DRAWN BY E Blake	SCALE 1/2

FIGURE 33

DETAILED DRAWING OF THE TEST FLANGES

ITEM	NO REQ'D	DESCRIPTION	MATERIAL
1	1	BOLT	½ DIA AN BOLT
2	2	SHIM	BRASS SHIM .032 THICK

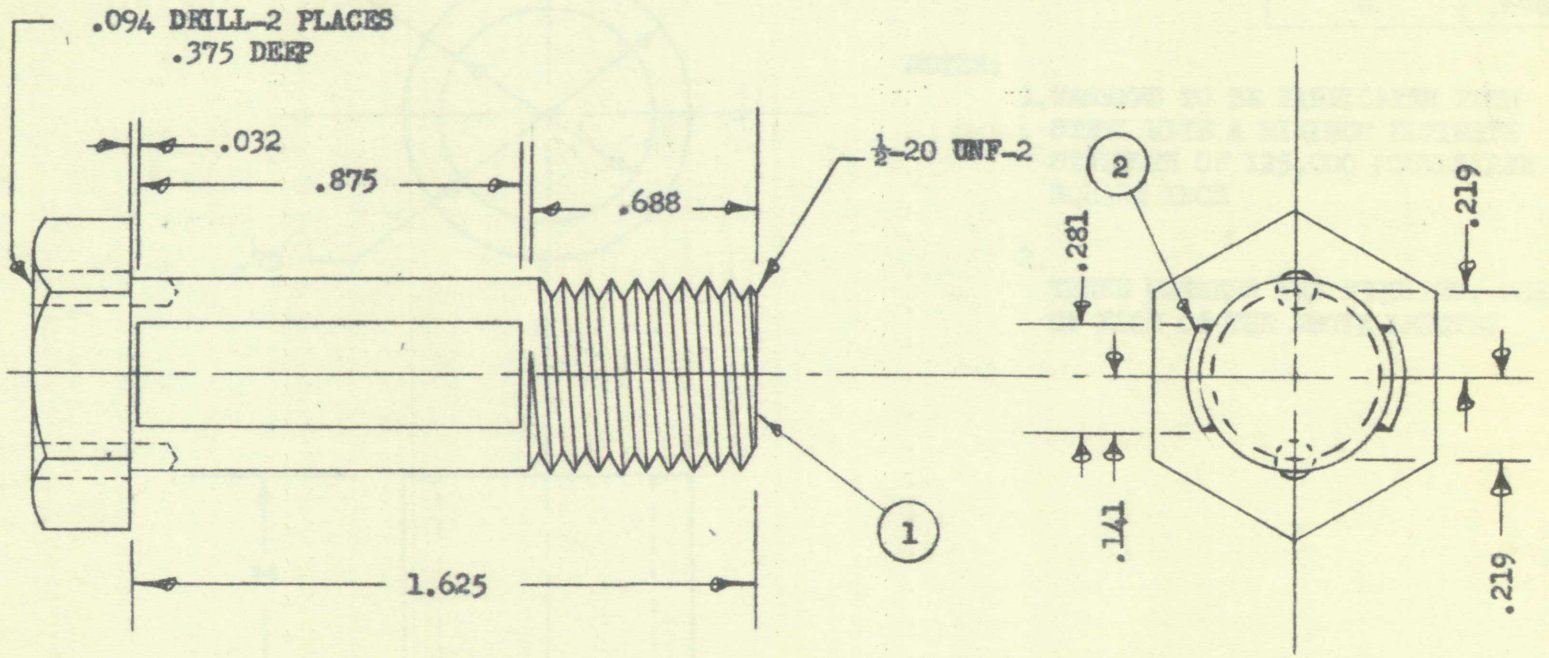

CAPSCREW	
MATERIAL - NOTED	DATE 1-1-56
DRAWN BY E Blake	SCALE 2=1

FIGURE 34

DETAILED DRAWING OF THE TEST BOLT

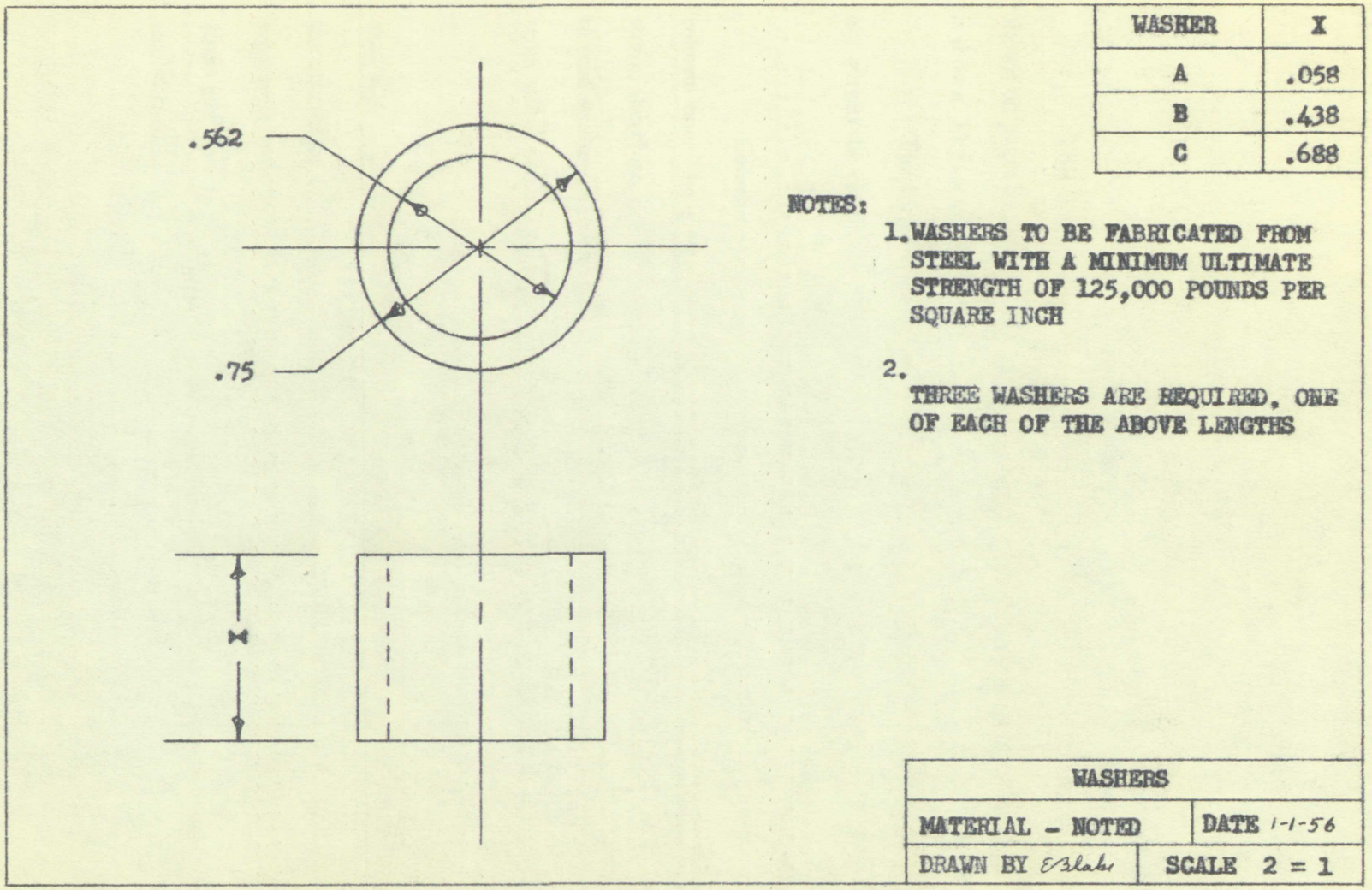

FIGURE 35

DETAILED DRAWING OF THE SPACER WASHERS

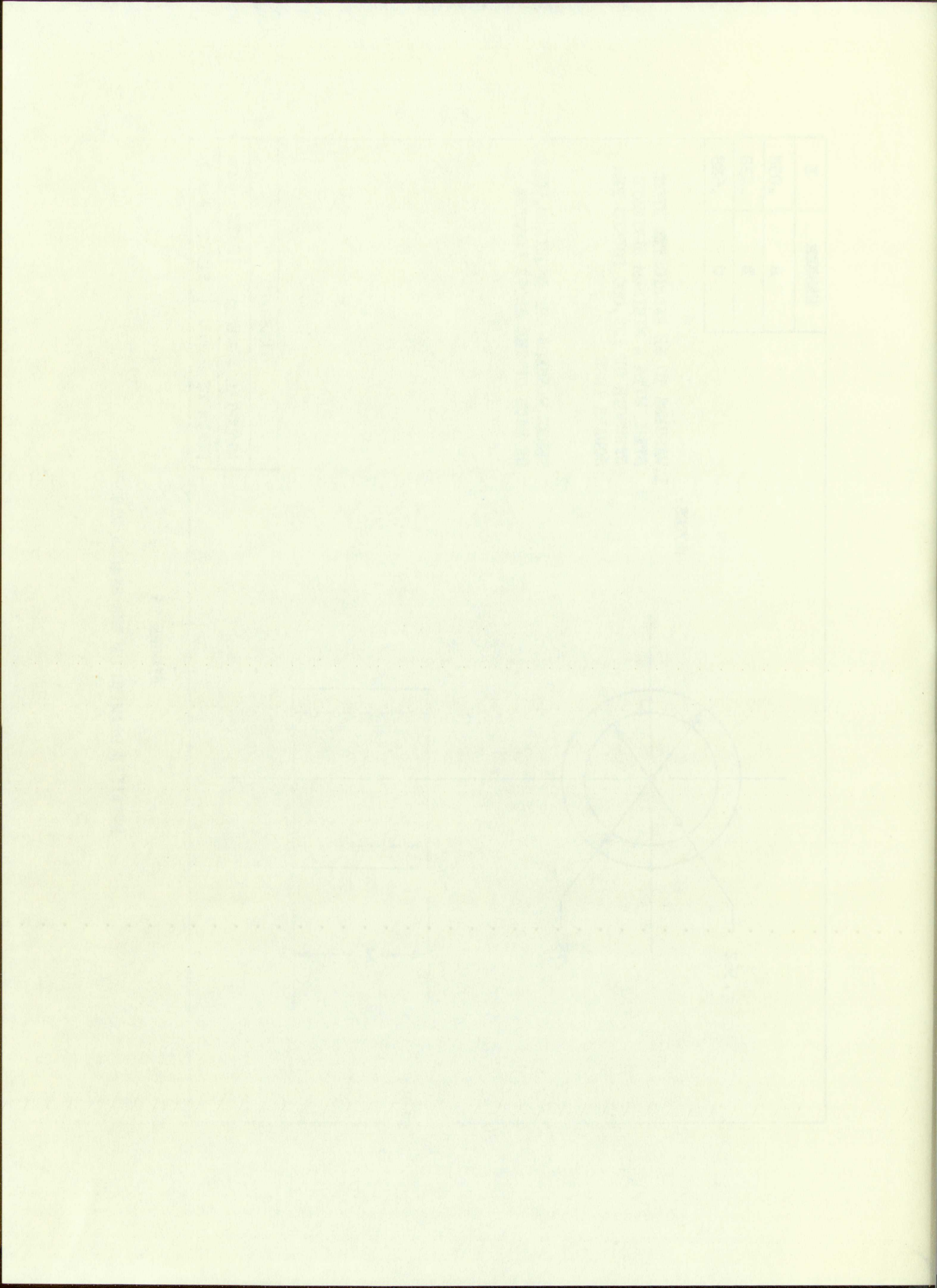

APPENDIX C

TABLES OF DATA AND METHODS USED FOR DATA REDUCTION

This appendix contains complete tables of all the original data. These tables are shown on pages 84 through 92 of this appendix. In addition, the reduced data as used in the text is shown. The formulas used to reduce the data are developed.

The formulas in the following paragraphs are developed assuming that all stresses are within the elastic limit. The letter symbols are defined in Appendix A.

Column I, Load Bolt strain. The strain measured on the Load Bolt is recorded in column one. The gages were connected in opposite arms of the bridge used for measuring the strain, therefore, only net tensile strains were obtained. The recording instrument is calibrated to read strains directly when two active gages are used. Consequently, the recorded data represents actual strain readings.

Columns II and III, Test Bolt strains, gages 1 and 2. The strain readings from the Test Bolt gage nearer the input load flange are tabulated in column II. The strain readings from the other Test Bolt gage are tabulated in column III. Since these strain readings were recorded separately, only one active gage was used in each bridge. Because of the calibration of the portable strain indicator the readings are the actual strain divided by two. To obtain the true strain, these readings must be doubled.

Column IV, Input Load. The tabulated data in this column is the actual load input, F_1, to the test flange. The data was obtained by multiplying the strain readings of column I by

the modulus of elasticity and the cross sectional area of the Load Bolt. Thus

$$F_1 = \varepsilon_9 E_b A_b (10^{-6}) \tag{1}$$

Column V, Test Bolt tensile load. The tensile load on the bolt, F_2, is tabulated in column V. This load was obtained by adding the strains of columns II and III to obtain the average tensile strain. The product of this strain, and the modulus of elasticity and cross sectional area of the Test Bolt, is the force F_2. It was not necessary to divide the strains in half since the individual readings were already divided in half because of the calibration of the recording instrument. The equation for this load is

$$F_2 = (\varepsilon_5 + \varepsilon_6) E_b A_b (10^{-6}) \ . \tag{2}$$

Column VI, maximum Test Bolt bending moment. From the strains at zero input load, it is obvious that bending stresses were present before any external load was applied. These stresses were undoubtedly introduced by non-parallelism of the different machined surfaces. Though it was not possible to eliminate the initial bending strains from the tests, it was possible to eliminate these strains from the reduced data. This was done by assuming that, had the parts been machined perfectly, the readings of the two gages ε_5 and ε_6 at zero external load would have been equal and their sum would have been equal to the strain produced by the initial bolt pre-tension. (It should be emphasized that the change in bending stress from zero load to maximum load was the important thing to be determined, rather than the absolute bending stress.) Consequently, a correction factor was determined which was equal to one half the difference between the larger reading and the smaller reading at zero external load. This correction factor was subtracted from the larger reading at zero load, and all other readings in that column. This same factor was also added to the smaller reading, at zero load, and all other readings in that column. The new readings thus obtained were called ε_5' and ε_6'. Thus a set of corrected strain readings was obtained. The sum of ε_5' plus ε_6' remained the same as ε_5 plus ε_6. However the in-

dividual readings were different.

From examination of the test setup it was obvious that each gage was recording strains due to both tensile and bending loads. The gage nearer the external load was reading the absolute sum of these two strains while the other gage was reading the absolute difference. Furthermore, the gages were not subjected to the maximum bending strains since they were not located on the axis of maximum bending. Figure 36 represents a cross section of the Test Bolt at the strain gages and shows the various axes. Thus if ε_8 was assumed to be the maximum strain due to bending, the bending strains recorded by each gage would actually be only $\varepsilon_8 \operatorname{Cos} \theta$. By assuming that the actual axial strain was ε_7, it was possible to set up two equations:

$$2\,\varepsilon_5' = \varepsilon_7 + \varepsilon_8 \cos\theta \tag{3}$$

and

$$2\,\varepsilon_6' = \varepsilon_7 - \varepsilon_8 \cos\theta\,. \tag{4}$$

The strains ε_5' and ε_6' were multiplied by two in each equation since the recorded strains ε_5 and ε_6 were only half the actual strain. Adding these two equations will give

$$\varepsilon_7 = \varepsilon_5' + \varepsilon_6'\,. \tag{5}$$

This equation shows the basis for derivation of equation (2) was correct since

$$\varepsilon_5' + \varepsilon_6' = \varepsilon_5 + \varepsilon_6\,. \tag{6}$$

By subtracting these two equations an equation

$$\varepsilon_8 = \frac{\varepsilon_5' - \varepsilon_6'}{\operatorname{Cos}\ \theta} \tag{7}$$

is obtained. The stress due to bending can be obtained by multiplying ε_8 by the modulus of elasticity of the bolt. The formula for the bending moment may be derived as

$$M_3 = \frac{\varepsilon_8 E_b I_b\,(10^{-6})}{r_1} \tag{8}$$

using standard formulas. Since the bending moment on the bolt is actually introduced at the head of the bolt, it would be greatest at that point. The moment M_3 just developed, was located at the strain gages, which were some distance from the bolt head. In order to obtain the maxi-

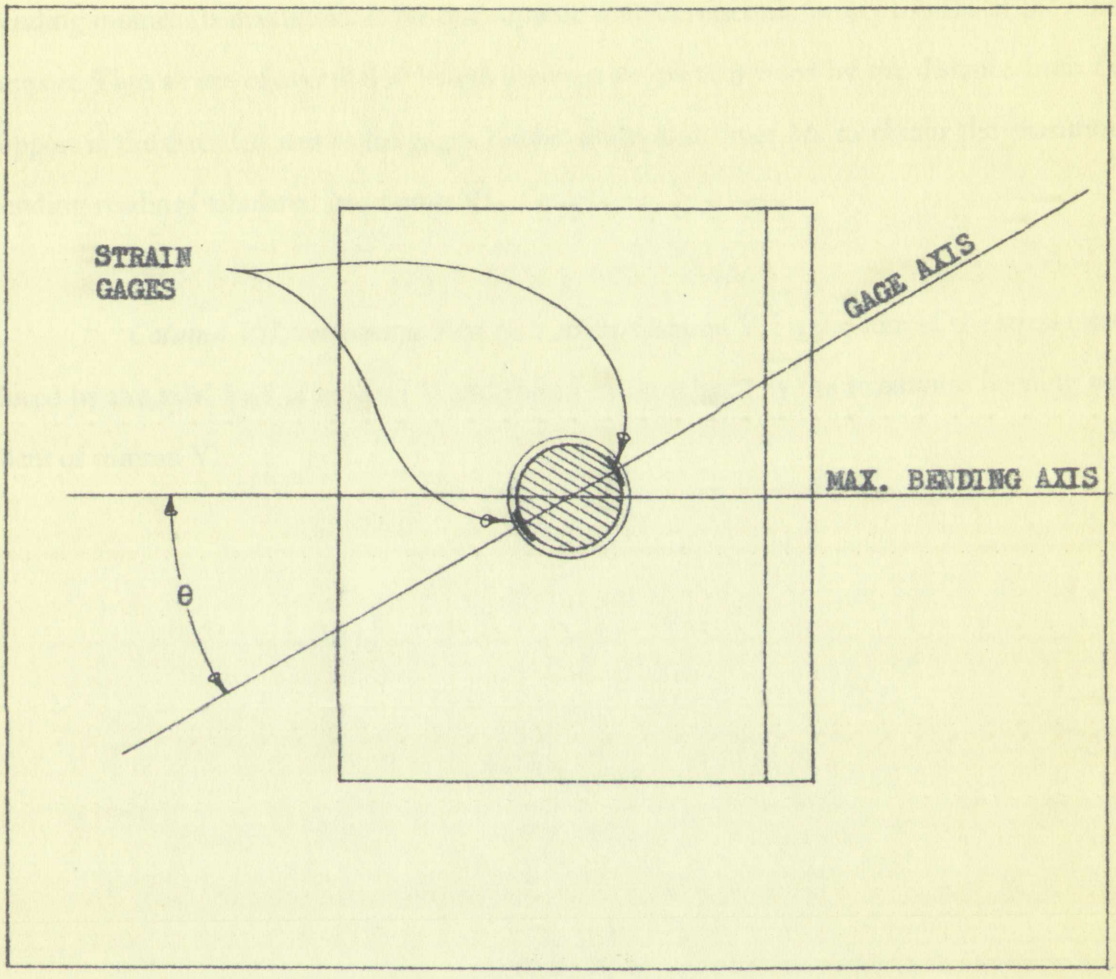

FIGURE 36

RELATION BETWEEN MEASURED BENDING STRAIN AND MAXIMUM BENDING STRAIN

mum bending moment it was assumed that the bolt was a simple beam pinned at the head and at a point, a distance equal to one half the thread engagement from the threaded end. It was further assumed that the entire bending moment was induced at the bolt head. In this case the bending moment is maximum at the one support and decreases uniformly to zero at the other support. Thus a ratio of overall bolt length between supports, divided by the distance from the support in the threaded area to the gages, can be multiplied times M_3 to obtain the maximum bending readings tabulated in column VI.

Column VII, maximum Test Bolt stress. Column VII is the sum of the stress introduced by the axial load of column V and the stress introduced by the maximum bending moment of column VI.

TABLE I

TEST DATA AND REDUCED DATA, FLANGE 2-1

TEST	LOAD BOLT STRAIN 1×10^{-6} *in*	TEST BOLT STRAIN GAGE 1 $.5 \times 10^{-6}$ *in*	TEST BOLT STRAIN GAGE 2 $.5 \times 10^{-6}$ *in*	INPUT LOAD *lbs*	TEST BOLT TENSILE LOAD *lbs*	MAXIMUM TEST BOLT BENDING MOMENT *in lbs*	MAXIMUM TEST BOLT STRESS *lbs per in²*
—1	0	0	180	0	1,060	0	5,400
	50	120	140	294	1,530	96	15,600
$\theta = 5°$	100	280	120	588	2,360	205	28,700
	150	435	110	883	3,208	304	41,200
	250	705	105	1,470	4,760	468	62,500
—2	0	230	230	0	2,700	0	13,800
	50	255	225	294	2,830	18	15,900
$\theta = 14°$	100	340	220	588	3,290	75	22,900
	150	455	215	883	3,940	148	32,200
	250	700	210	1,470	5,350	302	51,900
—3	0	545	270	0	4,790	0	24,400
	50	565	260	294	4,850	20	26,400
$\theta = 23°$	100	590	260	588	5,000	34	28,300
	150	640	250	883	5,230	75	32,800
	250	830	245	1,470	6,330	202	48,800
—4	0	745	345	0	6,410	0	32,700
	50	760	340	294	6,470	15	34,200
$\theta = 32°$	100	785	340	588	6,620	33	36,500
	150	815	335	883	6,760	57	39,100
	250	910	330	1,470	7,290	133	48,000

Table II

TEST DATA AND REDUCED DATA, FLANGE 2-2

Test	Load Bolt Strain 1×10^{-6} *in*	Test Bolt Strain Gage 1 $.5 \times 10^{-6}$ *in*	Test Bolt Strain Gage 2 $.5 \times 10^{-6}$ *in*	Input Load *lbs*	Test Bolt Tensile Load *lbs*	Maximum Test Bolt Bending Moment *in lbs*	Maximum Test Bolt Stress *lbs per in*^{2}
—1	0	— 80	215	0	794	0	4,100
	50	60	180	294	1,410	106	15,800
$\theta = 6°$	100	160	185	588	2,030	163	23,700
	200	365	190	1,176	3,260	284	39,900
	300	570	195	1,764	4,500	406	56,100
	400	780	195	2,352	5,730	531	72,500
—2	0	110	345	0	2,680	0	13,700
	50	170	320	294	2,880	51	18,900
$\theta = 1°$	100	255	305	588	3,300	111	25,900
	200	455	285	1,176	4,350	243	42,000
	300	655	275	1,764	5,470	368	57,900
	400	860	260	2,352	6,590	502	74,500
—3	0	365	330	0	4,080	0	20,800
	50	400	320	294	4,240	28	23,900
$\theta = 13°$	100	460	315	588	4,560	68	28,800
	200	600	300	1,176	5,290	163	40,300
	300	770	295	1,764	6,260	271	54,100
	400	945	290	2,352	7,260	381	68,100
—4	0	745	365	0	6,530	0	33,300
	50	760	360	294	6,590	15	34,800
$\theta = 30°$	100	775	360	588	6,680	24	36,100
	200	830	365	1,176	7,030	60	40,800
	300	930	365	1,764	7,620	129	49,400
	400	1,060	370	2,352	8,410	215	60,400

TABLE III

TEST DATA AND REDUCED DATA, FLANGE 2-3

TEST	LOAD BOLT STRAIN 1×10^{-6} *in*	TEST BOLT STRAIN GAGE 1 $.5 \times 10^{-6}$ *in*	TEST BOLT STRAIN GAGE 2 $.5 \times 10^{-6}$ *in*	INPUT LOAD *lbs*	TEST BOLT TENSILE LOAD *lbs*	MAXIMUM TEST BOLT BENDING MOMENT *in lbs*	MAXIMUM TEST BOLT STRESS *lbs per in²*
—1	0	20	110	0	765	0	3,900
	50	120	75	294	1,150	88	13,100
$\theta = 4°$	100	255	50	588	1,790	178	23,700
	200	440	40	1,176	2,820	295	38,600
	300	605	35	1,764	3,760	398	51,700
	400	780	30	2,352	4,760	505	65,500
	500	940	25	2,940	5,670	593	77,300
—2	0	100	290	0	2,300	0	11,700
	50	165	275	294	2,580	49	17,200
$\theta = 1°$	100	250	260	588	3,000	108	24,100
	200	445	240	1,176	4,020	238	40,000
	300	620	235	1,764	5,030	346	53,900
	400	790	225	2,352	5,970	453	67,500
	500	955	220	2,940	6,910	556	80,700
—3	0	435	300	0	4,320	0	22,000
	50	450	290	294	4,350	16	23,500
$\theta = 17°$	100	490	280	588	4,520	47	26,900
	200	620	270	1,176	5,230	135	37,700
	300	770	265	1,764	6,090	233	50,000
	400	915	260	2,352	6,920	326	61,900
	500	1,060	255	2,940	7,740	420	73,800
—4	0	865	330	0	7,030	0	35,800
	100	885	320	588	7,090	21	37,900
$\theta = 33°$	200	920	310	1,176	7,240	54	42,300
	300	990	305	1,764	7,620	108	47,700
	400	1,090	315	2,352	8,260	171	56,100
	500	1,195	320	2,940	8,910	244	65,400

TABLE IV

TEST DATA AND REDUCED DATA, FLANGE 4-1

TEST	LOAD BOLT STRAIN 1×10^{-6} *in*	TEST BOLT STRAIN GAGE 1 $.5 \times 10^{-6}$ *in*	TEST BOLT STRAIN GAGE 2 $.5 \times 10^{-6}$ *in*	INPUT LOAD *lbs*	TEST BOLT TENSILE LOAD *lbs*	MAXIMUM TEST BOLT BENDING MOMENT *in lbs*	MAXIMUM TEST BOLT STRESS *lbs per in*^{2}
—1	0	80	20	0	588	0	3,000
	50	320	— 80	294	1,410	225	25,600
$\theta = 25°$	100	500	—110	588	2,290	364	41,100
	200	795	— 85	1,176	4,180	543	65,600
	300	1,050	— 35	1,764	5,960	678	85,700
	400	1,260	20	2,352	7,530	782	102,200
	500	1,480	75	2,940	9,150	890	119,200
—2	0	200	150	0	2,060	0	10,500
	50	290	125	294	2,440	80	18,900
$\theta = 30°$	100	455	100	588	3,260	212	34,000
	200	700	160	1,176	5,060	339	53,400
	300	935	205	1,764	6,710	471	72,600
	400	1,145	260	2,352	8,260	578	89,200
	500	1,365	305	2,940	9,820	700	107,200
—3	0	—210	935	0	4,260	0	21,800
$\theta = 21°$	100	—150	925	588	4,560	42	26,600
	200	120	930	1,176	6,180	208	48,500
	300	350	950	1,764	7,650	329	65,800
	400	570	980	2,352	9,120	443	82,700
	500	780	1,010	2,940	10,530	583	101,100
—4	0	380	950	0	7,830	0	39,900
	100	395	940	588	7,860	15	41,300
$\theta = 0°$	200	455	930	1,176	8,150	57	46,200
	300	665	920	1,764	9,330	189	63,000
	400	890	925	2,352	10,680	321	80,700
	500	1,080	935	2,940	11,850	431	95,600

TABLE V

TEST DATA AND REDUCED DATA, FLANGE 4-2

TEST	LOAD BOLT STRAIN 1×10^{-6} *in*	TEST BOLT STRAIN GAGE 1 $.5 \times 10^{-6}$ *in*	TEST BOLT STRAIN GAGE 2 $.5 \times 10^{-6}$ *in*	INPUT LOAD *lbs*	TEST BOLT TENSILE LOAD *lbs*	MAXIMUM TEST BOLT BENDING MOMENT *in lbs*	MAXIMUM TEST BOLT STRESS *lbs per in²*
—1	0	—145	310	0	972	0	5,000
	50	—100	295	294	1,150	38	9,000
$\theta = 19°$	100	— 35	315	588	1,650	67	13,900
	200	160	340	1,176	2,940	175	29,300
	300	340	370	1,764	4,180	269	43,200
	400	505	415	2,352	5,410	347	55,900
	500	660	455	2,940	6,560	419	67,700
—2	0	150	275	0	2,500	0	12,800
	50	165	275	294	2,590	7	13,800
$\theta = 5°$	100	225	260	588	2,850	54	18,900
	200	390	260	1,176	3,820	153	32,000
	300	550	275	1,764	4,850	241	44,400
	400	705	295	2,352	5,880	323	56,300
	500	860	330	2,940	7,000	394	67,800
—3	0	515	235	0	4,410	0	22,500
	50	520	235	294	4,440	3	22,900
$\theta = 21°$	100	520	235	588	4,440	3	22,900
	200	635	230	1,176	5,090	80	32,400
	300	770	230	1,764	5,880	166	43,500
	400	905	240	2,352	6,740	248	54,600
	500	1,045	260	2,940	7,680	326	65,800
—4	0	690	330	0	6,000	0	30,600
	100	695	330	588	6,040	3	31,000
$\theta = 27°$	200	720	330	1,176	6,180	21	33,200
	300	850	330	1,764	6,950	109	44,300
	400	965	340	2,352	7,680	181	54,000
	500	1,090	350	2,940	8,480	259	64,300

TABLE VI

TEST DATA AND REDUCED DATA, FLANGE 4-3

TEST	LOAD BOLT STRAIN 1×10^{-6} *in*	TEST BOLT STRAIN GAGE 1 $.5 \times 10^{-6}$ *in*	TEST BOLT STRAIN GAGE 2 $.5 \times 10^{-6}$ *in*	INPUT LOAD *lbs*	TEST BOLT TENSILE LOAD *lbs*	MAXIMUM TEST BOLT BENDING MOMENT *in lbs*	MAXIMUM TEST BOLT STRESS *lbs per in*^{2}
—1	0	135	— 20	0	677	0	3,500
	50	195	— 50	294	854	57	9,000
$\theta = 16°$	100	320	— 90	588	1,350	160	19,900
	200	535	—135	1,176	2,360	321	38,200
	300	690	—140	1,764	3,240	420	50,700
	400	825	—120	2,352	4,150	492	61,300
	500	945	— 90	2,940	5,030	547	70,300
—2	0	235	50	0	1,620	0	8,300
	50	280	35	294	1,850	39	12,700
$\theta = 23°$	100	340	15	588	2,090	91	18,000
	200	480	— 5	1,176	2,800	195	30,200
	300	625	20	1,764	3,800	276	41,900
	400	750	40	2,352	4,650	342	51,600
	500	860	75	2,940	5,500	391	59,900
—3	0	50	770	0	4,830	0	24,600
	100	60	770	588	4,880	7	25,500
$\theta = 18°$	200	100	765	1,176	5,090	34	28,700
	300	185	760	1,764	5,560	91	35,800
	400	280	760	2,352	6,120	152	43,600
	500	380	765	2,940	6,790	212	51,700
—4	0	160	840	0	5,880	0	30,000
	100	170	835	588	5,920	10	31,000
$\theta = 15°$	200	195	835	1,176	6,060	24	32,900
	300	250	830	1,764	6,360	62	37,500
	400	345	825	2,352	6,890	124	45,200
	500	440	825	2,940	7,450	183	52,900

TABLE VI

TEST DATA AND REDUCED DATA, HI-RANGE 75

Test	Load Bolt Strain 1×10^{-6} in	Tare Bolt 1 Strain Gage 1 5×10^{-6} in	Tare Bolt 1 Strain Gage 2 5×10^{-6} in	Test Bolt Strain	Load Bolt Strain	Tare Bolt 1 Strain	Tare Bolt 2 Strain	Test Bolt Strain
—1	0	135	— 20					
	50	195	— 50					
$\theta = 16°$	100	320	— 90					
	200	535	—145					
	300	690	—140					
	400	825	— 120					
	500	945	— 90					
—2	0	235	30					
	50	280	35					
$\theta = 23°$	100	340	15					
	200	480	— 5					
	300	625	20					
	400	750	40					
	500	860	75					
—3	0	50	270					
	100	60	270					
$\theta = 18°$	200	100	265					
	300	185	260					
	400	280	260					
	500	380	265					
—4	0	160	340					
	100	170	335					
$\theta = 15°$	200	195	335					
	300	250	350					
	400	345	325					
	500	440	325					

TABLE VII

TEST DATA AND REDUCED DATA, FLANGE 7-1

Test	Load Bolt Strain 1×10^{-6} *in*	Test Bolt Strain Gage 1 $.5 \times 10^{-6}$ *in*	Test Bolt Strain Gage 2 $.5 \times 10^{-6}$ *in*	Input Load *lbs*	Test Bolt Tensile Load *lbs*	Maximum Test Bolt Bending Moment *in lbs*	Maximum Test Bolt Stress *lbs per in²*
—1	0	0	110	0	648	0	3,300
	50	165	55	294	1,300	132	17,400
$\theta = 3°$	100	340	0	588	2,000	270	32,200
	200	675	— 40	1,176	3,740	496	59,500
	300	940	— 5	1,764	5,500	635	79,800
	400	1,180	40	2,352	7,180	755	98,100
	500	1,420	90	2,940	8,890	867	116,000
—2	0	510	— 80	0	2,530	0	12,900
	50	530	— 85	294	2,620	16	14,700
$\theta = 28°$	100	665	—100	588	3,320	119	26,700
	200	910	— 95	1,176	4,800	284	47,600
	300	1,105	— 60	1,764	6,150	391	63,300
	400	1,305	— 5	2,352	7,650	488	78,800
	500	1,510	55	2,940	9,210	589	95,000
—3	0	—100	815	0	4,210	0	21,500
	50	— 90	850	294	4,210	15	22,700
$\theta = 28°$	100	— 55	795	588	4,360	44	25,800
	200	155	800	1,176	5,620	184	43,700
	300	340	830	1,764	6,880	287	58,500
	400	520	865	2,352	8,150	388	73,200
	500	705	910	2,940	9,510	482	87,800
—4	0	140	850	0	5,820	0	29,700
	100	170	840	588	5,940	26	32,500
$\theta = 18°$	200	285	820	1,176	6,510	111	42,300
	300	500	835	1,764	7,860	236	59,300
	400	675	855	2,352	9,000	333	73,100
	500	845	885	2,940	10,200	424	86,600

TABLE VIII

TEST DATA AND REDUCED DATA. FLANGE 7-2

TEST	LOAD BOLT STRAIN 1×10^{-6} *in*	TEST BOLT STRAIN GAGE 1 $.5 \times 10^{-6}$ *in*	TEST BOLT STRAIN GAGE 2 $.5 \times 10^{-6}$ *in*	INPUT LOAD *lbs*	TEST BOLT TENSILE LOAD *lbs*	MAXIMUM TEST BOLT BENDING MOMENT *in lbs*	MAXIMUM TEST BOLT STRESS *lbs per in*^{2}
—1	0	5	85	0	530	0	2,700
	50	150	25	294	1,030	125	15,500
$\theta = 10°$	100	270	— 5	588	1,560	217	25,700
	200	475	5	1,176	2,820	336	41,800
	300	635	60	1,764	4,090	400	53,500
	400	780	120	2,352	5,300	450	63,700
	500	920	180	2,940	6,480	500	73,800
—2	0	355	135	0	2,880	0	14,700
	50	360	135	294	2,920	3	15,100
$\theta = 25°$	100	445	120	588	3,320	70	22,700
	200	640	125	1,176	4,500	196	39,000
	300	755	150	1,764	5,320	254	47,900
	400	870	185	2,352	6,220	308	56,800
	500	1,000	220	2,940	7,180	370	66,900
—3	0	800	20	0	4,820	0	24,600
	50	805	25	294	4,880	0	24,900
$\theta = 47°$	100	810	20	588	4,880	10	25,700
	200	895	30	1,176	5,440	75	33,900
	300	1,030	60	1,764	6,420	166	46,300
	400	1,125	85	2,352	7,120	228	55,000
	500	1,205	120	2,940	7,800	269	61,700
—4	0	870	165	0	6,090	0	31,100
	50	870	165	294	6,090	0	31,100
$\theta = 42°$	100	875	165	588	6,120	5	31,600
	200	900	160	1,176	6,240	28	34,100
	300	1,050	180	1,764	7,240	134	47,900
	400	1,145	205	2,352	7,950	189	56,000
	500	1,240	230	2,940	8,650	248	64,300

Table IX

TEST DATA AND REDUCED DATA, FLANGE 7-3

Test	Load Bolt Strain 1×10^{-6} *in*	Test Bolt Strain Gage 1 $.5 \times 10^{-6}$ *in*	Test Bolt Strain Gage 2 $.5 \times 10^{-6}$ *in*	Input Load *lbs*	Test Bolt Tensile Load *lbs*	Maximum Test Bolt Bending Moment *in lbs*	Maximum Test Bolt Stress *lbs per in*^{2}
—1	0	— 60	160	0	588	0	3,000
	50	0	165	294	971	33	7,800
$\theta = 3°$	100	55	180	588	1,380	57	11,700
	200	180	195	1,176	2,210	124	21,400
	300	310	230	1,764	3,180	179	30,800
	400	415	270	2,352	4,030	226	39,000
	500	535	310	2,940	4,970	269	47,200
—2	0	430	50	0	2,820	0	14,400
	50	440	50	294	2,880	7	15,300
$\theta = 31°$	100	450	50	588	2,940	13	16,100
	200	530	60	1,176	3,470	64	22,900
	300	660	80	1,764	4,360	134	33,100
	400	770	110	2,352	5,180	196	42,400
	500	860	140	2,940	5,880	236	49,200
—3	0	40	830	0	5,120	0	26,100
	100	50	825	588	5,150	10	27,100
$\theta = 21°$	200	60	820	1,176	5,240	20	29,300
	300	100	820	1,764	5,410	46	31,400
	400	210	830	2,352	6,120	109	40,100
	500	320	850	2,940	6,890	166	48,600
—4	0	210	960	0	6,890	0	35,100
	100	220	960	588	6,950	7	36,000
$\theta = 16°$	200	225	955	1,176	6,950	13	37,500
	300	240	950	1,764	7,010	24	37,700
	400	280	950	2,352	7,240	51	41,100
	500	360	955	2,940	7,740	96	47,200

APPENDIX D

RIGID FLANGE THEORY

This appendix contains the derivations of the formulas for calculating bolt stress when using the rigid flange theory. This theory assumes that the flange will not deflect by bending, but that it is elastic and will compressively deform when subjected to loads. This theory further assumes that the flange is bolted to a rigid base which will neither bend nor compressively deform.

The first part of the appendix is devoted to the derivation of an expression for e_2, the compressive deformation of the flange at the bolt due to the initial bolt pre-tension. The solution for e_2 is required for the derivation of other formulas.

The next portion derives the expressions for the bolt tensile and bending loads when the flange is subjected to an external load, but prior to the opening of the joint between the flange and the base.

The final portion derives the expression for the bolt tensile and bending loads after the flange has started to separate from the base due to the external load.

Flange deformation due to initial bolt pre-tension. A free body diagram of a flange subjected to a force F_2, due to tightening the bolt and to the moment M_b at the attaching bolt is shown in Figure 37. The moment is caused by flange rotation which tends to tilt the bolt head slightly. A definition of all symbols used in this Appendix may be found in Appendix A. The force F_3 is the resulting force on the base of the flange. Force F_3 is located at the centroid of the pressure acting on the lower face of the flange. The shaded area represents a cross section of the volume of metal displaced by the pressure. (The vertical scale of this area is greatly exag-

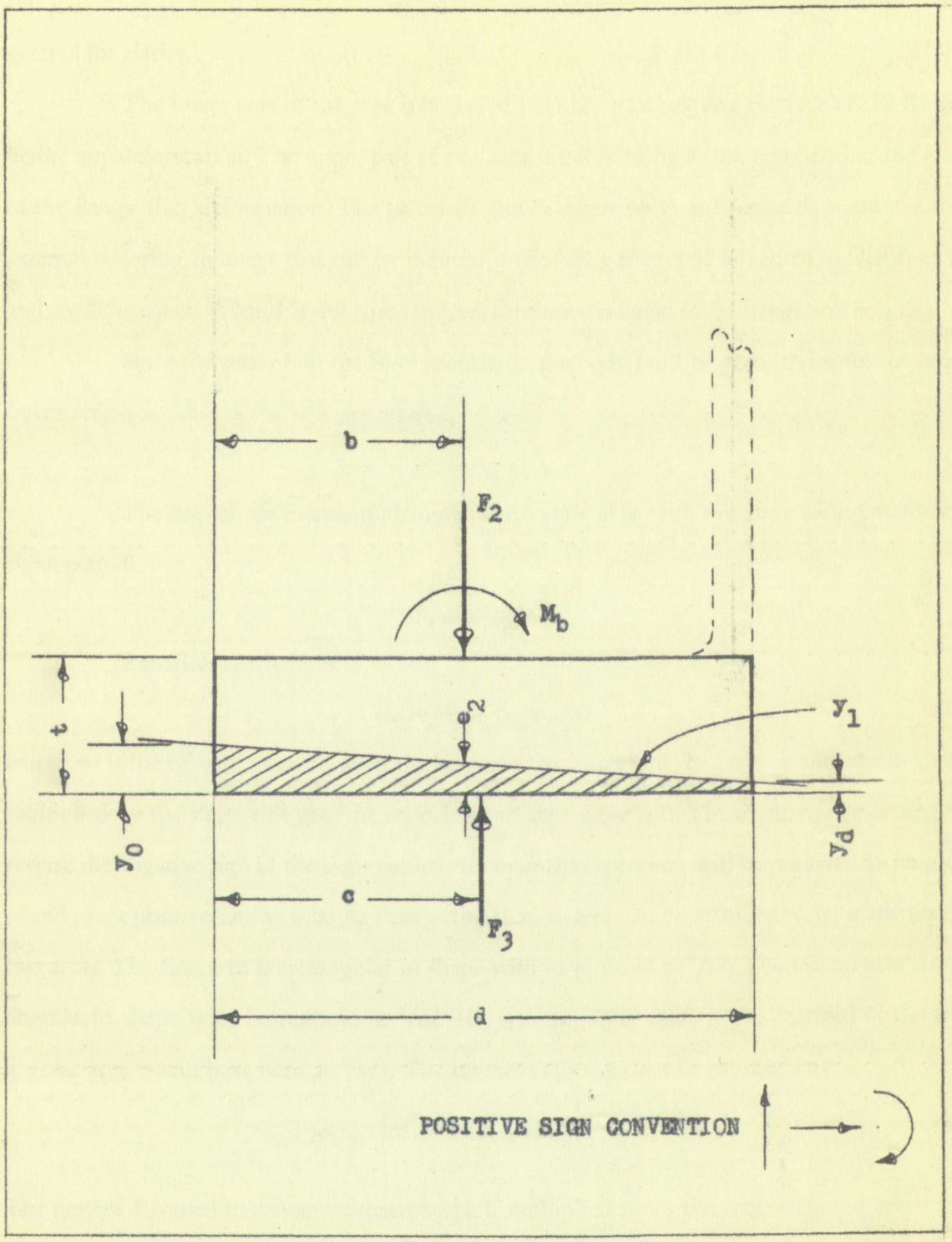

FIGURE 37

DEFORMATION OF RIGID FLANGE DUE TO BOLT PRE-TENSION, $1/3d < b < 2/3d$

gerated for clarity.)

The lower part of the area is bounded by a line representing the face of the flange before any deformation. The upper part of the area is bounded by a line representing the face of the flange after deformation. The forces F_2 and F_3 do not necessarily coincide because of the external restoring moment that can be induced if the flange rotates. If b is equal to $^1/_2d$, then b and c will be equal. When b is not equal to $^1/_2d$, then some rotation of the flange will occur.

Since the sum of all the forces acting on the body must be zero, and since the only forces acting are due to the bolt pre-tension,

$$F_2 = F_3 = F_t \,. \tag{1}$$

The sum of the moments acting on the body will be zero, therefore taking moments about point 0,

$$cF_3 = bF_2 + M_b \,. \tag{2}$$

Equation (2) reduces to

$$cF_3 = bF_2 + (-\, m_1 R_b) \tag{3}$$

where m_1 is the relative slope between the base and the flange and R_b is a constant which when multiplied by the slope will give the restoring moment at the bolt. The negative sign is used to reverse the negative sign of the slope so that the moment expression will be positive. As long as y_0 and y_d are positive, and y_0 is larger than y_d the shaded area can be assumed to be made up of two areas. The first area is rectangular in shape with its centroid at $^1/_2d$. The second area is triangular in shape with its centroid at $^1/_3d$. (If y_d were larger than y_0 the centroid of the triangular area would have been at $^2/_3d$). The moment cF_3 can then be expressed as

$$cF_3 = \frac{3Sd^2\, y_d + Sd^2\,(y_0 + y_d)}{6} \,. \tag{4}$$

The symbol S is used to denote a constant which multiplied times the cross-sectional area of a compressively deformed volume of the flange will give the force necessary to produce that deformation.

Using the point slope equation for a straight line, the line bounding the upper surface of the shaded area can be expressed as

$$y_1 = m_1 (x - {}^1/_2 d) + y_e \tag{5}$$

where it is assumed that the line passes through the point $x = {}^1/_2 d$ and $y = y_e$. The y ordinant has the value

$$y_e = {}^1/_2 (y_0 + y_d) . \tag{6}$$

Since y_e is the average height of the trapezoidal shaded area, an expression for F_3 involving y_e can be obtained as

$$F_3 = S d y_e . \tag{7}$$

By substituting the points $x = 0$, $y_1 = y_0$ and $x = d$, $y_1 = y_d$ into equation (5) the equations

$$y_0 = - {}^1/_2 (m_1 d) + y_e \tag{8}$$

and

$$y_d = {}^1/_2 (m_1 d) + y_e \tag{9}$$

are obtained.

Substituting these two equations into equation (4) and simplifying the result, gives the following equation:

$$cF_3 = \frac{S m_1 d^3 + 6 S d^2 y_e}{12} . \tag{10}$$

By solving equation (7) for y_e and substituting into equation (10), the expression

$$cF_3 = \frac{S m_1 d^3 + 6 F_3 d}{12} \tag{11}$$

is obtained which has only two unknowns, c and m_1. If equation (4) is re-written based on y_d being larger than y_0 the same equation as (11) will result. Therefore the original restriction on the relative sizes of y_0 and y_d was unnecessary.

By equating the right hand members of equations (3) and (11), substituting F_t for

F_3 and solving for m_1, the following equation results

$$m_1 = \frac{6F_t(2b - d)}{Sd^3 + 12R_b}. \tag{12}$$

By substituting this value of m_1 into equation (5) and substituting in the value of y_e in terms of F_t the general equation

$$y_1 = \frac{3SdF_t(2b - d)(2x - d) + F_t(Sd^3 + 12R_b)}{Sd(Sd^3 + 12R_b)} \tag{13}$$

is obtained. The solution for e_2 at $x = b$ is then

$$e_2 = \frac{3Sd\,F_t(2b - d)^2 + F_t(Sd^3 + 12R_b)}{Sd(Sd^3 + 12R_b)}. \tag{14}$$

In most cases the value of $12R_b$ is so small in relation to Sd^3 that the equation can be further simplified to

$$e_2 = \frac{F_t}{Sd}\left(\frac{3(2b - d)^2}{d^2} + 1\right). \tag{15}$$

In order to find the limiting positions of b for which both y_0 and y_d are positive, the points $x = 0$, $y_1 = 0$ and $x = d$, $y_1 = 0$, are substituted in the general equation (13). The result is that b must lie between $^1/_3d$ and $^2/_3d$ for the equation to hold. (Here it is assumed that the value of $12R_b$ is small enough to be disregarded without error.) Hence, equation (15) is true only when $^1/_3d < b < {}^2/_3d$.

It is necessary to derive formulas for e_2 when $0 < b < {}^1/_3d$ and $^2/_3d < b < d$. Since the value of e_2 will be the same for corresponding positions in either range of values, it is necessary to solve for e_2 for one set of values only. The solution derived below is for $0 < b < {}^1/_3d$. A free body diagram of the flange for this derivation is shown in Figure 38.

The summation of forces and the summation of moments in this instance will result in

$$F_2 = F_3 = F_t \tag{16}$$

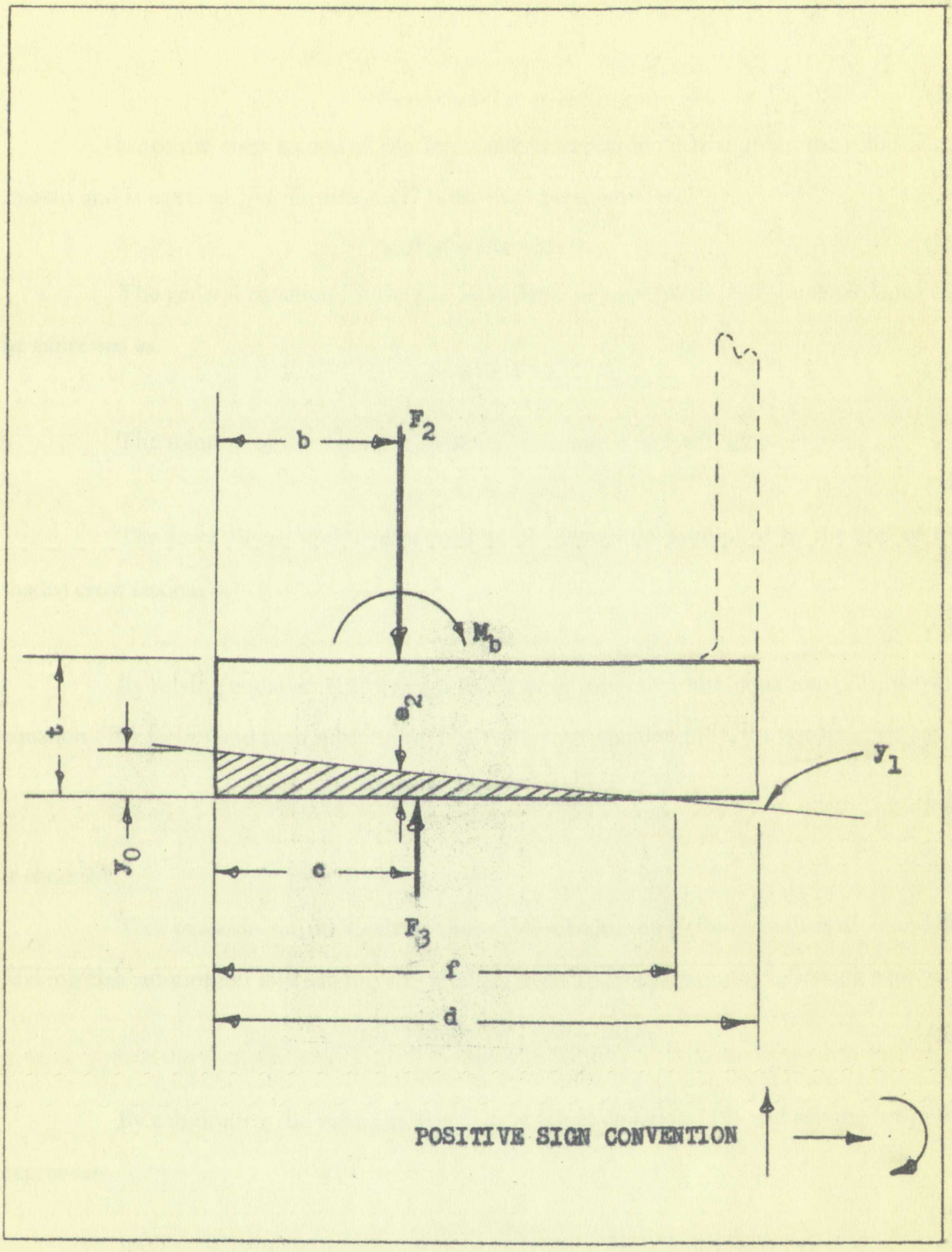

FIGURE 38

DEFORMATION OF RIGID FLANGE DUE TO BOLT PRE-TENSION, $0 < b < 1/3d$

and

$$cF_3 = bF_2 + (-m_1 R_b) . \tag{17}$$

Since the cross section of the area under compression is triangular, the value of c is known and is equal to $^1/_3 f$. Equation (17) can then be written as

$$^1/_3 (fF_3) = bF_2 - m_1 R_b . \tag{18}$$

The general equation for the line bounding the upper surface of the shaded area can be expressed as

$$y_1 = m_1 x + y_0 . \tag{19}$$

The solution of this equation, when $y_1 = e_2$ and $x = b$ will give

$$e_2 = m_1 b + y_0 . \tag{20}$$

The force F_3 can also be expressed as the constant S multiplied by the area of the shaded cross section, or

$$F_3 = {}^1/_2 (Sf y_0) . \tag{21}$$

By solving equation (21) for y_0, substituting this value into equation (20), solving equation (20) for m_1 and then substituting this value into equation (18), the equation

$$^1/_3(F_3) = \frac{fb^2 SF_2 + fS e_2 R_b - 2F_3 R_b}{fbS} \tag{22}$$

is obtained.

This equation can be further reduced by substituting F_t for the values of F_2 and F_3. Making this substitution and solving the resulting equation for e_2 gives the following equation.

$$e_2 = \frac{-{}^1/_3 (f^2 b F_t S) + b^2 f F_t S + 2R_b F_t}{f R_b S} . \tag{23}$$

By substituting the values of $x = f$, $y_1 = 0$ into equation (19) and solving for y_0 the expression

$$y_0 = -m_1 f \tag{24}$$

is obtained.

Substituting this value of y_0 into equation (21) results in another expression for

F_3, namely,

$$F_3 = -\,{}^1/_2\,(S\,m_1\,f^2)\,. \tag{25}$$

By scolwviningg equation (21) for y_0, substituting this value into equatin (20); solving equation (20) foor mn_1 : and then substituting this value into equation (25), th eqation

$$F_3 = -\,\frac{{}^1/_2\,Sf^2\,e_2 - F_3\,f}{b} \tag{26}$$

is obtained.

The soluutidon of equation (26) for e_2 is

$$e_2 = \frac{F_t\,f - F_t\,b}{{}^1/_2\,(Sf^2)} \tag{27}$$

where the force F_3 is replaced by its equal F_t.

The righht hand members of equations (23) and (27) may be eqiatd and solved to obtain

$$f^3\,bS - 3f^2\,b^2\,S - 6\,R_b\,b = 0\,. \tag{28}$$

The numnerrical value of e_2 may be obtained by solving equation (28) or f and substituting this value intoo eeither equation (23) or (27) to obtain the value of e_2.

Wlhern M_b, the restoring moment at the bolt, is small, little error will result from dropping the thiirdl teerm from equation (28) in which case the formula will reduce to

$$f = 3b\,. \tag{29}$$

By subsstitituating this value of f into equation (27), the solution for e_2 becomes

$$e_2 = \frac{4\,F_t}{9\,bS} \quad \text{for } 0 < \mathrm{b} < {}^1/_3\,\mathrm{d} \tag{30a}$$

and

$$e_2 = \frac{4\,F_t}{9\,(d-b)\,S} \quad \text{for } {}^2/_3\,d < b < d\,. \tag{30b}$$

It is mott ppossible to obtain a similar solution for e_2 by substituting equation (29) into equation (23), siince e_2 was introduced into this equation by the assumption that R_b had a value.

When R_b is assumed to be zero, the e_2 will drop out of equation (23).

Equation (30) can also be derived by assuming that e_2 will be $^2/_3$ f y_0, where the value of y_0 is obtained from equation (21) with f equal to $3b$.

Tensile and bending loads induced in the Test Bolt prior to flange separation from the base. A free body diagram of the flange is shown in Figure 39. The diagram is the same as Figure 37, except that the Force F_1 has been added.

As in the previous derivations, the formulas

$$F_2 = F_1 + F_3 \tag{31}$$

and

$$cF_3 + aF_1 = bF_2 - m_1 R_b \tag{32}$$

are obtained by taking the summation of the vertical forces equal to zero and the summation of moments about point 0 equal to zero. In this case $M_b = -m_1 R_b$.

As in formula (7), the force F_3 can be expressed as

$$F_3 = Sdy_e . \tag{33}$$

The formula for the line bounding the upper surface of the shaded area can be expressed as

$$y_1 = m_1 (x - {}^1/_2 d) + y_e . \tag{34}$$

Using the methods of derivation for equation (11), the moment cF_3 can be expressed as

$$cF_3 = \frac{Sm_1 d^3 + 6F_3 d}{12} . \tag{35}$$

Substituting the right hand member of equation (31) for F_2 in equation (32) and then solving for cF_3 results in

$$cF_3 = bF_1 + bF_3 - aF_1 - m_1 R_b . \tag{36}$$

The right hand members of equations (35) and (36), may be equated and solved for F_3 to give the equation

$$F_3 = \frac{F_1 (b - a) - m_1 R_b - {}^1/_{12} (Sm_1 d^3)}{({}^1/_2 d - b)} . \tag{37}$$

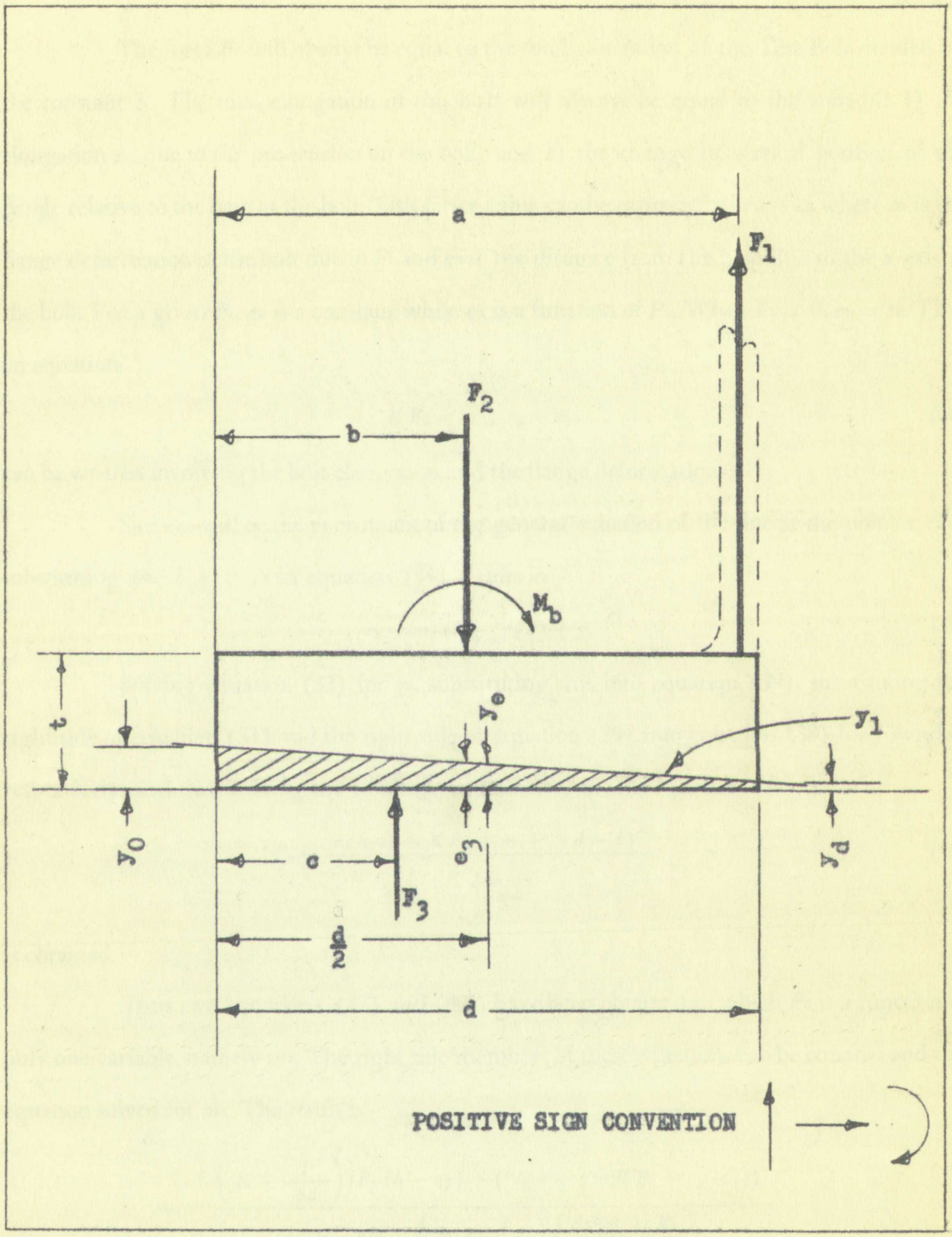

FIGURE 39

DEFORMATION OF RIGID FLANGE PRIOR TO SEPARATION FROM BASE

The force F_2 will always be equal to the total elongation of the Test Bolt divided by the constant K. The total elongation of this bolt will always be equal to the sum of: 1) the elongation e_2, due to the pre-tension on the bolt, and 2) the change in vertical position of the flange relative to the base at the bolt. This latter value can be expressed as $e_2 - e_3$ where e_2 is the flange deformation at the bolt due to F_t and e_3 is the distance from the base line to the x axis at the bolt. For a given F_t, e_2 is a constant while e_3 is a function of F_1. When $F_1 = 0$, $e_2 = e_3$. Thus an equation

$$K F_2 = e_1 + e_2 - e_3 , \tag{38}$$

can be written involving the bolt elongation and the flange deformations.

Since e_3 will be the y_1 ordinant of the general equation of the line at the point $x = b$, substituting $x = b$, $y_1 = e_3$ in equation (34) results in

$$e_3 = m_1 (b - {}^1/_2 d) + y_e . \tag{39}$$

Solving equation (33) for y_e, substituting this into equation (39), substituting the right side of equation (31) and the right side of equation (39) into equation (38) for F_2 and e_3 respectively, and then solving the resulting equation for F_3, the equation

$$F_3 = \frac{e_1 + e_2 - K F_1 + m_1 ({}^1/_2 d - b)}{K + \dfrac{1}{Sd}} \tag{40}$$

is obtained.

Thus two equations, (37) and (40), have been obtained in which F_3 is a function of only one variable, namely m_1. The right side members of these equations can be equated and this equation solved for m_1. The result is

$$m_1 = \frac{\left(K + \dfrac{1}{Sd}\right)[F_1 (b - a)] + ({}^1/_2 d - b)(K F_1 - e_1 - e_2)}{({}^1/_2 d - b)^2 + \left(K + \dfrac{1}{Sd}\right)\left(\dfrac{Sd^3 + 12 R_b}{12}\right)} . \tag{41}$$

The value of the axial load on the bolt, F_2, can now be obtained by combining equa-

tions (31), (40), and (41). The resulting equation is.

$$F_2 = F_1 + \left(\frac{1}{K + \frac{1}{Sd}}\right)\left(e_1 + e_2 - KF_1 + (1/2\,d - b)\right) \left(\frac{\left(K + \frac{1}{Sd}\right)[F_1(b-a)] + (1/2\,d - b)(KF_1 - e_1 - e_2)}{(1/2\,d - b)^2 + \left(K + \frac{1}{Sd}\right)\left(\frac{S\,d^3 + 12\,R_b}{12}\right)}\right). \tag{42}$$

Since this equation is cumbersome it is generally easier to solve for the value of m_1, from equation (41), substitute into equation (40) to obtain F, then substitute into equation (31), to obtain F_2. With F_2 known the axial stress of the bolt is easily determined.

The bending moment on the bolt is obtained by multiplying the slope m_1 by R_b and reversing the sign of the result to obtain a positive value for the moment. The bending stress is then obtained in the usual manner. The maximum bolt stress is the sum of the axial and the bending stresses.

It is to be noted that F_1 in equation (42) appears to the first power only. Therefore the relation between F_2 and F_1 is a straight line. This fact will prove useful since it will be necessary to locate only two points on a graph of F_2 versus F_1 in order to plot the curve of the function relating the two forces.

Tensile and bending loads induced in the Test Bolt after the occurrence of flange separation from the base. A free body diagram of the flange is shown in Figure 40. The diagram is the same as Figure 38, except that the force F_1 and the moment M_f have been added.

As in the previous derivations, the formulas

$$F_2 = F_1 + F_3 \tag{43}$$

and

$$cF_3 + aF_1 = bF_2 - m_1 R \tag{44}$$

are obtained by taking the summation of the vertical forces equal to zero, and the summation of

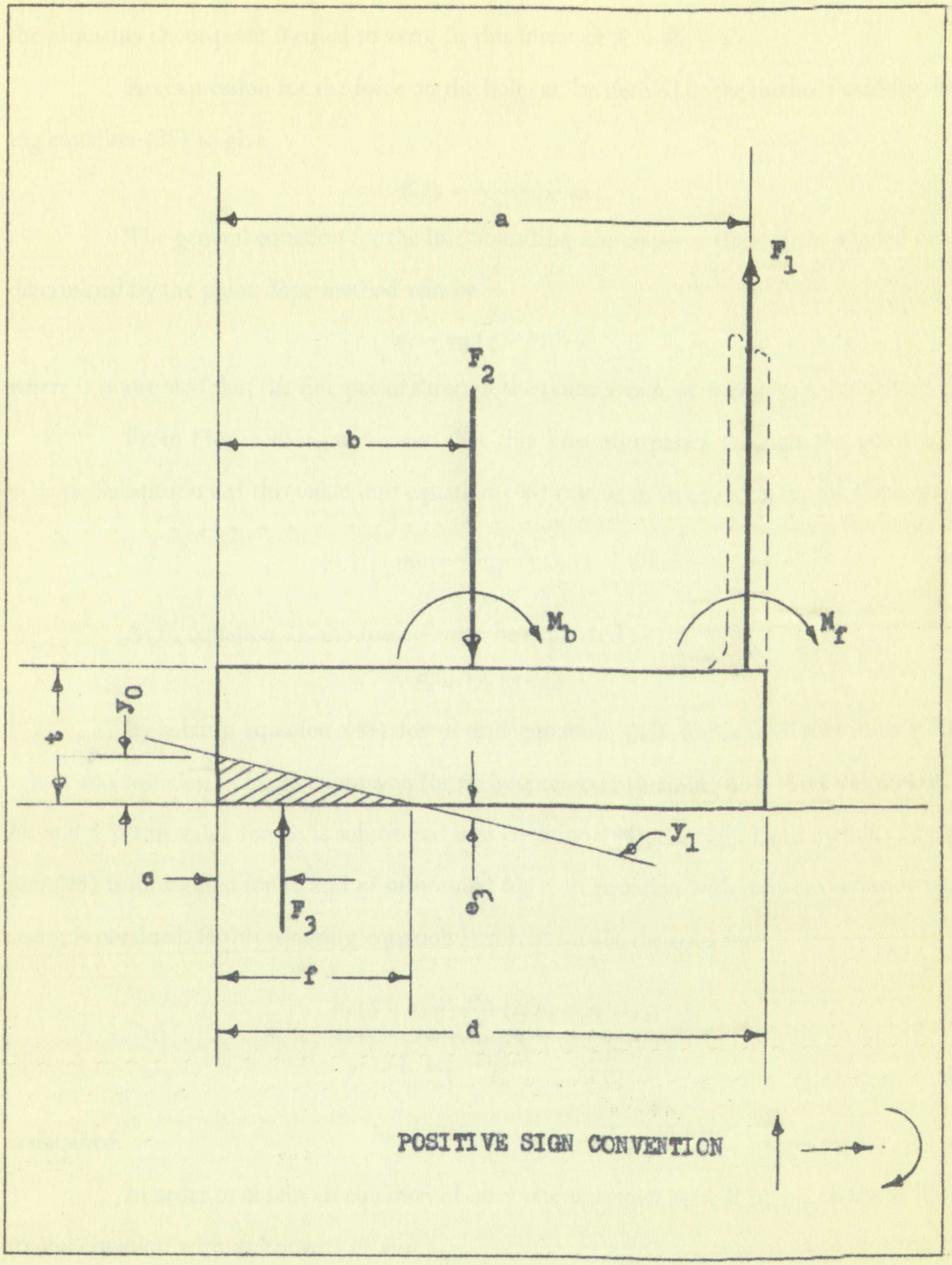

FIGURE 40

DEFORMATION OF RIGID FLANGE AFTER START OF SEPARATION

the moments about point 0 equal to zero. In this instance $R = R_b + R_f$.

An expression for the force on the bolt can be derived by the methods used for deriving equation (38) to give

$$K F_2 = e_1 + e_2 - e_3 . \tag{45}$$

The general equation for the line bounding the upper surface of the shaded area as determined by the point slope method will be

$$y_1 = m_1 (x - b) + e_3 \tag{46}$$

where it is assumed that the line passes through the point $x = b$, $y_1 = e_3$.

From Figure 40 it can be seen that this line also passes through the point $x = 0$, $y_1 = y_0$. Substitution of this value into equation (46) results in an equation for the slope m_1

$$m_1 = \frac{e_3 - y_0}{b} . \tag{47}$$

As in equation 21, the force F_3 can be expressed as

$$F_3 = {}^1/_2 (S f y_0) . \tag{48}$$

By solving equation (48) for y_0 and equation (45) for e_3 and substituting these values into equation (47), an expression for m_1 is obtained containing only three unknowns, F_2, F_3, and f. If this value for m_1 is substituted into equation (44), the right hand member of equation (43) is substituted for F_2 and gf substituted for c, an equation with only two unknowns, F_3 and f, is obtained. If this resulting equation is solved for F_3, the equation

$$F_3 = \frac{F_1 (b - a) + \frac{R}{b} (K F_1 - e_1 - e_2)}{gf - \left(b + \frac{R K}{b} \right) - \frac{2 R}{f b s}} \tag{49}$$

is obtained.

In order to obtain an equation of only one unknown it will be necessary to have a second equation with unknowns F_3 and f.

An equation involving F_3, f, and m_1,

$$F_3 = - {}^1/_2 (S m_1 f^2) , \tag{50}$$

can be derived using the same methods as were used in deriving equation (5).

By substituting the value of m_1 from equation (47), the value of y_0 from equation (48), the value of e_3 from equation (45), and the value of F_2 from equation (3) an equation involving only F_3 and f,

$$F_3 = \frac{S f^2 (K F_1 - e_1 - e_2)}{2 (b - f) - S K f^2} \tag{51}$$

is obtained.

By equating the right hand members of equations (49) and (51) and solving for F_1 the equation

$$F_1 = \frac{S f^2 (e_1 + e_2)\left[g f - \left(b + \frac{R K}{b} \right) - \frac{2 R}{f b s} \right] - \frac{R}{b} (e_1 + e_2) [2 (b - f) - S K f^2]}{S K f^2 \left[g f - \left(b + \frac{R K}{b} \right) - \frac{2 R}{f b s} \right] - \left(b - a + \frac{R K}{b} \right) [2 (b - f) - S K f^2]} \tag{52}$$

is obtained.

With a given g ($^1/_3$ for a triangular area) it is now possible to assume a value of f between $x = 0$ and $x = d$ and substitute it into equation (52) and obtain the force F_1 that will produce separation between the base and the flange to the point f. This value of F_1 can be substituted into either equation (49) or (51), along with f to obtain the value of F_3. The addition of F_1 and F_3 will give F_2. Knowing F_2, the axial stress on the bolt is easily determined.

The numerical value of y_0 and e_3 can now be determined from equations (48) and (45) respectively. Substitution of these values into equation (47) will give the value of the slope m_1. The bending moment on the bolt is then obtained by taking the product of m_1 and R_b and reversing the sign to obtain a positive value for the result. The bending stress may then be determined using standard formulas. If required, the bending moment on the external load carrying flange can be obtained from the product of m_1 and R_f.

APPENDIX E

FLEXIBLE FLANGE TTHEORY

This appendix contains the derivation of formmulas for the flexible flange theory. This theory assumes the flange is free to both compressively ddeform due to pressure and flex lue to bending loads. The derivation is based on the assumptionn that the base is completely rigd and neither bends nor compressively deforms.

Figure 41 is a free body diagram of a flexiblde flange shown compressed and bent, due to an external load. The shaded area, as in Appendilix D, represents the area of the flange that has been compressively deformed. In this instance i it is assumed to be made up of two areas, one triangular and one lens shaped. The product obf the shaded area and he appropriate constant will give the force equal and opposite to F_3. Foorce F_3 is shown dottel in Figure 41 since it is the resultant force obtained by combining the foorce F_4 associated with the triangular area and the force F_5 associated with the lens shaped areea. The line y_1 represents the surface of the base on which the flange is mounted. The line y_3 reppresents the flexural curve of the flange due to the force F_2. The actual flexural curve is unknown. It is obviously very complex because of the varying load applied to the one end due to the presssure between the flange and the base. In order to simplify the equations, it was decided to assume that the flange would deflect the same as a beam simply supported at each end with a conccentrated load F_2 located between the supports. The line y_2 is a line joining the outer lower edgee of the flange as determined by curve y_3, and the intersection of y_1 and y_3. The x axis is passed throough the inner and outer lower edges of the flange as determined by curve y_3. The y axis is passeed through the outer lower edge. The difference between y_1 and y_3 at any given x, represents the amount of compressive deformation of the flange at that point. As in previous derivations, e_3 represents the distance between the base and the bottom of of the flange at the bolt. In this case, howwever, it is necessary to have a new

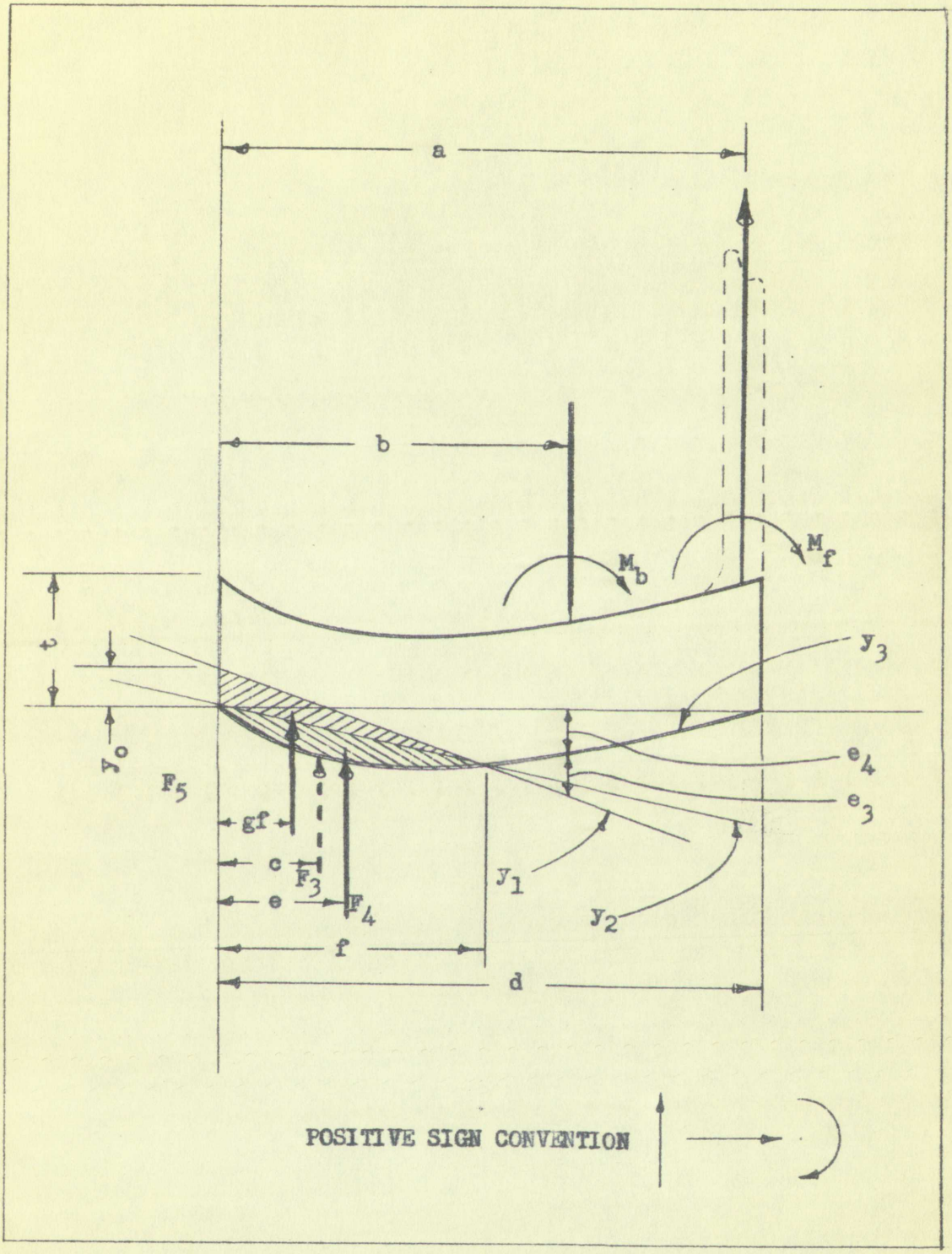

FIGURE 41

DEFORMATION OF FLEXIBLE FLANGE AFTER START OF SEPARATION

displacement e_4. This displacement, due to the force F_2, is the distance the flange has deflected relative to the x axis at the bolt.

As in the rigid flange theory (see Appendix D), the product of the constant S and the cross-sectional area of the compressively deformed volume of metal will give the force necessary to produce that deformation.

As in previous derivations, the summation of forces in the vertical direction and the summation of moment about point zero will give two equations.

$$F_2 = F_1 + F_4 + F_5 \tag{1}$$

and

$$eF_5 + gf\,F_4 + aF_1 = bF_2 + M_b + M_f\ . \tag{2}$$

From observation of Figure 41 it can be seen that

(3)

$$F_5 = S \int_0^f (y_2 - y_3)\, dx\ .$$

The formula for the deflection from 0 to b of a simply supported beam with a central load for the dimensions shown in Figure 41 is

$$y_3 = \frac{-F_2\,(a-b)\,[(2ab - b^2)\,x - x^3]}{b\,E_f\,I_f\,a} \tag{4}$$

which equals

$$y_3 = -F_2\,A_1\,[\,(2ab - b^2)\,x - x^3] \tag{5}$$

when simplified.

The formula for the line y_2 may be written as

$$y_2 = m_2 x\ . \tag{6}$$

When $x = f$, equations (6) and (4) can be re-written as

$$y_{2f} = m_2 f \tag{7}$$

and

$$y_{3f} = -F_2\,A_1\,[(2ab - b^2)\,f - f^3]\ . \tag{8}$$

Since y_{2f} and y_{3f} are equal when $x = f$, the right side of these two expressions may be equated and solved for m_2 with the result that

$$m_2 = -F_2 A_1 [(2ab - b^2) - f^2] . \tag{9}$$

The general equation of the line y_2 may then be re-written as

$$y_2 = -F_2 A_1 [(2ab - b^2) - f^2 x] . \tag{10}$$

By substituting the values of y_2 from equation (10) and y_3 from equation (5) into equation (3) and integrating between the limits of 0 and f, the equation

$$F_{55} = {}^1/_4 (S F_2 A_1 f^4) \tag{11}$$

may be obtained. If this value of F_5 is substituted into equation (1) and this equation then solved for F_2, the result is

$$F_2 = (F_1 + F_{44}) \left(\frac{1}{1 - {}^1/_4 (S A_1 f^4)} \right) \tag{12}$$

which can be simplified to

$$F_2 = (F_1 + F_4) A_8 . \tag{13}$$

An equation for eF_5 can be written as

$$eF_5 = S \int_0^f (y_2 - y_3) x dx . \tag{14}$$

A solution of this equation obtained in the same way as equation (3) will result in

$$eF_5 = {}^2/_{15} (S F_2 A_1 f^5) . \tag{15}$$

If the constants R_b and F_f are known, the sum of moments M_b and M_f can be expressed as

$$M_b + M_f = -(m_{11} - m_{3b}) R_b - (m_1 - m_{3a}) R_f \tag{16}$$

where m_{3b} and m_{3a} are the slopes of the curve y_3 at b and a respectively. The slope $m_1 - m_3$ in each case is the relative slope between the base and the flange at the points a and b. The constants R_b and R_f are the number of inch-pounds necessary to rotate the bolt and the attaching flange respectively, one radian.

From equation (4), the slope m_{3b} can be determined as

$$m_{3b} = -F_2 A_1 (2ab - 4b^2) \tag{17}$$

which can be simplified to

$$m_{3b} = -F_2 A_3 . \tag{18}$$

From the equation for the deflection y_3 from b to a, a similar expresiofor the slope m_{3a} can be derived as

$$m_{3a} = F_2 A_4 . \tag{19}$$

The equation for the slope of the line y_1 is

$$m_1 = \frac{e_3 + e_4 - y_0}{b} . \tag{20}$$

Since the total force on the bolt F_2 times the constant K will always be equal totheotal elongation of the bolt, an equation can be written where

$$K F_2 = e_1 + e_2 - e_3 . \tag{21}$$

From examination of Figure 41 it can be seen that an expression for F_4 can b obtined as

$$F_4 = {}^1/_2 (S f y_0) . \tag{22}$$

An expression for e_4 can be obtained by substituting the value $x = b$ into equatin).

$$e_4 = -F_2 A_2 . \tag{23}$$

By solving equation (21) for $e_3 + e_4$ (by first adding e_4 to each side of the eqatin), solving equation (22) for y_0 and substituting these values along with the value of e frcn equation (23) into equation (20) an expression for m_1 can be obtained.

$$m_1 = \frac{e_1 + e_2}{b} - F_2 \left(\frac{A_2 + K}{b} \right) - \frac{2 F_4}{S b f} . \tag{24}$$

By substituting the values of m_1 from equation (24), m_{3b} from equation (18)anc m_{3a} from equation (19) into equation (16), and gathering all like terms, then simplifying y sibstitution, an equation

$$M_b + M_f = F_2 A_5 + F_4 A_6 + A_7 \tag{25}$$

is obtained.

By taking the value of $M_b + M_f$ from equation (25), the value of eF_5 fron quaon (15), and the value of F_2 from equation (13) and substituting these into equation (2) an simplifying the result by combining terms and substituting, a value of F_4 can be obtainedwhe

$$F_4 = \frac{F_1 A_{10} + A_7}{A_{11}} . \tag{26}$$

Thus a relation between F_4, F_1 and f has been obtained. (The onsantA_{10} and A_{11} contain f). It will be necessary to develop another equation relating these hre vaables before a relation between F_1 and f can be determined.

As long as the difference between the slopes m_1 and m_2 remain snall,he force due to the triangular shaped area can be expressed as

$$F_4 = -\,{}^1/_2\,(m_1 - m_2)\,S\,f^2 . \tag{27}$$

Substituting the value of m_2 from equation (9) and m_1 from equation (24 ino euation (27) and collecting like terms, simplifying and solving for F_4 gives the equation

$$F_4 = \frac{F_1 A_8 A_{12} + A_{13}}{A_{14}} . \tag{28}$$

This equation is also a relation between F_4, F_1, and f (f is contained in theterns A_8, A_{12}, A_{13}, and A_{14}.)

The right hand members of equations (28) and (26) may be eqiated and the result solved for F_1 to obtain

$$F_1 = \frac{A_{11} A_{13} - A_7 A_{14}}{A_{10} A_{14} - A_8 A_{11} A_{12}} . \tag{29}$$

Thus it is now possible to solve for a given F_1 by substituting ino quaion (29), a value of f between $x = 0$ and $x = b$. The value of F_1 thus obtained along vith the value of f used to obtain F_1, can be substituted into either equation (28) or (26) to obtain a value of F_4. The value of F_1, F_4 and f may then the substituted into equation (10) to obtain F.

Since

$$M_b = -\,(m_1 - m_{3b})\,R_b , \tag{30}$$

it is possible to substitute in the values of m_1 from equation (24) and n_{3b} fron quation (18), then collect terms and simplify and obtain an expression for M_b of

$$M_b = R_b (F_2 A_{15} + F_4 A_{16} + A_{17}) . \tag{31}$$

Substitution of the values of F_2, F_4, and f into equation (31) will give he benlin moment on the bolt. The stress can then be determined using standard formulas.

APPENDIX F

FORMULA DERIVATION USING DIMENSIONAL ANALYSIS

The formulas developed in Appendices D and E were applied to several of the flanges tested. The results showed that no satisfactory relation between F_2 and F_t had been developed for that portion of the test after the flange had started separating from the base to which it was attached. Therefore, an attempt to describe this relationship by the use of Dimensional Analysis was made. This Appendix contains the formulas that were developed by the use of the Dimensional Analysis approach to the problem.

From an examination of the overall problem it was concluded that the following variables were of sufficient importance to warrant consideration.

Variable	*Units*	
F_2	lb.	(1)
F_1	lb.	(2)
F_t	lb.	(3)
$\frac{a}{b}$	dimensionless	(4)
$\frac{a}{h}$	dimensionless	(5)
t	in.	(6)
K	in.	(7)
C_1	$\frac{1}{\text{in.-lb.}}$	(8)
E_f	$\frac{\text{lb.}}{\text{in.}^2}$	(9)
I_f	in.^4	(10)
R_b	in.-lb.	(11)
R_f	in.-lb.	(12)

Variables	*Units*	
d	in.	(13)
w	in.	(14)
r_b	in.	(15)

It should be noted that all of these variables are not independent, therefore complete freedom in combining them does not exist. For example, the variable l involves r_b in addition to other variables.

The first eight variables were investigated in this problem. Even though many dimensionless ratios were possible when using the first eight variables, only four were found to be of use in describing the behavior of the flange. These were

$$\pi_1 = \frac{F_1}{F_2}, \tag{16}$$

$$\pi_2 = \frac{F_t}{F_2}, \tag{17}$$

$$\pi_3 = \frac{a}{b}, \tag{18}$$

and

$$\pi_4 = \frac{bh}{a^2}. \tag{19}$$

It was determined that these π terms would combine to form the equation

$$1 = \pi_1 \pi_3 \left(1 - \frac{F_t}{B_1}\right) + \pi_2 B_2 \pi_4. \tag{20}$$

By multiplying both sides of equation (20) by F_2 and substituting in the equivalents of the π terms, an equation involving all the variables is obtained.

$$F_2 = F_1 \left(\frac{a}{b}\right)\left(1 - \frac{F_t}{B_1}\right) + F_t B_2 \left(\frac{bh}{a^2}\right). \tag{21}$$

Methods used to derive the equations. From an observation of the graphs of resulting bolt load, F_2, versus input load, F_1, it may be seen that there is a marked similarity between

all the plots. The graphs may be found on pages 27 through 35. It is particularly noteworthy that the third portion of each curve, the part with relatively steep slope is very similar for each set of the flanges with the same $\frac{a}{b}$ ratio even though the three flanges in the set are of different thicknesses. It is also apparent upon adding the line $F_t = \frac{a}{b} F_1$ that this new line could quite easily be a member of the family of curves. Observation shows that, with increasing initial Test Bolt pre-tension, there is a decrease in slope of the third portion of each curve. This is consistent throughout all tests. If this third portion of the curve is actually a part of a straight line, then this line could be expressed as

$$F_2 = m F_1 + i \tag{22}$$

where m is the slope of the line and i is the intercept of the line on the y axis. A posible solution to equation (22) would be to allow m to be a π term and i to be the product of a π term and F_t.

Accordingly, a first degree equation was fitted to the third portion of each of the F_2 versus F_1 curves. A reduction of the data of the intercepts of all these curves showed the weighted average to be about 76% of F_t. (The intercepts were weighted to prevent the lower values of F_t from exerting undue influence, since an error of 10% on F_t of 100 pounds is not nearly as important as an error of 10% at an F_t of 1000 pounds.) No matter whether the flanges were grouped by thickness or eccentricity ratio, the average of the groups did not vary more than about 5% from the mean of 76%. One additional fact concerning this intercept was known, that is, it would have to be 0% of F_t when b was equal to a (when the bolt and the external load were in line). A more careful reduction of the intercept data showed the following:

1.) When $b = 0.6875$, $i = 77\%$ F_t with a standard deviation of $5.4\% F_t$.

2.) When $b = 1.125$, $i = 79\%$ F_t with a standard deviation of $6.1\% F_t$ and

3.) When $b = 1.3125$, $i = 73\%$ F_t with a standard deviation of $7.26\% F_t$.

With the value of $i = 0\%$ of F_t when $b = a$, a total of four points of the function was known. After plotting this function against the various dimensionless ratio terms, it was determined

that a π term made up of the reciprocal of the product of two of the original variables $\frac{a}{b}$ and $\frac{a}{h}$ would satisfy the required conditions. The equation for i was therefore

$$i = F_t B_2 \left(\frac{bh}{a^2}\right), \tag{23}$$

where B_2 is a dimensionless proportionality factor equal to 3.48.

The remaining factor to be determined was the slope m of equation (22). From examination of the plotted data it was apparent that the slope m could be expressed as a function of $\frac{a}{b}$ minus some function of $\frac{a}{b}$ and F_t. The plotted test data showed the slope would start out approximately equal to $\frac{a}{b}$ when F_t was equal to zero and would decrease as F_t became larger. It was determined that

$$m = \frac{a}{b}\left(1 - \frac{F_t}{B_1}\right) \tag{24}$$

would satisfy the available data. In this case B_1 was a constant equal to 16,000 pounds. While the term $\frac{F_t}{B_1}$ is dimensionless, it is not a dimensionless ratio and is applicable only to the flanges tested in this problem. No correlation could be found between the dimensionless ratios which could be determined from the variables examined in this problem and the term $\frac{F_t}{B_1}$. It is felt that the required π term will involve the modulus of elasticity and area of both the flange and the attaching bolt. These variables were not investigated in this problem.

Equation (20) for general use must then be reduced to

$$1 = \pi_1 \pi_3 + \pi_2 B_2 \pi_4, \tag{25}$$

This modification of equation (20) is necessary since no dimensionless ratio for $\frac{F_t}{B_1}$ could be developed from the variables investigated in this problem. Conversion of equation (25) to an equation of the variables involved yields

$$F_2 = \frac{a}{b} F_1 + B_2 \left(\frac{bh}{a^2}\right) F_t. \tag{26}$$

The results of applying this equation to an actual problem should be conservative since the third

portion of the curve will have a slope equal to the $\frac{a}{b}$ ratio and this portion of the curve will intersect the first portion of the curve (the portion where no separation from the base has occurred) at a lower F_1 than if the slope were decreasing with increasing h.